Bioactive Materials xxx (2017) 1–37

Contents lists available at ScienceDirect

Bioactive Materials

journal homepage: http://www.keaipublishing.com/en/journals/bioactive-materials/

3D bioactive composite scaffolds for bone tissue engineering

Gareth Turnbull [a, b], Jon Clarke [b], Frédéric Picard [a, b], Philip Riches [a], Luanluan Jia [c], Fengxuan Han [c], Bin Li [c], Wenmiao Shu [a, *]

[a] Department of Biomedical Engineering, Wolfson Building, University of Strathclyde, 106 Rottenrow, Glasgow, G4 0NW, United Kingdom
[b] Department of Orthopaedic Surgery, Golden Jubilee National Hospital, Agamemnon St, Clydebank, G81 4DY, United Kingdom
[c] Orthopaedic Institute, Department of Orthopaedic Surgery, The First Affiliated Hospital, Soochow University, Suzhou, Jiangsu, PR China

ARTICLE INFO

Article history:
Received 31 August 2017
Received in revised form
31 October 2017
Accepted 31 October 2017
Available online xxx

Keywords:
Bioactive composites
3D scaffold
3D printing
Bioprinting
Bone
Tissue engineering

ABSTRACT

Bone is the second most commonly transplanted tissue worldwide, with over four million operations using bone grafts or bone substitute materials annually to treat bone defects. However, significant limitations affect current treatment options and clinical demand for bone grafts continues to rise due to conditions such as trauma, cancer, infection and arthritis. Developing bioactive three-dimensional (3D) scaffolds to support bone regeneration has therefore become a key area of focus within bone tissue engineering (BTE). A variety of materials and manufacturing methods including 3D printing have been used to create novel alternatives to traditional bone grafts. However, individual groups of materials including polymers, ceramics and hydrogels have been unable to fully replicate the properties of bone when used alone. Favourable material properties can be combined and bioactivity improved when groups of materials are used together in composite 3D scaffolds. This review will therefore consider the ideal properties of bioactive composite 3D scaffolds and examine recent use of polymers, hydrogels, metals, ceramics and bio-glasses in BTE. Scaffold fabrication methodology, mechanical performance, biocompatibility, bioactivity, and potential clinical translations will be discussed.

1. Introduction

1.1. Clinical demand for bone grafts, bone substitutes & implants

The capacity for bone to self-regenerate has prompted study and intrigue since the times of Hippocrates and Galen [1]. Despite this, congenital and acquired pathologies including trauma, infection, neoplasm and failed arthroplasty remain capable of leaving patients with bone defects beyond a critical-size which the body cannot heal. Such patients often require invasive surgical intervention to aid healing. This can involve clinical use of bone grafts, bone substitute materials, growth factors, free fibula vascularized grafts and insertion of metalwork to aid stability and bone regeneration [2,3]. As a result, bone is the second most commonly transplanted tissue worldwide, with at least four million operations making use of bone grafts and bone substitute materials annually [4–6].

However, significant limitations affect current treatment options. Bone grafts taken from one part of a patient for use in their own body (autografts) are considered the gold standard but are restricted by the size of graft that can be harvested and carry a further risk of donor site morbidity including infection and ongoing pain following surgery [7,8]. Allograft tissue harvested from cadaveric and living sources (such as femoral heads removed during hip replacements) is in relatively greater supply compared to autograft tissue. However, allografts carry potential risk of disease transmission and immune response, whilst lacking a cellular component to aid tissue regeneration. Metalwork and bone substitutes can also be inserted to aid bone regeneration; limitations associated with their use include bone thinning due to stress shielding, wear and failure over time and risk of revision surgery [6]. Non-invasive therapies including ultrasound treatment have also show promise in aiding bone healing, although use is often restricted to stable, well aligned and well reduced fracture non-unions in adult patients [9].

To overcome the limitations of current treatment options, significant research in the field of bone tissue engineering (BTE) has been directed towards creating novel alternatives to traditional

* Corresponding author.
E-mail address: will.shu@strath.ac.uk (W. Shu).
Peer review under responsibility of KeAi Communications Co., Ltd.

https://doi.org/10.1016/j.bioactmat.2017.10.001

Please cite this article in press as: G. Turnbull, et al., 3D bioactive composite scaffolds for bone tissue engineering, Bioactive Materials (2017), https://doi.org/10.1016/j.bioactmat.2017.10.001

bone grafts. Porous 3D scaffolds fabricated through a variety of methods and including a range of biomaterials have been utilised to aid and direct bone regeneration [10–12]. However, the perfect scaffold material has yet to be encountered and clinical translation of 3D scaffolds has been limited as a result [13].

Bone is a heterogenous composite material with constituents including hydroxyapatite mineral ($Ca_{10}(PO_4)_6(OH)_2$) [14], a mixed organic component (type I collagen, lipids and non-collagenous proteins) and water [15,16]. During scaffold manufacture it would therefore seem logical to include a combination of materials to create a composite scaffold, potentially allowing greater scaffold bioactivity and structural biomimicry to be achieved.

Scaffold bioactivity is also increased by incorporating materials that possess the ability to interact with or bind to living tissues. Increased scaffold bioactivity can in turn lead to improved bone cell ingrowth (osteoconduction), stable anchoring of scaffolds to host bone tissue (osseointegration), stimulation of immature host cells to develop into osteogenic cells (osteoinduction) and increased vascularisation [17–20].

This review will therefore examine some of the significant bioactive composites that have been utilised recently in BTE after reference to the properties of an ideal scaffold and available scaffold manufacturing methods. 3D scaffolds that have successfully bridged bone defects whilst actively inducing bone regeneration will be highlighted.

2. Properties of an ideal scaffold

In general terms, the ideal 3D scaffold is composed of a biocompatible, biodegradable material with similar mechanical properties to the tissue which it is to be implanted in. Scaffolds by design are not intended to be permanent implants and will ideally facilitate host cells to deposit extracellular matrix (ECM) and replace the scaffold structure over time. The 3D architecture of the scaffold should be highly porous with an interconnected structure to allow cell and nutrient migration. The scaffold surface should also be optimised to facilitate cell attachment, proliferation and differentiation (see Table 1). Form a surgical point of view, it is also desirable for the scaffold material to be easily manipulated into different shapes and sizes to allow in-situ treatment of individual patient bone defects [13,21–23].

Scaffolds and their breakdown products must above all be biocompatible. This requires scaffold materials to be nontoxic to cells, easily eliminated from the body and to elicit negligible immune response through their presence [11,24,25]. Controlled biodegradability is also an essential characteristic for a scaffold to achieve; if a scaffold degrades too quickly, mechanical failure could occur. This is particularly relevant in BTE, as an implanted scaffold is likely to undergo load-bearing and could fracture if unable to provide mechanical support whilst new bone is forming. Similarly, if a scaffold does not degrade sufficiently quickly an inflammatory response could be triggered towards the foreign material of the scaffold, impairing tissue regeneration [26].

Growth factors also have a significant role to play in successful bone tissue engineering scaffolds. The processes of new bone formation and extracellular matrix deposition are regulated by a range of growth factors and biomolecules. Bone morphogenic proteins (BMP) play a critical role in bone and cartilage development, and have the ability to trigger proliferation and differentiation of osteoprogenitor cells [27]. There are several examples of scaffolds that have successfully incorporated BMPs resulting in improved bone formation. However, risk of bone formation within soft tissues, or heterotopic ossification, is also associated with use of BMPs [28–32]. Vascular endothelial growth factor (VEGF) has also frequently been included in scaffolds, with desirable properties including the ability to enhance blood vessel formation and bone formation *in vivo* [33–35]. Transforming growth factor β (TGF β), platelet-derived growth factor (PDGF), insulin-like growth-factor 1 (IGF-1), and fibroblast growth factors (FGFs) provide further examples of growth factors that have been utilised in bone and cartilage tissue engineering [36,37].

The microarchitecture of scaffolds is also centrally important in encouraging cell viability and fostering tissue ingrowth. An interconnected pore structure, in the absence of an engineered blood supply, allows inwards diffusion of oxygen and nutrients and outwards diffusion of waste products from the scaffold. Porosity also supports cell migration into the scaffold and improves available surface area for cell-scaffold binding and interaction with surrounding tissues [38–40] (Fig. 1A and B). Individual pore size within the scaffold is also an important consideration. It has previously been shown that scaffold pore density and size significantly impact upon cellular growth and attachment [41,42]. As pore size decreases, the surface area of the scaffold increases. This increases the availability of scaffold ligands for cells to bind to and interact with. However, if pore sizes become too small, cells may struggle to migrate into the scaffold structure. Scaffolds must therefore be precisely engineered with parameters favourable to the cells and tissue that they will be exposed to. For example, it has

Table 1
Summary of desirable scaffold properties.

Scaffold Characteristics	Desirable Features
Biocompatibility	• Non-toxic breakdown products • Non-inflammatory scaffold components, avoiding immune rejection
Biodegradability	• Controlled scaffold degradation which can complement tissue ingrowth whilst maintaining sufficient support • Degradable by host enzymatic or biological processes • Allows invading host cells to produce their own extracellular matrix
Bioactivity	• Scaffold materials that can interact with and bind to host tissue • Osteoconductive and osteoinductive properties • Inclusion of biological cues and growth factors to stimulate cell ingrowth, attachment and differentiation
Scaffold Architecture	• Interconnected pores allowing diffusion and cell migration • Microporosity to present a large surface area for cell-scaffold interactions • Macroporosity to allow cell migration and invasion of vasculature • Pore size tailored to target tissue and cells • Sufficient porosity to facilitate cell ingrowth without weakening mechanical properties • Inbuilt vascular channels to enhance angiogenesis *in vivo*
Mechanical Properties	• Compressive, elastic and fatigue strength comparable to host tissue allowing cell mechanoregulation to occur and structural integrity to remain *in vivo* • Scaffold material that can be readily manipulated in the clinical environment to treat individual patient bone defects

Please cite this article in press as: G. Turnbull, et al., 3D bioactive composite scaffolds for bone tissue engineering, Bioactive Materials (2017), https://doi.org/10.1016/j.bioactmat.2017.10.001

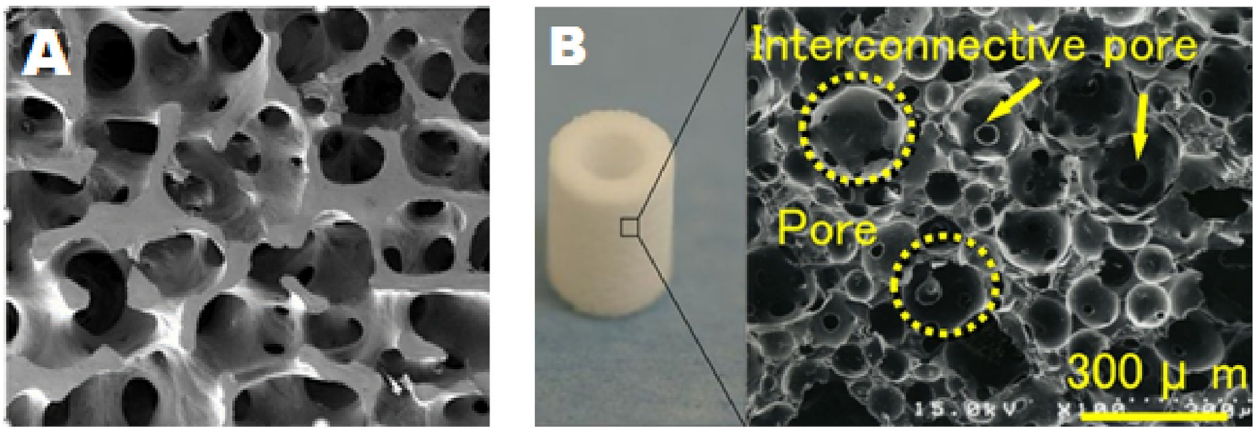

Fig. 1. (A) SEM image showing interconnected porous structure of human trabecular bone (B) Pores and interconnecting pores demonstrated in hydroxyapatite scaffold. Pores are circled; arrows indicate interconnecting pores which allow communication between pores. Adapted from Doi et al. [51].

been shown that scaffolds implanted *in vivo* with pore sizes close to 300 μm promote osteogenesis due to higher permeability and potential for vascularisation, whereas smaller pore sizes closer to 100 μm are more favourable for chondrogenesis [43–45]. Increased scaffold macroporosity has also been shown to improve angiogenesis *in vivo* [46], whilst a degree of microporosity (pores with diameters lower than 10 μm) can improve cell-scaffold interactions, resulting in osteogenic effects [47–49]. Scaffolds for BTE therefore need to contain a mixture of macropores allowing cell and osteon ingrowth *in vivo*, and micropores to encourage cell-scaffold ligand interactions [50].

In addition to pore size and overall porosity, mechanoregulatory effects are thought to be key in influencing bone tissue growth and cellular differentiation *in vivo*. If a scaffold is unable to replicate the mechanical forces transferred to cells in physiological conditions, cells may be stimulated to differentiate away from an osteogenic lineage towards an undesirable morphology [52–54]. Selecting scaffold materials with similar stiffness to native bone would therefore seem advantageous [55,56]. However, scaffold mechanical stiffness and porosity are directly conflicting physical properties, with mechanical strength inversely related to increasing scaffold porosity. In terms of load bearing, important scaffold mechanical properties include Young's modulus (also known as elastic modulus, a measure of the stiffness of a solid material), compressive strength (capacity of a scaffold to withstand loads tending to reduce size) and fatigue strength (the highest stress that a material can withstand for a given number of cycles without breaking) [11,57,58]. The ideal scaffold would have a compressive strength comparable to cortical bone, which along the long axis is approximately 100–230 MPa, with a Young's modulus close to 7–30 GPa and a tensile strength of 50–151 MPa [59–62]. Ideally this compressive strength would be complemented by a porosity between 60% and 90% and an average pore size of >150 μm [63,64].

Achieving a successful balance *in vivo* between the properties of a scaffold favourable to cellular function, cellular viability and mechanical integrity under load bearing therefore remains challenging [65,66].

3. Scaffold fabrication methods

A large variety of techniques have been used in the fabrication of 3D scaffolds, sometimes in combination. In general, it is difficult to create complex scaffold microarchitectures with precise control using conventional techniques. However, the integration into BTE of 3D printing using computer-aided design (CAD) modelling has greatly increased scaffold manufacture precision and repeatability, with control over scaffold macro- and microporosity possible. The advantages and disadvantages of conventional scaffold manufacturing methods and more recent 3D printing techniques will therefore be discussed and summarized in this section (see Table 2).

3.1. Conventional scaffold fabrication

Solvent casting/particulate leaching is a traditional method of scaffold manufacture that begins with dissolution of a polymer in an organic solvent (Fig. 2A). The technique uses porogens, substances that can be dispersed into a moulded structure and subsequently dissolved once the structure has set, resulting in the creation of pores. Porogens are added to the polymer solution to create a polymer-porogen network. The polymer is subsequently hardened as the solvent evaporates, with water then used to dissolve the porogen which is often a salt such as sodium chloride. A hardened polymer scaffold with a porous network is left behind, although it is difficult to control pore shape and pore interconnectivity of scaffolds produced by this method [67,68].

Gas foaming eliminates the use of solvents deployed in solvent casting/particulate leaching methods (Fig. 2B). This technique creates a porous structure through the nucleation and growth of gas bubbles dispersed throughout a polymer. Compression moulding is first used to create solid discs of a scaffold material, such as poly(lactic-*co*-glycolic acid), within a heated mould. Following this, the discs are saturated with carbon dioxide by exposure to high pressure CO_2 gas (5.5 MPa) for 72 h at room temperature, before solubility of the gas in the polymer is rapidly decreased by reducing CO_2 pressure to atmospheric levels (P^0CO_2). This causes the CO_2 gas to clump together, creating pores. Porosities of up to 93% and pore sizes of up to 100 mm can be obtained using this technique. However, it is difficult to control pore connectivity and pore sizes by gas foaming [7,68–70].

Freeze-drying begins with freezing of a polymer solution, resulting in the formation of solvent ice crystals surrounded by polymer aggregates (Fig. 2C). The surrounding pressure is then reduced via a vacuum, to a level lower than the equilibrium vapor pressure of the frozen solvent (P^0). The solvent is thus triggered to undergo sublimation directly into gas from the solid phase. When the solvent is completely sublimated, a dry polymer scaffold with an interconnected porous structure remains. Emulsification freeze drying can also be used as a primary scaffold fabrication method. The process begins by dissolving polymers/ceramics in a solvent

Please cite this article in press as: G. Turnbull, et al., 3D bioactive composite scaffolds for bone tissue engineering, Bioactive Materials (2017), https://doi.org/10.1016/j.bioactmat.2017.10.001

Table 2
Comparison of scaffold fabrication methods.

Manufacturing Method	Benefits	Potential Limitations
Solvent casting/ particulate leaching	• Relatively simple technique that allows creation of scaffolds with regular porosity, controlled composition and pore size.	• Use of organic solvents precludes cells and biomolecules being included directly in scaffolds • Can be difficult to control pore shape and interconnectivity • Limited thickness of structures and mechanical properties achievable
Gas Foaming	• Eliminates use of chemical solvents	• High pressures involved prohibits inclusion of cells and bioactive molecules directly into scaffolds • Temperature labile materials may be denatured during compression moulding step • Difficult to control pore sizes and ensure interconnectivity
Emulsification Freeze-Drying	• Does not require use of solid porogen	• Requires use of organic solvents • Small pore size and • Porosity often irregular • Long processing time
Phase Separation	• Eliminates leaching step of porogen • Can be combined with other techniques easily	• Small pore sizes limit use • Use of organic solvents inhibits use of bioactive molecules or cells during scaffold fabrication
Electrospinning	• Creates scaffold with large surface area for cell attachment • Simple and inexpensive technique	• Organic solvents may be required, which can be harmful to cells • Limited mechanical properties • Difficult to incorporate precise microarchitecture into constructs
3D Printing • SLA • SLS • FDM • Inkjet • Laser-assisted • Microvalve • Microextrusion	• Complex 3D shapes with high resolution, controlled pore size & morphology and controlled internal structures can be fabricated. Improved capacity to incorporate vascular structures into constructs • Depending on technique used, cells may be included in high concentration directly in scaffold materials	• Some techniques are limited by printable materials • Set up costs can be expensive for machinery

and then mixing with water, to obtain an emulsion. The mixture is poured into a mould and frozen before the two phases can separate. The frozen emulsion is then freeze-dried to remove the solvent and dispersed water, creating pores in a solidified scaffold [72].

Phase separation relies on changes in thermal energy to induce the de-mixing of a homogenous polymer/solvent solution. When a polymer such as PLLA is dissolved in a solvent, it can become thermodynamically unstable at a low temperature and spontaneously separate into a polymer-rich phase and a solvent-rich phase. Phase separation scaffold manufacture takes advantage of this phenomenon and begins with dissolution of a polymer in a high-boiling, low molecular weight solvent at an elevated temperature, typically around the melting point of the polymer, allowing formation of a homogenous melt-blend. The solution is then cast into a desired scaffold shape, and cooled in a controlled manner to induce phase separation and precipitation of the solution into a polymer-rich phase and a solvent-rich phase, creating a nanofibrous matrix (Fig. 2D). The solvent which is in the solvent-rich phase will then be removed through extraction, evaporation, or sublimation. This creates a porous scaffold, as removal of the solvent leaves pores behind in the polymer matrix.

Electrospinning is another popular scaffold fabrication technique with the ability to create nanofibrous interconnected porous scaffolds (Fig. 2E). This method uses an externally applied electric field to draw charged threads of polymer solutions or polymer melts as thin jets from a capillary tube towards a collector plate. Fibres in the micro- and nanometre range can be created and deposited sequentially to create a scaffold, with potential to include composite materials and biomolecules [73–76].

3.2. 3D printing techniques

The traditional methods of scaffold fabrication that have been discussed in brief so far generally offer limited control over pore size, geometry and interconnectivity. Overtime there has been an improvement in the ability to spatially control scaffold microarchitecture and spatial content as technologies such as 3D printing have emerged. In general, 3D printing fabricates objects via layer-by-layer processing of powder, liquid or solid material substrates. Starting from the bottom and building up, each newly formed layer is triggered to adhere to the previous layer, resulting in the creation of construct of gradually increasing size. The structure of a 3D printed object is dictated by a computer-aided design (CAD) model loaded onto a 3D printer. CAD models describe 3D objects in a series of cross-sectional layers, allowing 3D printers to physically reproduce models through an additive process.

Patient specific CAD models can be created by converting computed tomography (CT) or magnetic resonance imaging (MRI) of clinical defects into (CAD) models. Further software is then used to slice CAD models into G-code, which encodes 3D CAD models in a format that can control 3D printers. Parameters such as print speed, layer height, print head temperature and pressure can all be modified and optimised through G-code.

Several 3D printing methods have been adapted into BTE, with stereolithography (SLA) representing one of the earliest 3D printing techniques to have been developed (Fig. 3A).

It relies on the directed use of a laser to polymerize liquid UV-curable photopolymer resin layer-by-layer, resulting in a solidified 3D model. The UV laser can solidify the model's cross-section,

Please cite this article in press as: G. Turnbull, et al., 3D bioactive composite scaffolds for bone tissue engineering, Bioactive Materials (2017), https://doi.org/10.1016/j.bioactmat.2017.10.001

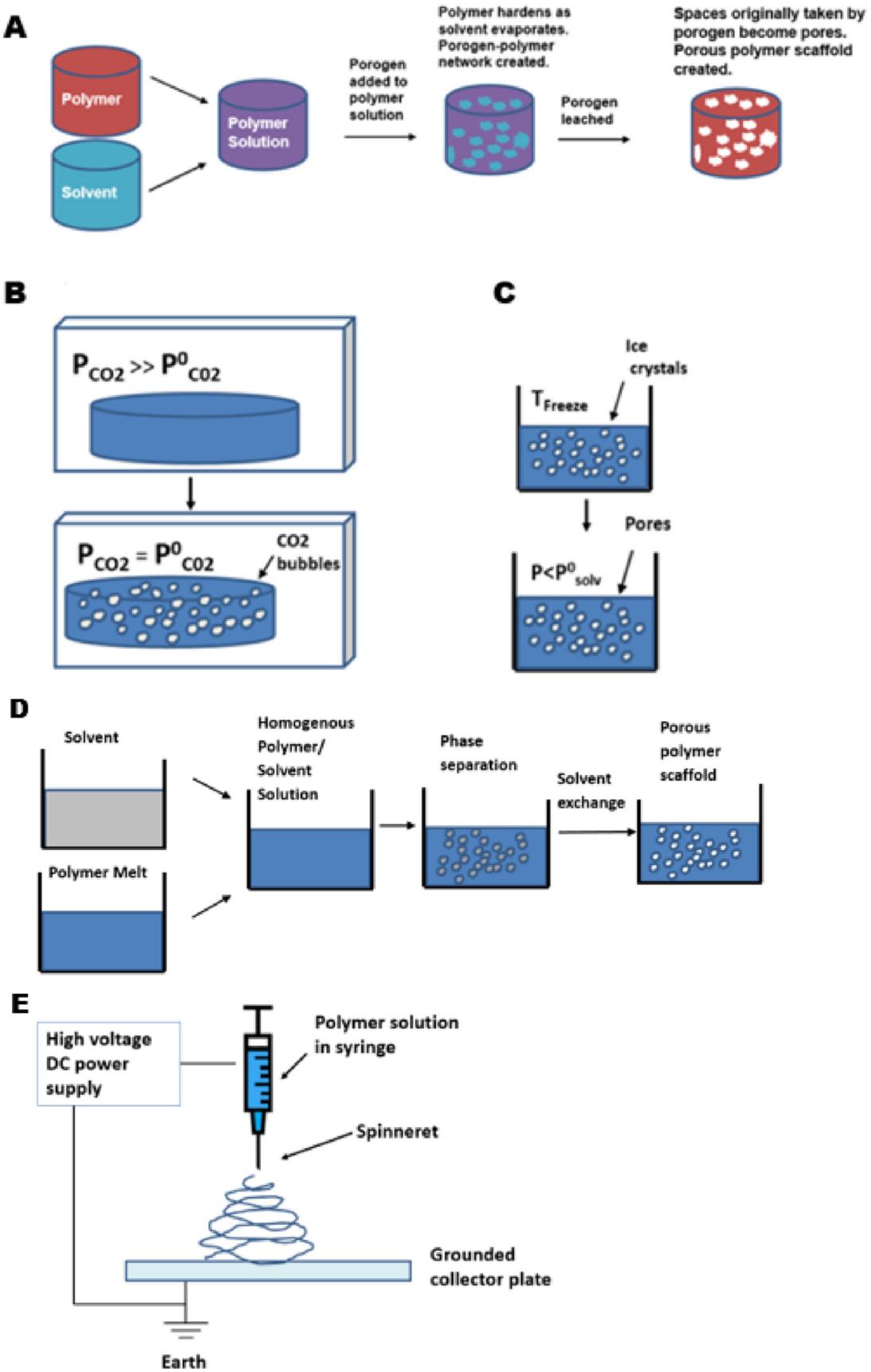

Fig. 2. Common scaffold fabrication techniques. (A) Solvent casting-particle leaching process (B) Gas foaming (C) Freeze-drying (D) Phase separation (E) Electrospinning. Adapted from Puppi et al. [71].

Please cite this article in press as: G. Turnbull, et al., 3D bioactive composite scaffolds for bone tissue engineering, Bioactive Materials (2017), https://doi.org/10.1016/j.bioactmat.2017.10.001

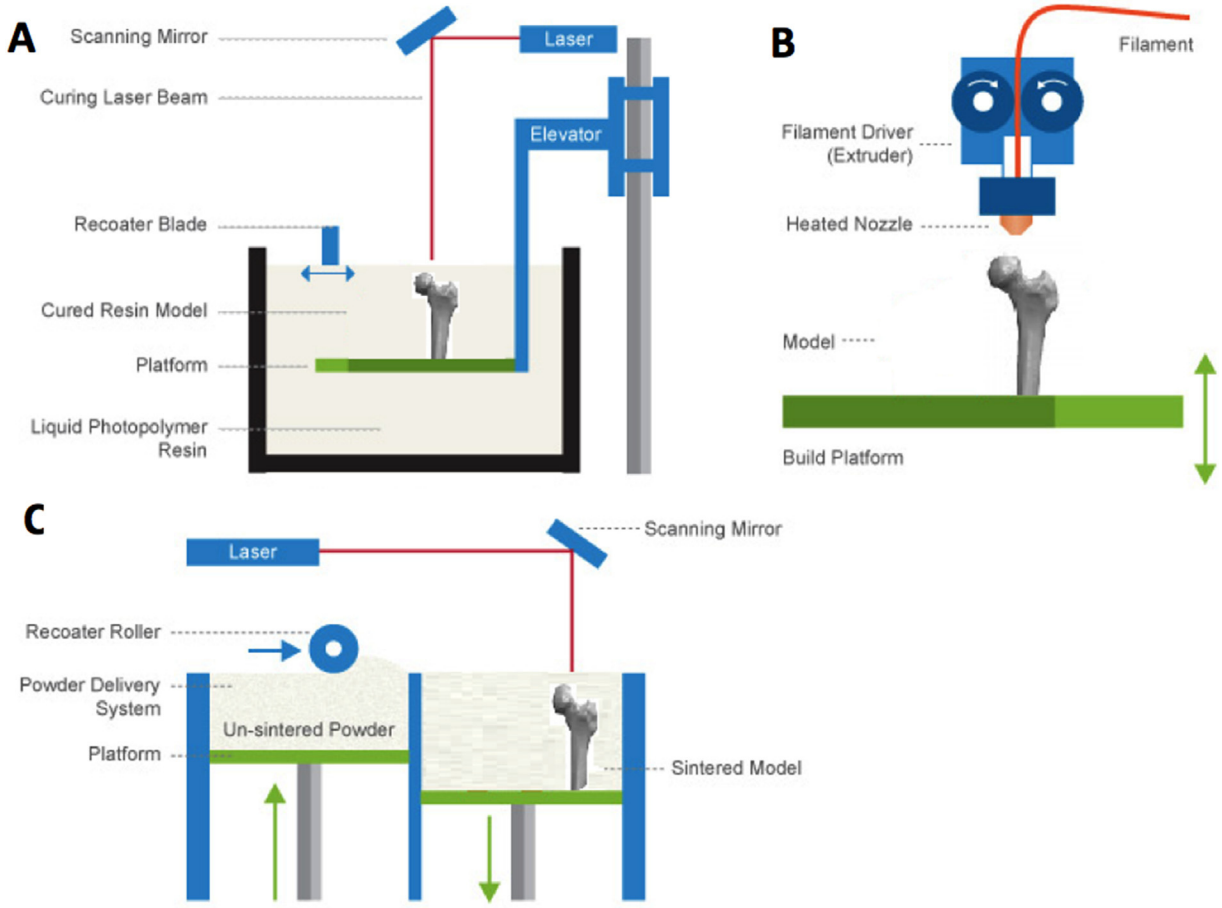

Fig. 3. Common 3D Printing Techniques. (A) Stereolithography (B) Fused deposition modelling (C) Selective laser sintering. Adapted from Jaster L [77].

leaving remaining areas in liquid form. After each cross-section, the print platform moves down, covering the solid polymer with another layer of resin for curing. Excess resin that has not been cured is then removed from the 3D structure, allowing rapid fabrication of a structure that can be cured further in an oven. Whilst SLA can quickly produce scaffolds with controlled architecture and micrometre-level resolution, there is a limited number of materials applicable to this costly technique [78].

Fused deposition modelling (FDM) uses a temperature controlled printhead to deposit thermoplastic material onto a platform in a layer by layer manner to build up a 3D construct (Fig. 3B). A thermoplastic filament is driven into a heated printhead, causing the filament to melt, allowing thin layers of a semi-molten polymer such as polycaprolactone to be precisely deposited sequentially. The molten filament cools in the air of the print environment, allowing filaments to fuse together rapidly to create a scaffold. FDM has been successfully adapted into BTE as method of producing synthetic scaffolds, although the elevated temperatures involved limit the inclusion of biomolecules and hydrogels [79,80].

Selective laser sintering (SLS) involves the use of a computer controlled laser beam to fuse layer-upon-layer of a powder, sintering the powder material together to build a solid 3D structure (Fig. 3C). Some success with this technique has been demonstrated, through the production of bioactive, composite scaffolds with similar mechanical properties to trabecular bone [81,82]. However, the elevated temperatures involved in the process limit the inclusion of cells and biomaterials directly into SLS scaffolds.

3.3. 3D bioprinting

As an emerging technology, 3D bioprinting offers a potential solution to help ease the burden of arthritis and other cause of bone defects within orthopaedics. Bioprinting can be used to deposit living cells, extracellular matrices and other biomaterials in user-defined patterns to build complex tissue constructs “from the bottom up.” The potential to create inherent vascular structures is also improved by bioprinting, as internal channels containing vascular cells can be printed into constructs, fostering the ingrowth of blood vessels *in vivo*. By contrast, the conventional tissue engineering method of seeding cells onto a pre-fabricated scaffold does not allow for precise 3D placement of cells or biological content, limiting capacity to create complex hierarchical tissue constructs [83,84].

The process of bioprinting typically begins with the selection of cells and biomaterials for inclusion in bioprinted constructs (Fig. 4). Cells for printing can be sourced from tissue biopsies, blood samples and from other sources, and expanded in number through culture to maximise cell density on bioprinting. The additional step of 3D cell culture may also be performed to creating aggregates of cells for printing. Cell aggregates or spheroids have superior intercellular communication and extracellular matrix development when compared to cells grown in 2D culture, potentially accelerating the growth of printed constructs towards functional tissue after bioprinting [85]. Mesenchymal stem cell spheroids also exhibit enhanced *in vitro* and *in vivo* osteoregenerative potential compared to MSCs cultured in monolayer [86,87].

Please cite this article in press as: G. Turnbull, et al., 3D bioactive composite scaffolds for bone tissue engineering, Bioactive Materials (2017), https://doi.org/10.1016/j.bioactmat.2017.10.001

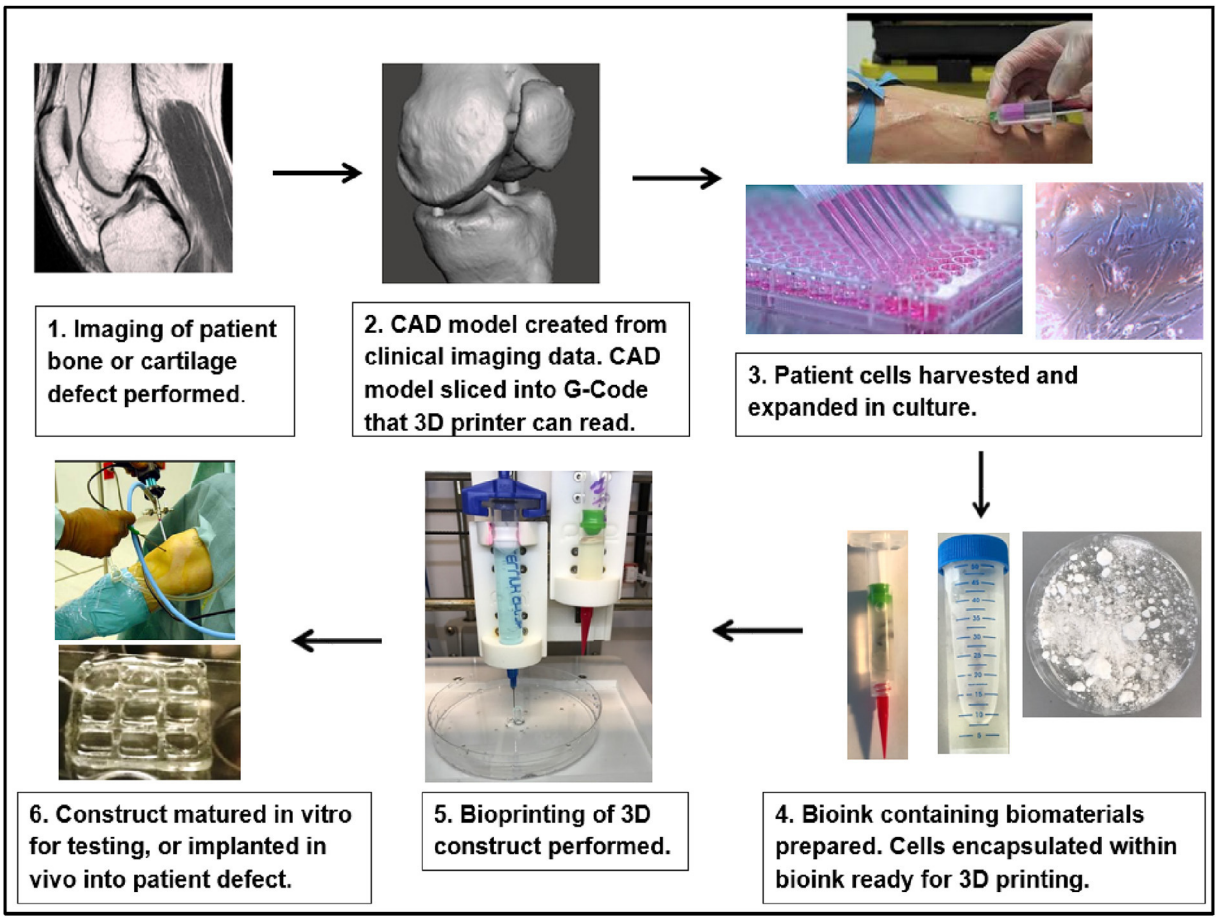

Fig. 4. Summary of bioprinting process.

Following culture, cells and selected biomaterials such as hydroxyapatite are encapsulated in a delivery medium, or bioink. Print cartridges containing bioink are then loaded into a 3D bioprinter, which dispenses the bioink in a pre-determined 3D geometry according to a CAD model. Bioprinters often have multiple print nozzles, allowing combinations of cells and biomaterials to be included within a printed construct. A high degree of spatial control can therefore be achieved over construct architecture and content [88,89]. Following printing the construct can be directly implanted into a patient, or alternatively matured first *in vitro*. Biologically active culture environments known as bioreactors are available to help direct and support cell growth towards specific tissue types.

3.4. 3D bioprinting techniques

Commonly used bioprinting techniques include inkjet, laser-assisted, microvalve and extrusion bioprinting.

Inkjet bioprinting (or drop-on-demand bioprinting) uses thermal or acoustic forces to eject droplets from a pint head nozzle (Fig. 5A). Thermal inkjet printers use heat to generate a pressure pulse within a print head for a brief period, causing ejection of a droplet of bioink. Other systems rely on piezoelectric crystals, which become mechanically stressed by the application of a voltage and as a result change shape. This generates an acoustic wave which in turn creates sufficient pressure to eject droplets from a nozzle. As a technology adapted form desktop inkjet printers, benefits include low cost, wide availability and high print speed. However, limitations include frequent nozzle clogging, risk of exposing cells and materials to thermal and mechanical stress and nonuniform droplet size. The liquid droplet deposited is also of low viscosity, relying on further gelation or crosslinking to create a solid structure [90–92].

Laser-assisted bioprinting (LAB) systems avoid the use of a nozzle; instead they rely on a pulsed laser beam to generate a high-pressure bubble, which in turn propels cell-containing materials toward a collector substrate from an initial print material “ribbon” (Fig. 5B). Recently Keriquel et al. used LAB to print mesenchymal stromal cells, associated with collagen and nano-hydroxyapatite, directly in situ onto a mouse cranial defect to aid bone regeneration [93]. Some limitations of LAB include potential heat-induced damage to cells, difficulty of creating 3D structures, high system costs and the time-consuming nature of creating ribbons with high cell and biomaterial concentrations [94].

Microvalve bioprinting is a droplet-based system where fluids under a constant pneumatic pressure are dispensed from cartridge tips by opening and closing a small valve (Fig. 5C). The valve in question can be controlled mechanically, electrically or magnetically. Microvalve systems can print cells including MSCs with high viability and functionality, with deposition of other biomaterials also possible such as collagen and bone morphogenic protein [95–97].

Extrusion bioprinters deposit continuous filaments of materials rather than individual droplets (Fig. 5D). Pneumatic or mechanical pressure is applied to a syringe to cause bioink extrusion through a nozzle. A significant advantage of this approach is the ability to deposit very high cell densities, with some studies manging to

Please cite this article in press as: G. Turnbull, et al., 3D bioactive composite scaffolds for bone tissue engineering, Bioactive Materials (2017), https://doi.org/10.1016/j.bioactmat.2017.10.001

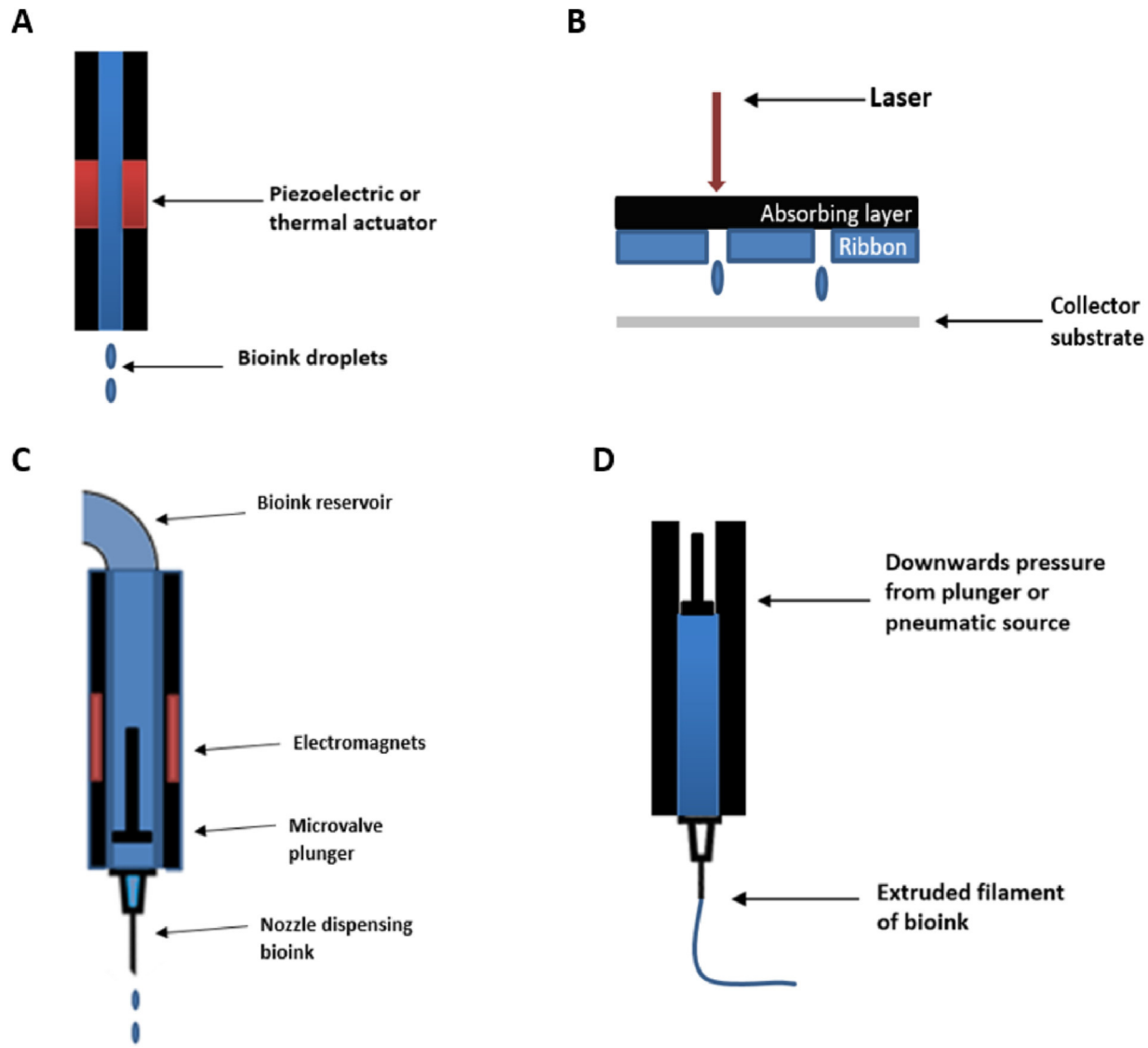

Fig. 5. Common bioprinting techniques: (A) Inkjet, (B) Laser-assisted, (C) Microvalve, and (D) Extrusion bioprinting.

purely print cells, for example as filaments of cartilage [98]. A broad range of bioinks have been successfully extrusion bioprintined, including tissue spheroids, tissue strands, cell pellets, decellularized matrix components and cell-laden hydrogels. Potential limitations and challenges include achieving high print resolution, shear stress effect on cells within print nozzles and development of printable bioinks [99].

4. Materials used within bone tissue engineering

Materials that have been utilised within bone repair and regeneration include metals, ceramics, polymers, hydrogels and related composites. Groups of materials will be reviewed in the following corresponding sections and summarized (see Table 3).

4.1. Metals

Metal alloys such as cobalt-chromium, zirconium, titanium and stainless steel have excellent biocompatibility and strength [21,100]. As such, they are commonly used in joint replacement and fracture fixation implants to offer support for healing bone [101]. However, a lack of biodegradability makes them less suited to BTE where the aim is for native tissue to resorb and replace implanted constructs. Additional surgery is often required to remove metallic implants, particularly when they are used in paediatric patients who have not reached skeletal maturity [102]. The superior elastic modulus of metals relative to bone can also predispose to stress shielding occurring. In this phenomena, mechanical bypass of loads occurs in the bone surrounding implants, leading to bone resorption and increased fracture risk [103]. Despite these limitations, some success has been achieved through creation of composite metal scaffolds. Strontium (Sr) was combined via freeze-drying with hydroxyapatite (HA) and chitosan (CS) by Lei et al. to create composite nanohybrid scaffolds. The presence of SrHA nanocrystals in the scaffolds was found to significantly enhance cell proliferation and osteogenic differentiation of human bone marrow mesenchymal stem cells (hBMSCs) [104]. Hierarchical structure was developed by Wu et al. on a microporous nickel-titanium composite (NiTi) scaffold by treating the surface with sodium hydroxide in a hydrothermal reaction. This led to the creation of a nanostructured, microporous exposed surface on an already microporous NiTi scaffold. Improved surface hydrophilicity, deposition of

Please cite this article in press as: G. Turnbull, et al., 3D bioactive composite scaffolds for bone tissue engineering, Bioactive Materials (2017), https://doi.org/10.1016/j.bioactmat.2017.10.001

Table 3
Comparison of scaffold materials.

Manufacturing Material	Benefits	Potential Limitations
Hydrogels	• High water content/growth media inclusion allows for cell encapsulation and growth • Mechanical properties can be modified through crosslinking • Controlled drug/growth factor release possible • Ease of patterning via 3D printing to mimic tissue microarchitectures	• Mechanical properties limit use in load bearing constructs • Optimising printing conditions for individual hydrogels can be time consuming • Physical manipulation of constructs can be difficult • Loading evenly with cells can be challenging
Polymers	• Natural polymers can be derived from extracellular matrix, ensuring high biocompatibility and low toxicity • Biodegradable • Often contain biofunctional molecules on their surface • Synthetic polymers offer improved control over physical properties	• Natural and synthetic polymers generally lack mechanical properties for load bearing • Pathological impurities such as endotoxin may be present in natural polymers • Synthetic polymers are often hydrophobic and lack cell recognition sites
Ceramics	• Osteoconductive and osteoinductive properties allow strong integration with host tissue • Similar composition to host bone mineral content • Can be delivered as granules, paste or in an injectable format	• Hard and brittle when used alone • May display inappropriate degradation/resorption rates, with decline in mechanical properties as a result
Bioactive glasses	• Osteoconductive, osteoinductive properties • Adapted into clinical prosthesis already	• Inherent brittleness • Difficult to tune resorption rate • Manipulation of constructs into 3D shapes to treat specific defects challenging • Potential for release of toxic metal ions
Metals	• Biocompatible • Superior strength • Superior mechanical properties can be advantageous in situations where slow bone growth likely	• Superior modulus can lead to stress-shielding • Poor biodegradability may result in further surgery/impairment of tissue ingrowth • Secondary release of metal ions may cause local and distal toxicity

hydroxyapatite, accelerated cell attachment and proliferation was seen *in vitro* as a result [105]. Titanium based scaffolds were also fabricated by Chen et al., who sintered microporous Ti spheres and Ti powder. Maximum porosity of 50% was achieved, with scaffold compressive strength reported to be up to 109 MPa. *In vitro*, the microporosity of the scaffolds helped promote attachment and growth of mesenchymal stem cells (MSCs) [106].

Chou et al. utilised 3D inkjet printing to create iron-magnesium (FeMg) composite scaffolds (Fig. 6). Following 3D printing, the FeMg constructs were found to have an open, porous structure with similar tensile mechanical properties to cancellous bone. *In vitro* analysis found good cell viability on exposure to the scaffolds, with cell infiltration into pores also seen [107].

Selective laser sintering (SLS) is another 3D printing method that has used to successfully produce composite metallic scaffolds. Layer-upon-layer of a titanium powder and silica sol slurry were sintered by Liu et al. to produce composite titanium-silica scaffolds with complex geometry [108]. Scaffold compressive strength was increased by heat treatment post-fabrication, with significant human sarcoma cell (MG63) proliferation seen over 7 days. However, the significant heat involved in manufacturing metallic scaffolds using SLS and other methods limits the potential to directly include biomolecules. Attempts have therefore been made to coat the surface of metallic scaffolds with bioactive ceramics such as HA and calcium silicate [75].

Stainless steel, titanium and cobalt chromium alloys have all been combined using SLS and secondarily modified using phosphonic acid. This process results in the creation of a composite scaffold with a biocompatible phosphonic layer on the scaffold surface. Biomolecules and drugs including paracetamol and antibiotics have then been successfully deposited on scaffold phosphonic acid surfaces, improving bioactivity [109,110].

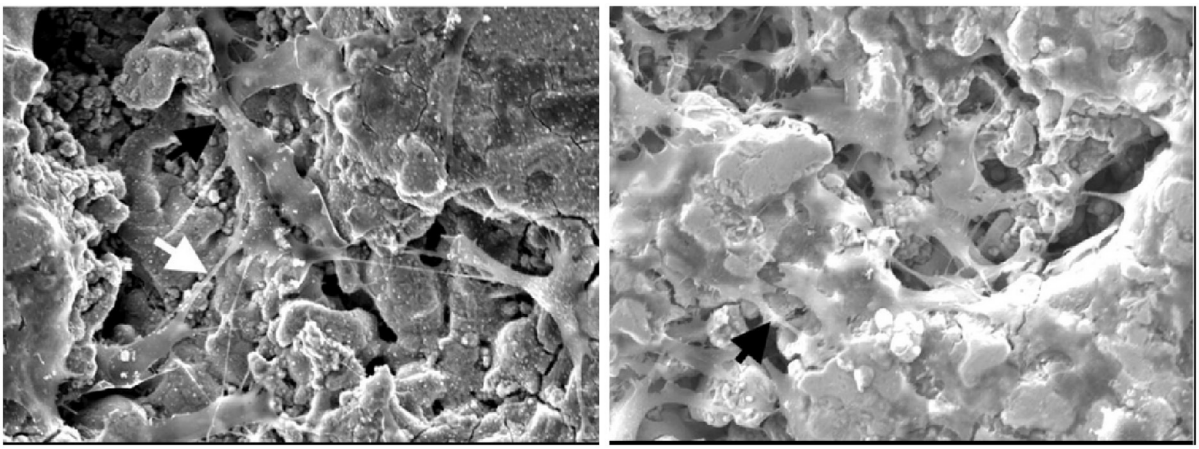

Fig. 6. SEM images of MC3T3 cells on the surface of 3D-printed Fe–Mg scaffold. White arrow denotes a cell–cell junction after one day; black arrows denote cellular extensions to pore walls after 3 days [107].

Please cite this article in press as: G. Turnbull, et al., 3D bioactive composite scaffolds for bone tissue engineering, Bioactive Materials (2017), https://doi.org/10.1016/j.bioactmat.2017.10.001

4.2. Bioceramics

Bioceramics, including ceramic composites, amorphous glasses and crystalline ceramics, show great promise within BTE as mechanically strong materials, with favourable bioactivity [111]. Further material properties can include corrosion resistance, resistance to compression, and a weakness to shearing and tensile forces, resulting in brittleness [112].

Perhaps the most frequently utilised crystalline bioceramics in BTE are calcium phosphates (CaPs), partly due to their prevalence in native bone tissue [113]. Hydroxyapatite (HA), tricalcium phosphate (TCP) and a composite of both substances known as biphasic calcium phosphate (BCP) have all been adapted in BTE scaffolds. Cell mediated degradation of these ceramics *in vivo* produces calcium and phosphate ions, which promote new bone formation through osteoinduction [114,115]. CaPs also share a large degree of similarity in structure and chemical composition to the mineral content of native bone. This allows CaP constructs to provide a biocompatible, osteoconductive interface capable of facilitating integration with host tissue without formation of scar tissue [116,117].

HA has excellent properties for BTE, including biocompatibility, controlled degradation and lack of cytotoxicity. HA also has a strong compositional similarity to bone, with proven osteoinductive and osteoconductive properties allowing HA constructs to form a strong bond with surrounding bone [118,119]. HA can also stimulate endogenous expression of osteogenic growth factors such as bone morphogenetic protein (BMP) and enhance alkaline phosphatase (ALP) activity in mesenchymal stem cells (MSCs). This is particularly important as ALP activity is pivotal in the early mineralization process associated with bone formation [120–122]. However, in common with other ceramics, HA has properties of being hard and brittle, which limits HA construct load-bearing and manipulation into shapes specific to individual bone defects. HA also has a slow degradation rate *in vivo* which can predispose to mechanical failure at implant sites [114,119]. To overcome these mechanical limitations, HA has been combined with several naturally occurring and synthetic polymers to create composite scaffolds, as will be discussed later [17,30,123–129].

Dicalcium phosphate (DCP) has been used much less frequently than HA within BTE, due to weak, brittle mechanical properties and a high *in vivo* resorption rate [115]. Although DCP/synthetic polymer composites have been produced resulting in improved mechanical properties, success has been limited in comparison to HA and tricalcium phosphate based scaffolds with degradation rates difficult to control [130–132].

Tricalcium phosphate (TCP) is another popular bioceramic that has been adapted into BTE, with commercial products already available. Beta-TCP (β-TCP) beads have been combined with alginate gels to create injectable 3D scaffolds, capable of supporting *in vivo* osteogenic differentiation of MSCs [133] (Fig. 7). The β-TCP allotrope has also been combined with type I collagen to produce porous scaffolds with equivalent clinical performance to autografts in a spinal fusion model [134]. Nanocomposite TCP/collagen scaffold performance has also been compared favourably to HA scaffolds *in vivo*. Histologically advanced bone formation was found after 45 days in TCP/collagen scaffolds that had been implanted in a rabbit segmental femur bone defect, with superior results found

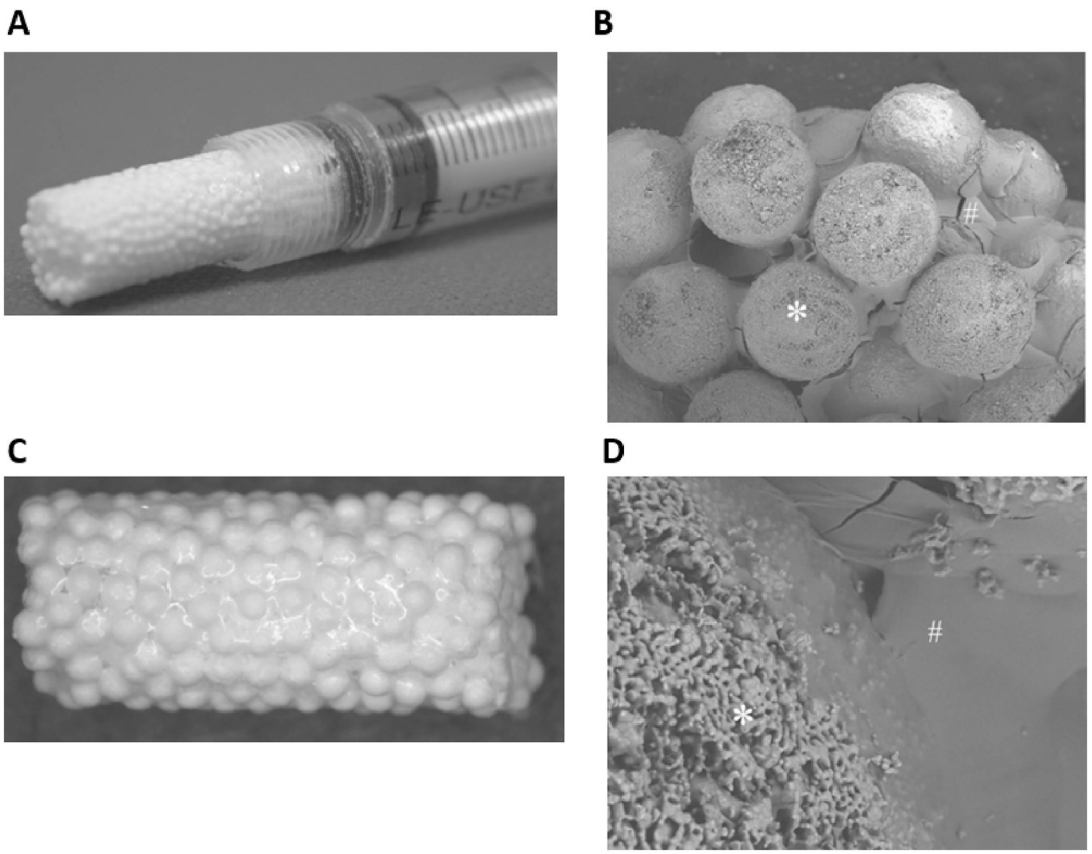

Fig. 7. Photograph of injectable 3D-formed composite of β-TCP beads and alginate capable of triggering MSC osteogenic differentiation *in vivo*. (A) and light microscope photograph of the composite (B). SEM photographs of the composite (C) and surface of the composite (D). The composite was composed of β-TCP beads (*) and alginate (#). Adapted from Matsuno et al. [133].

Please cite this article in press as: G. Turnbull, et al., 3D bioactive composite scaffolds for bone tissue engineering, Bioactive Materials (2017), https://doi.org/10.1016/j.bioactmat.2017.10.001

compared to implanted HA scaffolds [135].

Tarafder and Bose 3D printed a TCP scaffold, with polycaprolactone (PCL) and alendronic acid coating (AL) of the scaffold performed post-fabrication [136]. It was found that *in vivo* local AL delivery from PCL-coated TCP scaffolds led to increased early bone formation compared to bare TCP and PCL coated TCP scaffolds.

A further study 3D printed a composite 3D TCP scaffold, with magnesium oxide and silicon dioxide doping incorporated into the scaffold design [137]. Significantly higher bone and blood vessel formation was seen in Mg and Si containing scaffolds compared to bare TCP controls *in vivo*. However, the hard material based scaffold lacked a soft niche to support neo-angiogenesis *in vivo*. This ultimately impaired integration of the construct into host rat tissue. Overall the results suggest that magnesium and silicon incorporated into 3DP TCP scaffolds could have potential for future bone tissue repair and regeneration.

Rakovsky et al. employed salt leaching to create a composite β-TCP and polylactic acid (PLA) scaffold. Composite scaffolds were produced with 50% porosity and a large pore size (300–420 μm), potentially favourable to BTE. Further analysis found a compressive strength of ~5 MPa, comparable to trabecular bone, although *in vivo* cellular response was not assessed [138].

Silica-based bioceramic composites have also received significant attention within BTE. The ionic breakdown products of Si-containing scaffolds have the attractive property of being osteoconductive [75,139–142]. Feng et al. created a calcium silicate matrix via SLS as a starting point and incorporated HA whiskers to improve scaffold strength. It was found that compressive strength of scaffolds with ~45% porosity increased from 15 MPa to 27 MPa with the addition of 20 wt% HA whiskers. Furthermore, scaffold degradation rate decreased as HA whisker content increased. Mineralization of apatite occurred on the scaffold surfaces *in vitro*, with osteoblast-like MG-63 cells seen to infiltrate the scaffolds and proliferate with increasing culture time [143] (Fig. 8).

Dai et al. sintered $CaCO_3$ and SiO_2 to create a novel, porous β-dicalcium silicate (β-Ca_2SiO_4) scaffold. Mechanical analysis found maximum scaffold compressive strength of 28.1 MPa and porosity of up to 71%. Good biocompatibility was also evident, with MG-63 cells and MSCs proliferating on the scaffolds *in vitro*, with surface apatite formation also seen. *In vivo* analysis in mice found bone tissue generation in the scaffolds after 9 weeks, suggesting osteoinductive scaffold properties [144].

Feng et al. utilised 3D printing in the form of SLS to fabricate composite akermanite ($Ca_2MgSi_2O_7$) scaffolds reinforced with nano-titania particles. They reported a maximum compressive strength of 23 MPa for scaffolds with ~58% porosity after addition of 5 wt% nano-titania. Fracture toughness, hardness, compressive strength and stiffness were significantly increased with increasing nano-TiO_2 content from 0 to 5 wt%. Bone-like apatite was formed on the scaffolds *in vitro*, with MG-63 cells adhering to the scaffolds and proliferating well [145].

Properties such as corrosion resistance, biocompatibility and stiffness have led to widespread use of bioceramics within clinical orthopaedics. Thousands of patients already benefit from ceramic joint replacement components, and ceramic powders and granules used for filling bone defects [146,147]. However, within the context of BTE, ceramic scaffolds can be prone to brittleness. In common with metallic based scaffolds, they also have degradation rates that can be difficult to finely control. Increasing attention has therefore been applied to developing ceramic/polymer composite scaffolds, which will also subsequently be reviewed.

4.3. Bioactive glasses

Bioactive glasses (BGs) represent a subgroup of ceramic materials that have been extensively researched within the field of BTE. BGs can be considered as surface reactive glass-ceramic biomaterials with amorphous structures. This group of materials was first pioneered by Professor Larry Hench at the University of Florida in the late 1960s, as he sought to find a bone substitute materials to treat Vietnam War veterans [148]. The field of BGs began with development of Na2O–CaO–SiO2–P2O5 glasses, the most bioactive of which is known as 45S5 Bioglass®. Once implanted, BG dissolution helps create a biologically active layer of HA on the surface of the glass, which in turn interacts with the collagen fibrils in host bone to create a strong bond. In fact, the bond formed with bone is so strong that BG often cannot be removed with breaking the surrounding bone [149]. Dissolution products such as calcium and silica ions are also thought to stimulate host cells to produce bone matrix [18,150]. Within bone, BGs can act as osteoconductive materials, although evidence for osteoinductive properties is more limited [151,152]. The interconnected porous structure of BGs is similar to trabecular bone, providing cells with a temporary template to regenerate into [153].

The two main manufacturing processes used to make glass are melt-quenching and the sol-gel route. Melt-quenching involves melting oxides together at elevated temperature, before quenching them together in water or a graphite mould; 45S5 BG and other commercial bioactive glasses are made by this method. Components of different size and shape can be produced through this method, including prosthetic middle ear ossicles [154].

Clinical applications of BGs have so far included prostheses used in the fields of orthopaedic and maxillofacial surgery; granules and particulates have also been used in place of conventional bone

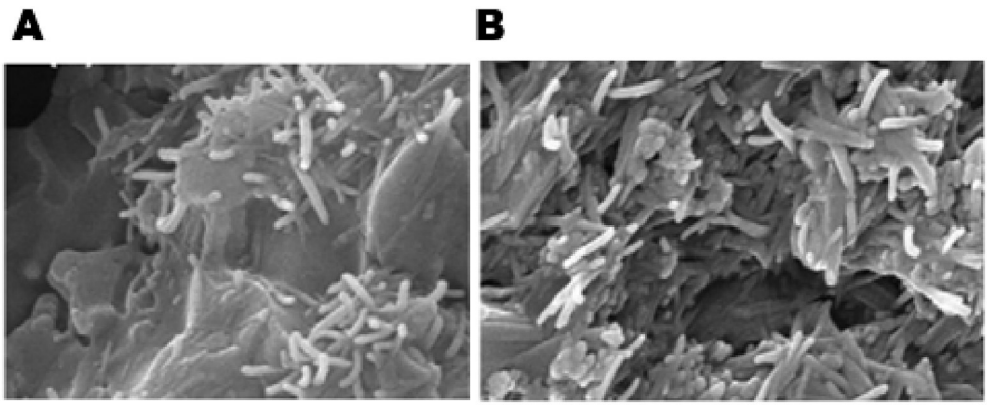

Fig. 8. SEM images of (A) 10% and (B) 30% HA whiskers present in calcium silicate matrix. Adapted from Feng et al. [143].

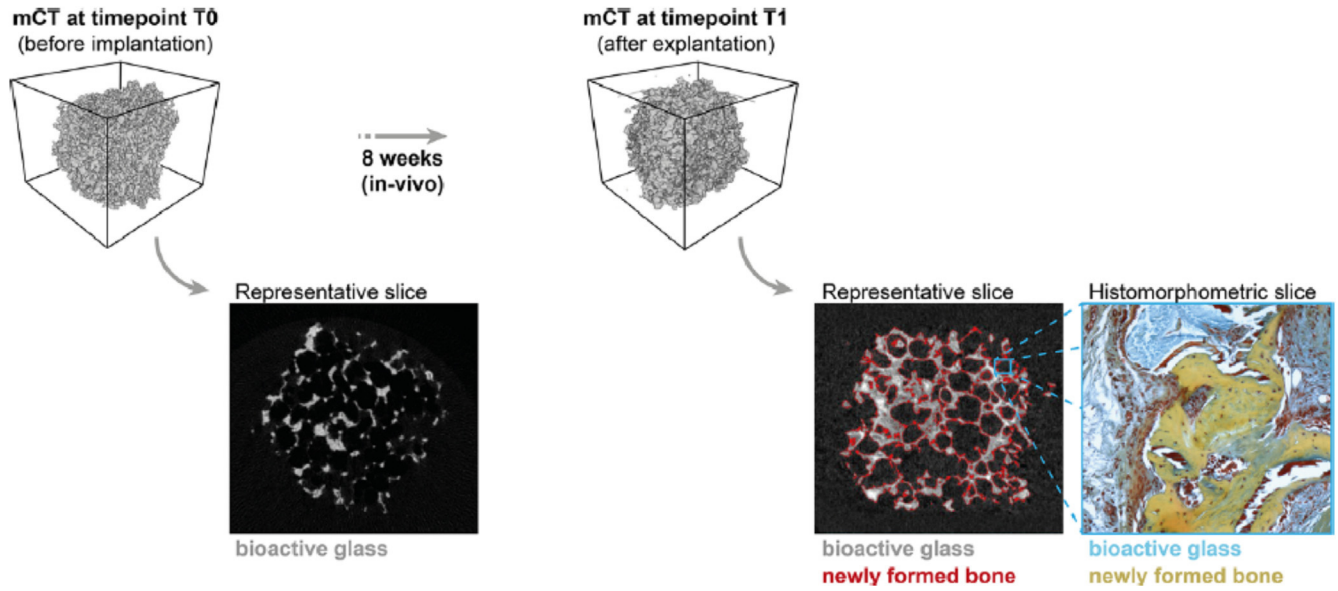

Fig. 9. Micro-CT and histomorphic analysis showing new bone formation in polymer-coated BG scaffolds implanted in mice for 8 weeks [166].

grafting to aid treatment of chronic osteomyelitis, soft tissue defects and wounds [18,155,156]. More than a million patients within orthopaedics and maxillofacial surgery have now had bone defects repaired with 45S5 Bioglass® [148]. Within the field of spinal surgery, a study comparing 45S5 Bioglass® versus iliac crest autograft for spinal fusion in adolescent idiopathic scoliosis (AIS) demonstrated positive results in a series of 88 patients. 45S5 BG® was found to be as effective as iliac crest graft, the current gold standard for spinal fusion, in terms of ability to achieve deformity correction and spinal fusion in AIS patients. Additionally, the morbidity of harvesting an iliac crest graft was avoided in BG patients, who also experienced fewer complications [157].

Whilst properties such as bioactivity and osteoconductivity are attractive, the inherent brittle nature of bioactive glasses represents a major potential limitation in their clinical application [155,158]. Through incorporation of biodegradable polymers to create BG composites, properties such as porosity, degradation rate and elastic modulus can be improved [159,160].

Vergnol et al. investigated the potential of a polylactic acid (PLLA)-bioactive glass composite for bone fixation devices. PLLA has previously been reported to require up to 4 years to fully degrade in humans and lacks osteointegration ability [161]. The *in vivo* behaviour of PLLA-HA composites has already been investigated, with osteointegration found to be significantly improved in PLLA-HA composites compared to pure PLLA structures [162–165]. Vergnol et al. therefore attempted to characterise the performance of 45S5 BG® -PLLA composites *in vitro* and *in vivo*. Composites containing increasing 45S5 BG® content with PLLA were manufactured by injection moulding and tested for up to 56 days in simulated body fluid (SBF). Whilst formation of a mineralised or HA layer was not seen on the surface of PLLA polymer, crystallisation of HA and calcite was evident on composite 45S5 BG® -PLLA scaffolds on X-ray diffraction analysis. Larger 45S5 BG® content, especially 30–50%, led to rapid HA crystallisation on the surface of composite scaffolds. However, degradation of composites containing 50% 45S5 BG® occurred rapidly within 7 days *in vitro*. Therefore, it was concluded that composites with 30% 45S5 BG® seemed to exhibit the best balance between bioactivity and stability at least during the first weeks of immersion in contact with SBF. *In vivo* analysis of the 30% 45S5 BG® -PLLA composite within rabbits also found strong osseointegration a month after implantation.

Westhauser et al. investigated the osteoinductive properties of different polymer coated 3D-45S5 BG® scaffolds seeded with human MSCs (hMSCs) *in vivo* [166]. 45S5 BG® scaffolds were dip-coated with either gelatin, cross-linked gelatin, or poly(3-hydroxybutyrate-*co*-3-hydroxyvalerate). After seeding with hMSCs, the scaffolds were implanted into immunodeficient mice. Histomorphometry and micro-computed tomography (micro-CT) was then performed after 8 weeks (Fig. 9). Although bone formation was detected in all scaffolds, gelatin-coated 45S5 BG® scaffolds performed the best overall with further studies required to fully evaluate their potential for BTE on a larger scale.

Murphy et al. utilised 3D extrusion bioprinting to create a composite polycaprolactone (PCL)/BG scaffold containing human adipose-derived stem cells (ASCs). Borate glass and PCL were initially dissolved in organic solvent to create a paste with printable viscosity. ASCs suspended in Matrigel were then co-printed via a second syringe as droplets into the PCL-BG scaffold. Degradation of the scaffolds in SBF was analysed, with 23.2 ± 4% weight loss due to controlled BG dissolution found at 14 days. Cell viability after 24 h was 70 ± 10% and after 7 days was 58 ± 11%. Scaffold pore sizes ranged from 100 to 300 μm, making it ideally suited for BTE. Bioactivity of the BG component was also seen, with formation of HA crystals witnessed on the scaffold surface. This study therefore demonstrated the potential for solvent-based 3D bioprinting to fabricate a scaffold containing cells and BG-polymer composites for BTE applications [167].

Baino et al. utilised a sponge template method involving sintering to fabricate a silicate-based glass-ceramic scaffold. Their intention was to create a scaffold capable of repairing large defects in load-bearing bones. Total scaffold porosity was 56%, with pore sizes ranging from 100 to 500 μm on micro-CT analysis. When tested under compression, the scaffolds had an elastic modulus of 380 MPa and a compressive strength of 18 MPa [168].

Eqtesadi et al. utilised the 3D printing technique of robocasting to fabricate 13–93 BG scaffolds with a pore size of ~230 μm and 51% overall porosity. The scaffolds unfortunately showed brittle characteristics with a compressive strength of 86 MPa and a modulus of rupture of 15 MPa. PCL was therefore added to the BG to create composite scaffolds, as an attempt to address the brittleness and

Please cite this article in press as: G. Turnbull, et al., 3D bioactive composite scaffolds for bone tissue engineering, Bioactive Materials (2017), https://doi.org/10.1016/j.bioactmat.2017.10.001

flexural strength of scaffolds. Whilst compressive strength of the scaffolds was maintained, brittleness was significantly reduced as 13–93/PCL composite scaffolds were able to survive large stains [169].

BGs have also been used to improve the surface bioactivity of 3D printed β-TCP scaffolds, with promising results found. Zhang et al. spin-coated mesoporous (pores with diameters between 2 and 50 nm) bioactive glass (MBG) nanoparticles onto porous β-TCP scaffolds to create a 100 nm layer of MBG on scaffold surfaces [170]. This resulted in a hierarchical pore structure with both MBG mesopores and BG macropores present in the scaffold. The compressive strength and mineralization of MBG-β-TCP scaffolds were also significantly enhanced as compared to β-TCP scaffolds without the MBG nanolayer. Culture of human umbilical vein endothelial cells (HUVECs) found increased cell attachment, viability and angiogenic gene expression compared with conventional BG-modified β-TCP (BG-β-TCP) and pure β-TCP scaffolds. Furthermore, MBG-β-TCP scaffolds significantly enhanced the formation of new bone *in vivo* as compared to BG-β-TCP and β-TCP scaffolds.

The majority of drugs used in clinical practice are measured on the nanometre scale and can therefore be introduced into mesoporous bioglass structures, potentially improving bioactivity and drug delivery [171]. Jiang et al. coated mesoporous BG scaffolds with amides, with subsequent gentamicin loading onto the scaffold mesoporous surface achieved. As a result, higher gentamicin loading and longer drug release were achieved *in vitro* compared to BG scaffolds that had not undergone amination. *In vitro* bioactivity was also improved, with increased formation of surface hydroxyapatite found after soaking in simulated body fluid for 3 days (Fig. 10) [172]. MBGs have been utilised by several other studies to create composite scaffolds with increased bioactivity [170,173–175].

BG composites have also been used as injectable cements in some studies, with antibiotic [176], natural polymer [177] and synthetic polymer [178] composites found to be cell friendly and capable of treating *in vivo* bone and cartilage defects. Zhang et al. prepared a strontium-doped, borate bioactive glass (BBG)-chitosan composite cement and evaluated *in vitro* and *in vivo* performance [179]. The Sr-BBG cement showed the valuable ability to set in situ (initial setting time = 11.6 ± 1.2 min) and a compressive strength of 19 ± 1 MPa. The Sr-BBG cement was also found to enhance the proliferation and osteogenic differentiation of hBMSCs *in vitro* when compared to a similar cement composed of chitosan-bonded BBG particles without Sr. The cement was then injected into rabbit femoral condyle defects, with new bone formation supported by the Sr-BBG cement. It would therefore appear to be a promising treatment for treating irregularly shaped bone defects through minimally invasive surgery.

4.4. Polymers

Use of natural polymers in scaffolds has attracted great interest within BTE due to favourable properties including ductility, biocompatibility and biodegradability. As a further benefit, natural polymers often contain biofunctional molecules on their surface that can aid cell attachment, integration and differentiation on scaffolds. Naturally occurring polymers that have been investigated in BTE include collagen, silk, alginate, chitosan and hyaluronic acid. However, use of naturally occurring polymers can also be subject to limitations including presence of pathogenic impurities such as endotoxin [180], lack of tuneability of degradation rates and degradation related inhibition of local cells. Mechanical properties of natural polymers are also suboptimal for BTE, although cross-linking of polymers can enhance structural properties [181–183].

Synthetic polymers that have been deployed in BTE include poly(lactic acid) (PLA), poly(glycolic acid) (PGA), poly(caprolactone) (PCL) and poly(ethylene glycol) (PEG). Co-polymers including poly(lactic-*co*-glycolic acid) (PLGA) have also been used. Synthetic polymers can be created with tailored pore size, porosity, degradation rate and mechanical strength as required [184–187]. However, they are often hydrophobic and lack cell recognition sites, limiting application without secondary modification to improve bioactivity [188,189]. Synthetic and natural polymers in general have relatively poor load bearing capacity when used alone, with low elastic moduli compared to metallic and ceramic compounds [190,191]. However, the mechanical requirements of BTE scaffolds are complex, with compressive, tensile and fatigue properties all required for load bearing [192].

One approach that has proved popular in addressing these limitations is the combination of polymers with bioceramics or bioglasses to produce composite scaffolds. Most often, bioceramics or bioglasses are added as a coating or filler to a polymer matrix to improve bioactivity in addition to ramifying mechanical properties [180,193,194]. Porosity can also be added to composite polymer-ceramic scaffolds with varying levels of precision using techniques including 3D printing [80] and electrospinning [127,195]. These techniques are capable of depositing material with gaps between fibres to allow interconnectivity. Alternatively, porogens

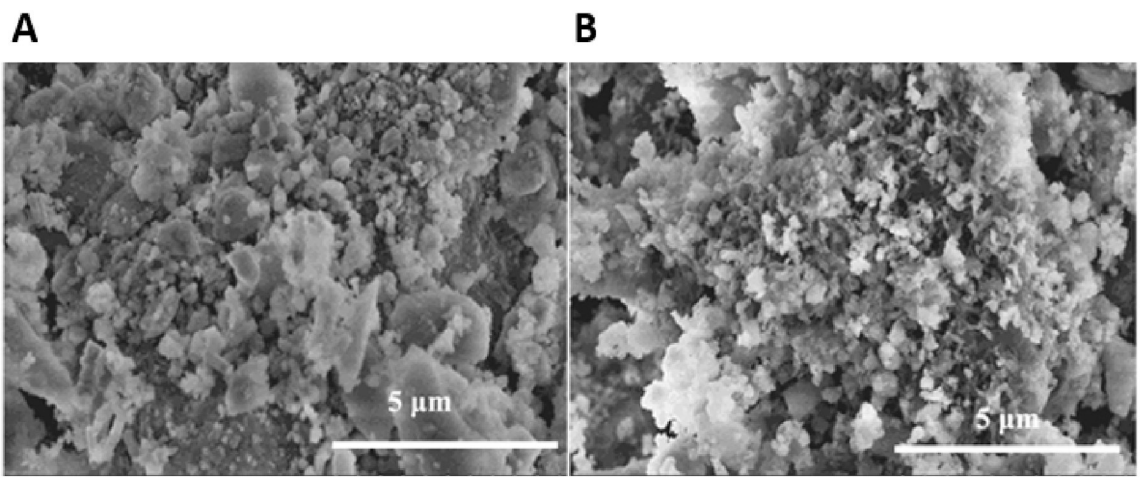

Fig. 10. SEM images of the amine-coated MBG before (A) and after (B) soaking in SBF. Formation of a crystalline HA layer was confirmed on Fourier transform infrared spectroscopy [172].

can be incorporated into the structure before being dissolved out, or chemically triggered to release gas, to create pores [196–198]. Combining use of porogens with techniques such as 3D printing during manufacturing can increase micro and macroporosity. Polymer-based scaffold surfaces have also been secondarily chemically treated to increase microporosity, through use of organic solvents [199,200]. Scaffold performance can also be increased by surface modification with bioactive substances including growth factors and surface ligands to aid cell adhesion and proliferation [121,193,201–203].

4.4.1. Collagen –based composite scaffolds

Amongst the natural polymers used in bone tissue engineering, collagen is perhaps the most frequently adapted into scaffolds. Collagen composes 90% of the total weight of bone extracellular matrix proteins and is therefore a logical choice for inclusion in a composite BTE scaffold. Although there are approximately twenty-nine known types of collagen, type I collagen has been used most frequently within BTE due to the lack of immune reactivity associated its use [204]. As part of the normal ECM it is inherently biocompatible, biodegradable and can stimulate cell proliferation and differentiation [205,206]. Furthermore, the mechanical and degradation properties of collagen can be tailored through the process of crosslinking [207]. However, in common with other natural polymers, collagen has mechanical properties that are insufficient for creating a load-bearing scaffold [208]. It is therefore often combined with more robust materials within BTE to create composite scaffolds. As the major inorganic component of bone, hydroxyapatite (HA) has frequently been combined with collagen in composite scaffolds.

Villa et al. developed a collagen-HA (Col-HA) scaffold through a co-precipitation and freeze casting process [209]. The scaffold created had a high degree of permeability suitable for cell infiltration, attachment and osteogenesis with 99% interconnectivity of pores. Mouse bone marrow derived mesenchymal stem cells (BMSCs) were seeded onto the scaffold and seen to be well attached after 12 h *in vitro* culture. Subsequently the scaffolds were implanted into a mouse calvarial defect. After three weeks *in vivo*, near complete filling of the calvarial defects with bone on radiographic and mineralization analysis was found. After several weeks, host matrix metalloproteinase breakdown of collagen had to led to scaffold degradation occurring. By contrast, Marcacci et al. previously found that a pure HA scaffolds failed to degrade 6 years after insertion into 4 patients with long bone defects [210]. However, compliant mechanical properties of the Col-HA scaffold were observed making it perhaps best suited for non-load bearing applications such as craniofacial repair [209]. Alternatively, it could be used to aid treatment of a complex fracture in the same way that bone substitutes or bone grafts are commonly used, in combination with mechanical fixation [211].

Calabrese et al. also demonstrated the osteoinductive potential of a type 1 collagen (30%) -HA (70%) scaffold. The scaffold in this instance was prepared by a freeze casting process, with the addition of a magnesium to create bioactive Mg-doped HA (MHA) nanocrystals. Human MSCs isolated from adipose tissue were seeded onto the scaffold and cultured *in vitro* in the absence of specific osteogenic inducing factors. Analysis through quantitative PCR and immunohistochemistry at up to 8 weeks demonstrated osteogenic differentiation of MSCs. This study therefore showed that the scaffold materials alone could trigger osteogenic differentiation of MSCs, with extracellular matrix production, gene expression and mineralization analysis all demonstrating the osteoinductive potential of the scaffold. Nevertheless, osteogenic differentiation was found to be significantly accelerated with the addition of osteogenic factors to the culture medium [123]. *In vivo* analysis was then performed of the scaffold in mice, with ectopic osteoinductive and angiogenic performance of the Col-MHA composite scaffold compared to a pure collagen scaffold. Bone augmentation and angiogenesis were found to spontaneously occur into the composite Col-MHA scaffold, with recruitment of host cells into the structure. The Col-MHA scaffold performed significantly better than the collagen alone scaffold, with less fibrotic tissue and more osteogenic tissue deposited at up to 16 weeks [212].

Grigolo et al. also utilised a scaffold composed of type 1 collagen and Mg doped-HA. The scaffold was designed to be biomimetic, with three distinct layers included to replicate the cartilaginous, tidemark and subchondral layered structure of articulating bone [213,214]. The cartilaginous layer was composed of purely type 1 collagen; the intermediate layer type I collagen (60%) and Mg-HA (40%); and the sub-chondral layer type I collagen (30%) and Mg-HA (70%). The scaffold was manufactured by combining a sintering and a freeze-drying technique, to obtain an integrated monolithic composite. Human MSCs (hMSCs) were seeded onto the single layers of the composite scaffold individually, and onto the integrated composite scaffold. Cells were then grown in either chondrogenic or osteogenic media for comparison. Immunostaining confirmed chondrogenic differentiation of hMSCs in the collagen-only cartilaginous layer when using chondrogenic media. Chondrogenic differentiation did not occur in the Mg-HA bone layer despite use of chondrogenic media. Immunostaining also confirmed osteogenic differentiation of hMSCs in both layers containing Mg-HA, and infiltration into the cartilaginous layer when osteogenic media was used, but this did not occur in the presence of chondrogenic media. Therefore, the processes of osteogenic and chondrogenic differentiation tended to depend mainly on the media used for culture, rather than the biomaterial composition in this study [215] (Fig. 11). Human bone marrow concentrate was then used in place of hMSCs on the three-layered scaffold in a

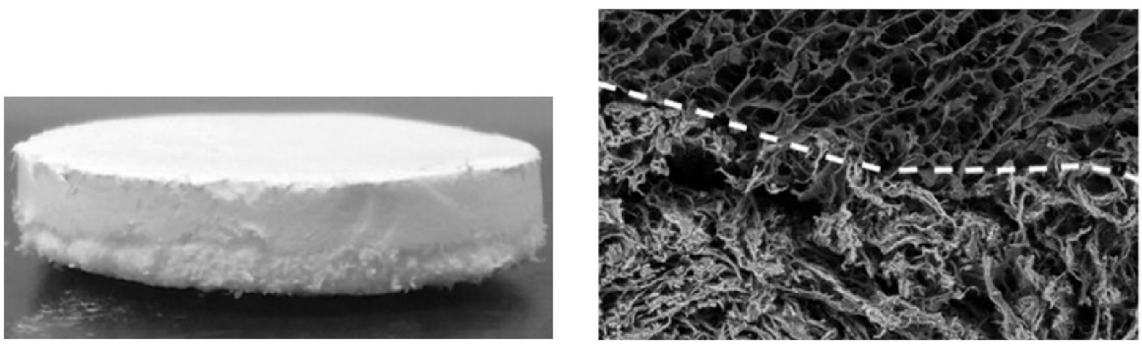

Fig. 11. Photograph of the biomimetic scaffold showing the external appearance and layered structure; SEM images showing the interface between scaffold layers [215].

Please cite this article in press as: G. Turnbull, et al., 3D bioactive composite scaffolds for bone tissue engineering, Bioactive Materials (2017), https://doi.org/10.1016/j.bioactmat.2017.10.001

further study. Having found a lack of osteogenesis in the cartilaginous layer, and a similar lack of chondrogenesis in the bone layer, they decided to induce chondrogenic differentiation only in the cartilaginous layer and osteogenesis in the composite layer (type I collagen (60%) and Mg-HA (40%)) and bone layer (type I collagen (30%) and Mg-HA (70%)). After 52 days *in vitro*, cell viability remained high and differentiation of cells down both the chondrogenic and osteogenic pathways was demonstrated on histological and immunohistochemical analysis. This biomimetic, nanocomposite material would therefore appear to offer a potential option for treating osteochondral lesions. In combination with patient-derived bone marrow concentrate, chondrogenic and osteogenic areas could be combined into the same scaffold to offer a "one step" transplantation procedure for osteochondral defects [216].

Kane et al. looked to improve upon the mechanical properties of collagen-HA scaffolds previously described by modifying the freeze-drying process most commonly used in their manufacture [217–219]. Attempting to improve scaffold porosity and mechanical strength, they used compression moulding to combine HA, paraffin micro-spheres and concentrated collagen fibrils. The paraffin micro-spheres were then leached out, acting as porogens, and the collagen was chemically cross-linked [126]. Interconnected pores of 300–400 μm in size with walls 3–100 μm thick were found on micro-CT analysis, with overall 85–90% porosity. This is significant, as scaffold pores greater than 300 μm have been shown to be favourable for osteointegration [160]. Mechanical testing found scaffolds with 60% HA to exhibit fully elastic deformation upon loading to 50% compressive strain, maintained over greater than 100 000 cycles. Compared to Col-HA scaffolds created through freeze-drying, the compressive modulus of the scaffold created in this study was a magnitude greater at approximately 1 MPa. These properties make the scaffold well suited to clinical application, as elastic deformation would potentially facilitate surgical handling and manipulation, whilst the compressive modulus demonstrated would potentially facilitate a degree of load bearing. *In vitro* bioactivity was investigated by seeding murine adipose derived stromal cells (mASCs) onto the scaffolds and culturing in osteogenic media. After 14 days, significant increases in ALP activity were seen, with complete infiltration of the scaffold by mASCs. HA containing scaffolds showed vastly superior bioactivity compared to collagen-only scaffolds, in keeping with other studies [180,220,221], with increased osteogenic differentiation and ALP levels found. However, increasing HA content beyond 40% had no significant benefit. *In vivo* angiogenesis and osteogenesis in 40% HA scaffolds was then evaluated by implanting acellular scaffolds subcutaneously in mice for 8 weeks. *In vivo* the scaffold was shown to be conducive to the infiltration and differentiation of endogenous cells, with osteogenesis and angiogenesis observed on histological analysis, suggesting the scaffold is osteoinductive. Therefore, the collagen-HA scaffolds in this study would appear to have potential for clinical use as a synthetic bone graft replacement, given their superior mechanical properties to scaffolds prepared by freeze-drying and favourable osteoinductive and angiogenic properties.

Meagher et al. investigated the impact of HA volume fraction on the *in vivo* performance of Col-HA scaffolds produced by compression moulding. Acellular collagen scaffolds containing 0, 20, and 40 wt% HA were implanted subcutaneously for up to 12 weeks in mice. Endogenous cell infiltration after 6 weeks was increased in scaffolds containing HA versus collagen alone. Angiogenesis, remodelling of the original scaffold matrix, mineralization and osteogenic gene expression was evident in scaffolds containing HA, but not observed in pure collagen scaffolds. Increasing scaffold HA content was found to be directly correlated with improved vascularity, cell density, matrix deposition and mineralization on histological and micro-CT analysis. It would therefore seem that HA promotes the recruitment and differentiation of endogenous cell populations, leading to angiogenic and osteogenic activity in collagen scaffolds. Contrastingly, collagen scaffolds exhibited no matrix deposition, mineralization, osteogenic gene expression and a significantly lower cell infiltration density [222].

Perdisa et al. demonstrated the osteoinductive potential of Col-HA scaffolds further in a prospective clinical study involving patients with patellar osteochondral defects [223] (Fig. 12). Cell-free Col-HA scaffolds were implanted into knee or patellar osteochondral lesions, with MRI imaging performed 24 months following surgery. The composite scaffold in this study utilised the same three-layered approach as used by Grigolo et al. [215]; the cartilaginous layer was made of type I collagen with a smooth surface; the intermediate layer had a combination of type I collagen (60%) and HA (40%); and the lower layer was a mineralised blend of type I collagen (30%) and HA (70%), mimicking subchondral bone composition. Patient functional outcome scores improved significantly at 12 and 24 months follow up, with MRI showing complete filling of the cartilage in 87.0% of the lesions, complete integration of the graft in 95.7% of lesions, and intact repair tissue surface in 69.6% of patients. However, osteophytes or more extensive bony overgrowth was also documented in.8% of the patients, though no correlation was found between MRI findings and clinical outcome [223].

4.4.2. Chitosan – based composite scaffolds

Chitosan (CS) is a polysaccharide normally found in the shell of crustaceans including crabs, lobsters and shrimp. As a versatile, semi-synthetic polymer it has favourable biocompatibility and biodegradability in addition to antibacterial and bioadhesive characteristics [197,224,225]. Within BTE chitosan has been combined with a number of materials in scaffolds including calcium phosphate [226], calcium sulfate [227], hydroxyapatite [228] and other natural polymers including silk [229–231].

Microparticle-based chitosan scaffolds have been produced by several groups [106,232–234]. Jiang et al. produced a composite CS/poly(lactic acid-*co*-glycolic acid) (CS/PLAGA) sintered microsphere scaffold, functionalizing the scaffold surface further with heparin molecules [235]. Scaffolds had a mean pore size of 172 μm, with a compressive strength in the region of trabecular bone. Mechanical testing showed that heparinization of chitosan/PLAGA scaffolds did not significantly alter scaffold mechanical properties or porosity. Osteoblast-like cells were observed to proliferate faster on CS/

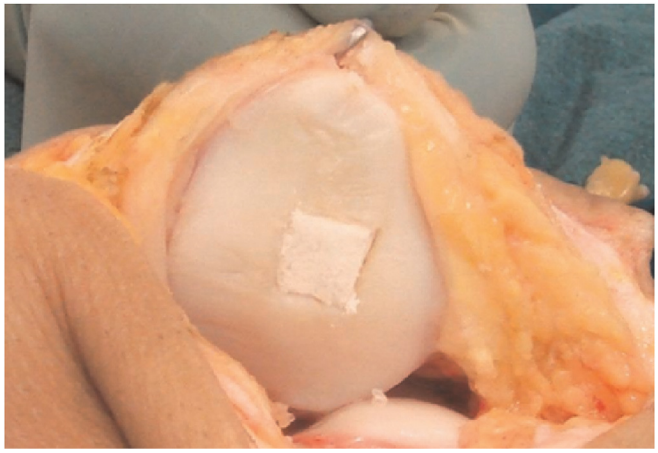

Fig. 12. Osteochondral scaffold, sized and press-fit into a patella defect. Adapted from Perdisa et al. [223].

PLAGA scaffolds as compared to pure PLAGA scaffolds. Furthermore, it was shown that the presence of CS on microsphere surfaces increased the ALP activity of the cells cultured on the composite scaffolds and up-regulated gene expression of osteopontin and bone sialoprotein. This study therefore demonstrated the potential of functionalized chitosan/PLAGA scaffolds.

Nano-fibre based composite chitosan scaffolds have also been investigated within BTE, fabricated using methods such as wet spinning [236,237] and electrospinning [238] and including materials such as silicon [239] and nano-hydroxyapatite (nHA) [240]. However, electrospinning of CS can be difficult and scaffold stability inside aqueous solutions is unreliable. Secondary crosslinking with agents such as poly(ethylene oxide) (PEG) and blending with other polymers such as silk, collagen and PCL to create composites can however significantly reduce the degradation rate of CS in electrospun scaffolds and improve bioactivity [241].

CS has also been combined with collagen and bone morphogenic protein (BMP) in composite scaffolds, with *in vivo* performance in dog and rabbit models analysed [31,242].

Shi et al. encapsulated BMP in poly-L-lactide-*co*-glycolide (PLGA) biodegradable microspheres, before dispersing them in a chitosan/collagen composite scaffold. The scaffolds were implanted in dog mandibles for 4 weeks, with histologically enhanced bone formation found in BMP/PLGA microsphere loaded scaffolds compared to control chitosan/collagen scaffolds also containing BMP. It was therefore concluded that sustained release of BMP from microspheres was more effective in inducing implant osseointegration compared to BMP bound to scaffolds.

Hou et al. prepared chitosan microspheres (CMs) and combined them with an absorbable collagen sponge with freeze-drying performed, to achieve controlled-release of BMP. The BMP-loaded composite scaffolds were implanted into 15 mm radius defects of rabbits and the bone-repair ability was evaluated. Defects were found to be bridged by new bone as early as 4 weeks, with complete healing and recanalization of the bone-marrow cavity at 12 weeks evident on X-ray and histological analysis. These results demonstrated that the composite CS-Col scaffold is a promising carrier of BMP-2 for the treatment of segmental bone defects [242].

Wu et al. developed a novel, composite scaffold of poly(L-lactic acid)/nHA/Alendronate-loaded chitosan microspheres (CS-ALs) with promising application for drug delivery and BTE demonstrated *in vitro* and *in vivo* [243] (Fig. 13). Alendronic (AL) acid has been used in an increasing number of BTE studies, with known properties including potent osteoinduction and inhibition of bone resorption [244,245]. Using a room temperature moulding/particle leaching method [246], followed by compression moulding, porous scaffolds of PLLA/nHA/CS-AL were prepared with the concentrations of CS/nHA-AL ranging from 0 to 20%. Porous PLLA/nHA scaffolds with only PLLA and nHA were also produced for use as controls. SEM found the scaffolds to exhibit a homogeneously interconnected porous structure, with the pore diameters of 150–250 μm. Scaffolds with 10% of CS/nHA-AL were then analysed *in vitro*, having been found to possess the most favourable drug release, degradation and mechanical properties. Culture of rabbit adipose stem cells (ASCs) found rapid cell proliferation and ECM production after 5 days, with no apparent cytotoxicity seen. Growth in osteogenic media led to significantly increased ALP activity and calcium deposition, with CS-AL scaffolds containing CS/nHA-AL having significantly better results than control scaffolds. Scaffolds containing 10% and 0% CS-ALs were then implanted into a rabbit bone defect model to further evaluate *in vivo* bone regeneration. Bone defects were healed with new bone formation seen during 4–8 weeks of implantation. New bone formation was significantly higher in CS-ALs (10%) group when compared with CS-ALs (0%), an effect that increased with time on histological analysis. Sustained release of AL was also found for up to 30 days. This study therefore showed promising application of CS-AL microsphere loaded (10%) scaffolds for both drug delivery and bone tissue engineering.

4.4.3. Hyaluronic acid – based composite scaffolds

Hyaluronic acid (HLA) is a natural glycosaminoglycan found widely throughout connective, epithelial and neural tissues. As one of the chief components of the extracellular matrix, HLA contributes significantly to cell proliferation and migration. It typically has a very large molecular weight and has been adapted into attempts at both hard and soft tissue engineering, particularly as a hydrogel (as discussed in the later hydrogel section) [247,248]. The mechanical properties of HA can be readily improved through processes such as crosslinking [79,249], whilst it is naturally viscoelastic, biodegradable and biocompatible, making it an ideal material for BTE [250].

HLA has been implemented in composite scaffolds by several groups. Kim et al. recently looked to combine favourable properties of multiple materials in fabricating a graphene oxide (GO)–Chitosan (CS)–Hyaluronic acid (HLA) based bioactive composite scaffold also containing an osteogenesis-inducing drug simvastatin (SV) [251]. Interestingly, SV is capable of initiating osteoblast differentiation of human adipose derived stem cells (hADSCs) and is well known for its property to enhance bone morphogenic proteins (BMPs). In fact, there are several examples in the literature of SV being used in composite scaffolds and injectable gels for bone regeneration, with improved osteogenesis seen [252–258]. The SV

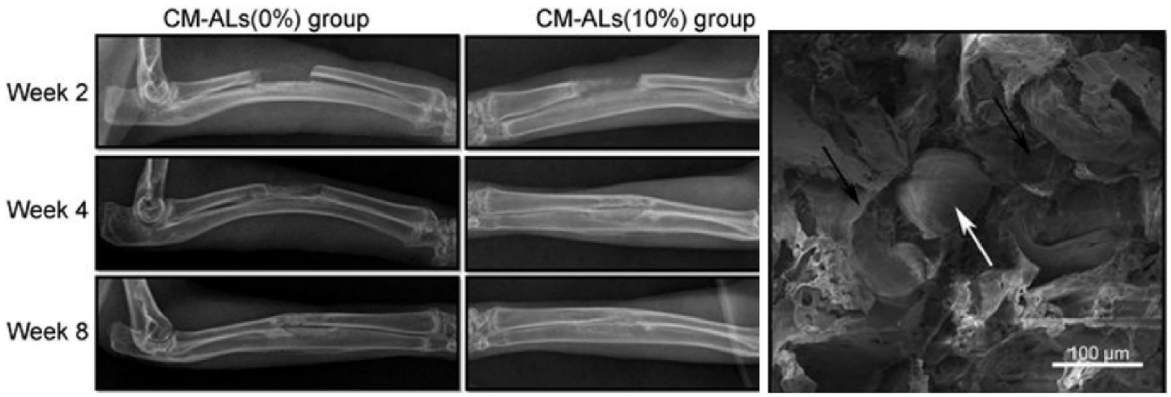

Fig. 13. Comparison of CS-ALs (10%)-implanted group to CS-ALs (0%) found significantly higher new bone formation, a finding which increased with time. SEM images of the CS-AL scaffold, with black arrows indicating the PLLA/nHA matrix and the white arrow indicating a CS/nHA-AL microspheres [243].

loaded GO–CS–HLA scaffold in this study was prepared in brief by mixing dissolved CS and HLA, with GO added through continuous stirring to create a composite blend, before a freezing and lyophilisation step to add SV was performed. Finally, the obtained composite scaffolds were cross-linked with N,N-(3-dimethylaminopropyl)-N-ethylcarbodiimide (EDC). Electron microscopy found the scaffolds to have an interconnected porous morphology. The addition of GO also resulted in less swelling and ultimately contributed to enhanced structural integrity of the scaffold. However, introduction of GO also caused a 35% reduction in porosity of the GO–CS–HLA scaffold. MC3T3 (Osteoblasts) cells were seen to adhere and proliferate better on SV loaded GO–CS–HLA scaffolds throughout 48 h of *in vitro* analysis. This was reflected by significantly higher scaffold mineralization being found in SV loaded scaffolds after 14 days of analysis. Overall, the SV loaded GO–CS–HLA scaffold appeared to offer a successful option for BTE, with the addition of SV significantly accelerating bioactivity and osteogenesis.

Jing et al. also combined HLA and CS in a porous scaffold for bone tissue engineering [259]. Mixing CS and HLA together as liquids, they used a freeze-drying approach to form porous, 3D scaffolds. By performing a further cross-linking step, the elastic modulus and structural integrity of the scaffold was increased. Stem cell colonisation and proliferation within the scaffold was demonstrated by DNA assays and confocal imaging. Correia et al. also used a freeze-drying processed to prepare composite scaffolds of chitosan and HLA, though directed their scaffolds at cartilage tissue engineering. Within this study incorporation of HLA enhanced cartilage ECM production, chondrocyte proliferation and cell adhesion to scaffold surfaces [260].

Kim et al. combined HLA and collagen in a scaffold directed at regenerating cartilage [261]. The hybrid scaffolds were prepared by adding 0.1, 0.3 or 0.5 wt% collagen to HLA. The HLA was then crosslinked with ethylene glycol diglycidyl ether, followed by a freeze-drying process. The resulting composite scaffolds had a three-dimensional structure with interconnected pores and showed an increase in tensile strength with increasing collagen concentration. The degradation time of the hybrid scaffolds *in vitro* increased with increasing collagen concentration. *In vitro* chondrocyte growth on the scaffolds was also improved by increasing collagen concentration over 2 weeks in culture. Furthermore, glycosaminoglycan (GAGA) concentration in the hybrid scaffolds was higher than in pure HLA scaffolds. These composite scaffolds would therefore seem to have potential for *in vivo* cartilage regeneration.

HLA has also been used as a delivery agent to improve bioactivity in bone substitute materials. Chang et al. investigated whether the use of HLA as an aqueous binder of hydroxyapatite/beta-tricalcium phosphate (HA-βTCP) particles could reduce the amount of bone graft needed and increase ease of graft handling in clinical situations [262] (Fig. 14). HA/βTCP was loaded into cross-linked HLA to form a novel HLA/HA-βTCP composite, which was then injected into rabbit skull defects *in vivo*. Histological and micro-CT analysis found that HLA allowed bone regeneration to be maintained even when HA-βTCP particle numbers were reduced. In fact, compared to the control scaffold, HLA/HA-βTCP samples had 1.7 times larger bone formation after 2 weeks. Overall, the addition of HLA to bone grafts not only promoted osteoconduction but also improved handling characteristics in clinical situations.

4.4.4. Silk - based composite scaffolds

Silk fibroin (SF) is a natural protein-based polymer mainly produced by silkworms and spiders. SF possesses several characteristics desirable for use in bone tissue engineering, including biocompatibility, low immunogenicity, limited bacterial adhesion, tuneable biodegradability, mechanical integrity and the ability to support the differentiation of mesenchymal stem cells along the osteogenic lineage [263–265].

McNamara et al. developed a new technique in fabrication of porous HA-silk scaffolds. Firstly, they mixed silk together with HA powder before addition of silk macroporogens. The mixtures were then sintered, with silk acting as a sacrificial polymer creating porosity. The resulting silk-HA scaffolds could be moulded into large, complex shapes, and further machined post-sinter to generate specific three-dimensional geometries. Scaffolds also supported bone marrow-derived MSC attachment and proliferation, with no signs of cytotoxicity [266].

Kweon et al. compared the performance of HA-coated silk scaffolds and HA-coated collagen scaffolds. They implanted both scaffold variants into rat tibias, with histological analysis of bone formation around the scaffolds performed after 6 weeks *in vivo*. They found that coating silk based scaffolds with HA promoted bone regeneration and bone to scaffold contact, with superior results demonstrated compared to HA-coated collagen scaffolds [267].

Silk has also been used to coat BTE scaffolds, with encouraging results found. In one study, PCL nanofibers were coated with silk and combined with biphasic calcium phosphate (BCP) in a composite scaffold [268]. Addition of silk-coated PCL nanofibers improved scaffold compressive strength (from 0.07 MPa for BCP to

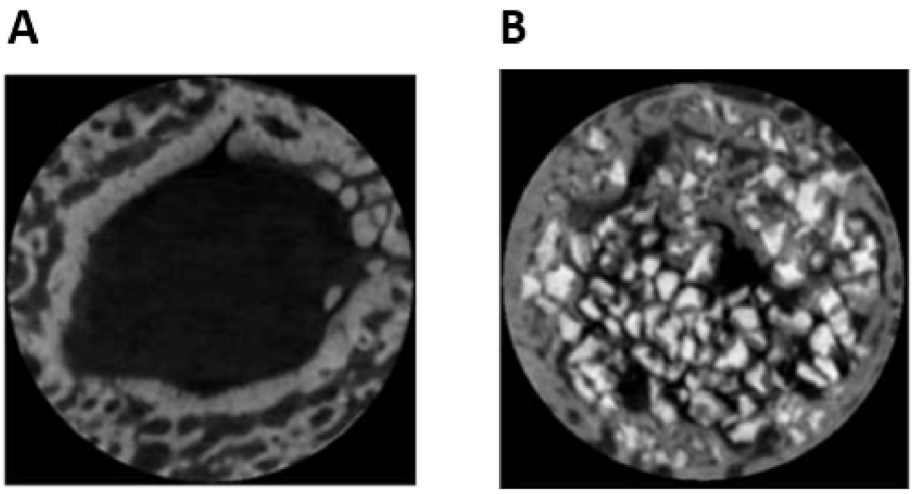

Fig. 14. Micro-CT images of the artificial skull defects after 4 weeks, showing significant bone regeneration in HLA/HA-β-TCP composites (B) compared to control (A).

Please cite this article in press as: G. Turnbull, et al., 3D bioactive composite scaffolds for bone tissue engineering, Bioactive Materials (2017), https://doi.org/10.1016/j.bioactmat.2017.10.001

0.42 MPa), elastic modulus (from 5 MPa for BCP to 25 MPa), and bioactivity whilst also preserving porosity (85%) and interconnectivity (99%). Furthermore, osteoblast proliferation and differentiation rates were increased in the BCP/PCL-silk scaffolds compared to that in the BCP/PCL and BCP scaffolds. Jaio et al. also modified BCP scaffolds with silk, applying multiple coatings to the scaffold surface. In doing so they managed to significantly enhance scaffold mechanical performance, with properties comparable to native bone tissue found. Once again osteogenesis by hMSCs was found to be positively influence by silk over an extended period in culture [269].

Cao et al. used a HA-mineralised silk to mechanically reinforce an injectable bone cement [270]. In this study, a hydroxyapatite (HA)—silk fibroin (SF) complex was synthesised through a co-precipitation method and added to an injectable CPC/SF composite. The compressive strength of the three-component composite, CPC/HA—SF/SF, kept increasing as HA—SF content was increased to 3 wt%. The setting time of CPC/HA—SF/SF composites also decreased as a function of HA—SF content, with no apparent effect on injectability. Furthermore, the CPC/HA—SF/SF composites showed good biocompatibility both *in vitro* and *in vivo*. It was therefore suggested that the composite could hold promise for orthopaedic applications, including serving as filler materials for minimally invasive surgeries to treat vertebral fractures.

In a further study, attempts were made to enhance the mechanical properties of electrospun SF scaffolds by uniformly dispersing hydroxyapatite (HA) nanoparticles within SF nanofibers [271]. Addition of HA content up to 20 wt% increased the mechanical properties of the composite scaffolds, while further increases above 20 wt% disrupted the polymer chain networks within SF nanofibers and weakened overall mechanical strengths.

4.4.5. Synthetic polymer composites

Use of natural polymers such as type I collagen in composite scaffolds has many advantages, including increased ease of enzymatic degradation, biocompatibility and improved scaffold similarity to natural bone extra-cellular matrix. However, natural polymers such as collagen used within scaffolds can have weak mechanical properties [42,272—274]. Significant research has therefore looked to optimise and improve scaffold properties by developing hybrid synthetic polymer/ceramic scaffolds for bone tissue engineering. Synthetic polymers that have been used frequently within BTE include polycaprolactone (PCL), polylactic acid (PLA), polyglycolic acid (PGA), and copolymers of PLA-PGA (PLGA). These poly(α-ester)s have key characteristics of being biodegradable, nontoxic and biocompatible [275—277].

4.4.6. Polycaprolactone (PCL) — based composite scaffolds

Polycaprolactone has been widely used in BTE for the fabrication of 3D scaffolds. Advantages of this polyester include biocompatibility, relatively slow degradation rate, less acidic breakdown products in comparison to other polyesters and potential for load-bearing applications [191,278—280]. In terms of hard tissue engineering, the high mechanical strength and slow degradation rate of PCL are particularly advantageous characteristics, potentially allowing load-bearing whilst native tissue gradually ossify a BTE scaffold [281]. However, due to the poor cellular adhesion properties of PCL, numerous attempts have been made to create PCL composites with improved bioactivity [282,283].

Kim et al. demonstrated the potential of PCL/alginate composite scaffolds, showing superior *in vitro* results in 3D printed PCL/alginate composite scaffolds compared to pure PCL scaffolds [284]. Alginates have desirable characteristics for use in 3D scaffold fabrication, including biocompatibility, low cost, controlled degradation and rapid gelation in the presence of calcium ions [224,285,286]. However, they also have poor mechanical properties and excessive hydrophilicity, making it difficult to control scaffold structure and shape [287,288]. Kim et al. therefore attempted to combine the favourable properties of alginate and PCL by melting PCL and alginate powders together at 130 °C, before extruding the melted composite through a 250-μm nozzle to create a 3D scaffold. Compared to a pure PCL scaffold fabricated by the same method, PCL/alginate scaffolds showed increased osteoblast cell viability, calcium deposition, ALP activity and greater cell-seeding efficiency over 7 days in culture.

Kim et al. used a combination of 3D printing, electrospinning and a physical punching process to create composite PCL/alginate constructs with nanofibrous content and improved mechanical strength. Electrospun layers of PCL/alginate were sandwiched by layers of micro-sized PCL struts; the final scaffold was then punched to create micro-sized pores travelling through the consecutive layers of electrospun and 3D printed material (Fig. 15). Compared to pure PCL scaffolds, PCL/alginate composite scaffolds showed significantly enhanced cell viability at 7 days, ALP activity and calcium deposition at 14 days and greatly increased water absorption due to the improved hydrophilicity contributed by the scaffold alginate content [271].

Hydroxyapatite has also been combined with PCL by several groups attempting to create more bioactive, composite scaffolds for BTE. Gonçalves et al. utilised silicon-doped nanocrystalline HA, PCL, and carbon nanotubes in 3D printed composite scaffolds [124]. In using three distinct materials, they hoped to merge properties favourable to bone regeneration including biocompatibility,

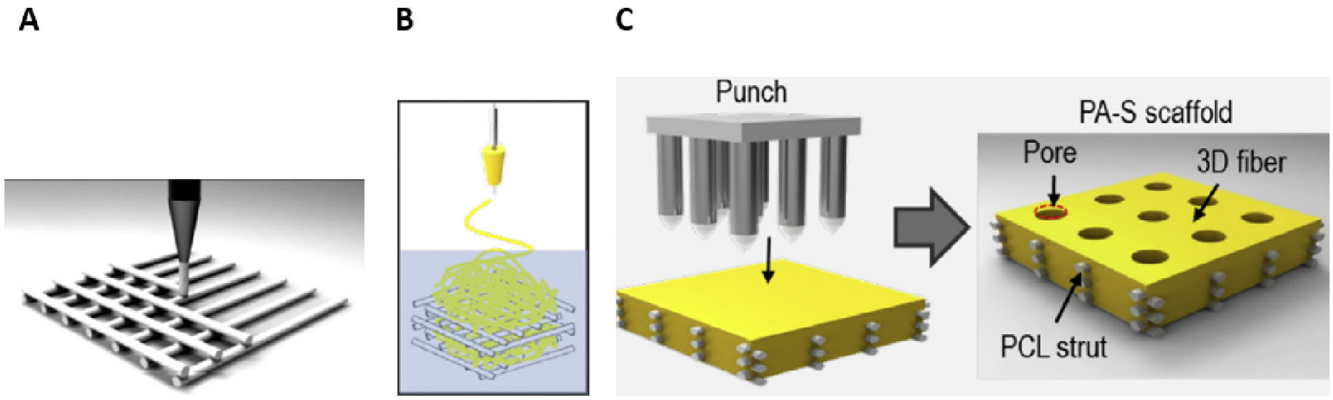

Fig. 15. PCL/Alginate scaffold fabrication method. (A) 3D printing of micro-sized PCL struts (B) electrospinning of PCL/alginate onto PCL struts (C) punching process to create micro-sized pores in final PCL/alginate (PAS-S) scaffold. Adapted from Kim et al. [271].

Please cite this article in press as: G. Turnbull, et al., 3D bioactive composite scaffolds for bone tissue engineering, Bioactive Materials (2017), https://doi.org/10.1016/j.bioactmat.2017.10.001

osteointegration ability and biodegradability [193,289,290]. Nanocrystaline silicon-doped HA was chosen as a ceramic material due to the chemical composition being comparable to the inorganic part of native bone. It has also been shown that the *in vivo* bioactivity of silicon-doped HA (SiHA) is significantly improved compared to pure HA, with enhanced bone apposition, bone ingrowth and cell-mediated degradation found on SiHA implants [291,292]. Carbon nano-tubes (CNTs) have been shown to influence and enhance cell differentiation and adhesion, by increasing electrical stimulation to cells [293–296]. PCL was incorporated into the scaffold to add ductile properties to the ceramic SiHA. Additionally, PCL has a relatively low melting temperature (approximately 60 °C), making it ideal for 3D printing [297,298]. To combine the materials, PCL and HA were dissolved independently in dicholoromethane. CNTs were then added to the HA in solution, and the PCL solution was then added to the HA-CNT suspension. The slurry was mixed and slowly heated to allow the dichloromethane to evaporate until a suitable viscosity for 3D printing was achieved. Scaffolds of differing CNT content were then printed, with CNT content ranging from 0 to 10%. Scaffolds containing 10% CNTs had significantly greater apatite deposition and osteoblast-like cell adhesion after 6 days *in vitro*. Additionally, electrical resistance of the scaffolds decreased as CNT content increased. This would suggest that CNTs have beneficial effects on cell function through modifying surface charge, as suggested by previous studies [293–295]. In terms of the mechanical properties, scaffold load-bearing capacity was improved by a CNT content of up to 0.75%. Beyond 2% CNT content, there was a clear detrimental effect on compressive strength. Nevertheless, compressive strength values for pure PCL-SiHA and PCL-SiHA scaffolds with CNT content up to 0.75% were comparable to those found in the literature for trabecular bone [299]. Morphologically, the scaffolds were found to have interconnected pores with sizes from 450 to 700 πm. Overall, the scaffolds with 2% CNTs offered the best combination of mechanical behaviour, cell viability and electrical conductivity.

Jakus et al. also utilised organic solvents to create a composite HA-PCL biomaterial, described as “hyperelastic bone,” or “ HB.” HA powder and either PCL or PLGA were added to a trisolvent mixture of excess dichloromethane (DCM), 2-butoxyethanol (2-Bu) and dibutylphthalate (DBP) [300]. The resulting solutions were then stirred in an open environment to allow solvent evaporation, until a viscosity ideal for 3D printing was reached. The synthetic composites composed of 90% HA and either 10% PCL or PLGA could be rapidly 3D printed (up to 275 cm^3/hour) from room temperature extruded liquid inks. Mechanical testing of HB found elastic properties; although not as elastic as their pure polymer counterparts, both HA-PLGA and HA-PCL versions of HB retained a high degree of elasticity, capable of undergoing 36.1 ± 4.3% and 61.2 ± 6.4% strain and having similar tensile elastic moduli of 4.3 ± 0.4 MPa and 10.3 ± 1.3 MPa, respectively (Fig. 16). To examine biocompatibility *in vivo*, HA-PLGA scaffolds were implanted subcutaneously in mice. After 7 days, native tissue had already begun to infiltrate the scaffolds, with vascularisation seen to develop on histological analysis. Further to this, HB capacity to induce bone regeneration was assessed *in vivo* within a rat spinal fusion model. Pure HA-PLGA scaffolds and HA-PLGA scaffolds with additional of recombinant human bone morphogenic protein 2 (rhBMP-2) were implanted. A demineralised bone matrix (DBM) scaffold was used for comparison, with fusion rates of 50–60% usually seen with this control [301]. After 8 weeks *in vivo*, bone formation and spinal fusion rates were similar in the HA-PLGA scaffold compared to the DBM control. These findings suggest that without any added growth factors, the scaffold has intrinsic osteoinductive properties comparable to the commercially available DBM. HA-PLGA scaffolds with rhBMP-2 were found to have superior new bone formation and spinal fusion rates compared to both the alone and DBM. HA-PLGA HB Scaffolds were also implanted into primate calvarial defects, to evaluate performance in larger cortical bone defects. After 4 weeks *in vivo*, implants were excised from the calvarial defects and examined. Evidence of heavy vascularisation and mineralised tissue advancing into the implants from the cortical bone was seen; areas not in direct contact with native bone were also seen to develop mineralised tissue, suggesting up-regulation of osteogenic gene expression by native MSCs without the addition of any growth factors, indicating HB osteoinductive potential. In summary, 3D printed HB demonstrated several properties favourable to clinical use. Compared to DBM, 3D printed HA-PLGA could offer a cheap and potentially readily available osteoinductive material for clinical applications, without risk of disease transmission.

Cheng et al. also looked to combine HA and PCL in a 3D printed

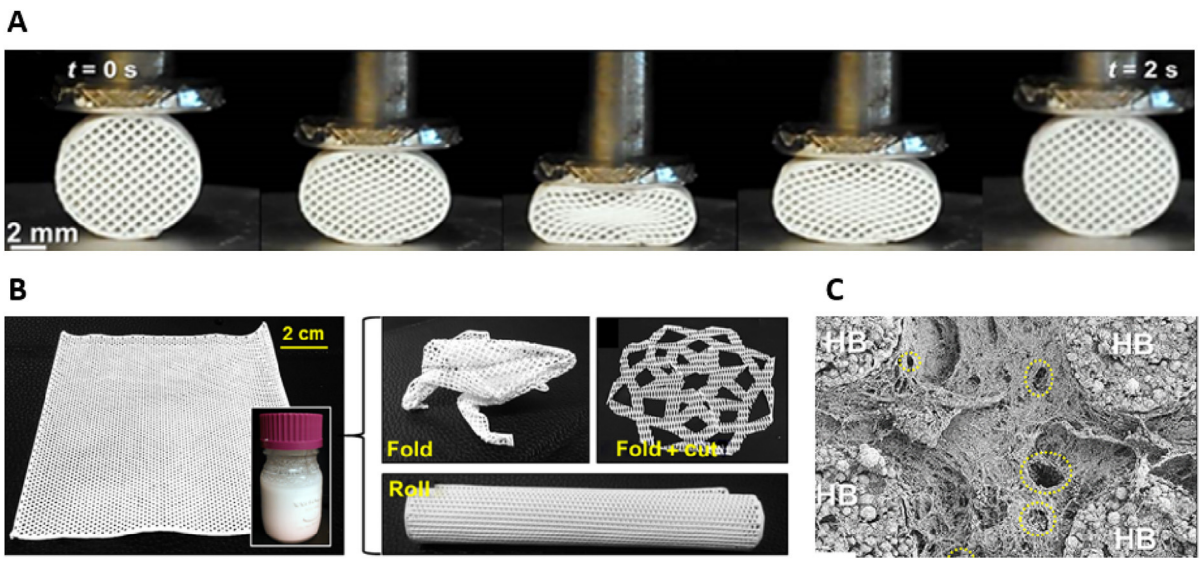

Fig. 16. (A) Photograph series showing the compression and recovery of a 1-cm-diameter 3D-printed HB cylinder over a single compression cycle (B) 12 × 12 cm sheet of HB printed from 100 ml HB ink, with ease of manipulation into complex folded structures shown (C) SEM image of explanted HB scaffold after 35 days *in vivo*; blood vessels indicated by yellow circles, with soft tissue filling space between HB fibres. Adapted from Jakus et al. [302].

composite scaffold using stereolithography, which creates 3D structures through spatially controlling the solidification of liquid photo-polymerizable resin [78,303,304]. Pure PCL scaffolds were first fabricated via a custom designed 3D printer. The scaffolds were then modified by immersing them in poly-dopamine (PDA), before mineralization with HA nanocrystals was achieved on the scaffold surfaces through a precipitation reaction. Scanning electron microscopy (SEM) was used to examine HA/PDA/PCL scaffold microstructure; mean pore sizes of scaffolds 400 πm were found, which has previously been shown to be optimal for bone tissue regeneration [305]. Sterilised scaffolds were then seeded with hMSCs and incubated in appropriate media. Cellular attachment, osteogenesis and angiogenesis of hMSCs was found to be significantly increased in dopamine-coated scaffolds compared to pure PCL variants. Furthermore, hMSC proliferation, ALP activity, osteogenesis-related proteins, and angiogenesis-related protein secretion all increased as scaffold PDA concentration was increased. These results demonstrated that dopamine scaffold surface modification could have significantly beneficial effects for BTE. Dopamine analogues have previously been shown to be important in allowing mussels to attach themselves to rocks [306]. Dopamine has also been applied to various materials to improve their cell adhesive properties; metals, oxides, polymers and carbon-based materials have all been coated with improved cell attachment and differentiation seen [203,307–309]. Dopamine has also been shown to help inhibit peri-implant osteolysis caused by inflammation [307].

4.4.7. Poly(lactic acid) (PLA) – based composite scaffolds

Poly (lactic acid) is a biodegradable, bioactive thermoplastic polyester that has been used to make a number of medical implants including bone screws, fixation devices and vascular grafts [310]. PLA is formed by the polymerization of lactic acid and can be obtained from renewable sources including starch and sugar. Several distinct forms of PLA exist due to the chiral nature of lactic acid, including poly-L-lactide (PLLA) and poly-D-lactide (PDLA) which are produced from the polymerization of L-lactide and D-lactide respectively [311].

Yang et al. recently fabricated hierarchical macroporous biocompatible (HmPB) scaffolds containing a matrix of PLA, PCL and hydrophobically modified silica nanoparticles (h-SiO2) [312]. PCL and PLA were first dissolved in an organic solvent, with h-SiO2 nanoparticles then added as a particulate emulsifier. After solvent evaporation, the resulting composite material was 3D printed into scaffolds with over 98% porosity. The scaffolds had a hierarchical structure (including macropores, medium pores and small pores) and supported the adhesion and proliferation of MSCs, suggesting good biocompatibility.

Holmes et al. created a PLA based scaffold using a fused deposition modelling 3D printer. The scaffolds were designed to have highly interconnected 3D microvascular-mimicking channels, to facilitate osteogenic bone regeneration as well as vascular cell growth. The resulting scaffolds were also chemically conjugated with nHA to enhance osteo-differentiation of seeded hMSCs. SEM imaging demonstrated printing of vertical microchannels with both a 500 and 250 μm radius, within a porous bone matrix. Mechanical testing also demonstrated that the scaffolds could withstand normal mechanical loading, exhibiting elastic behaviour. Analysis of *in vitro* hMSC adhesion, proliferation and osteogenic differentiation found enhanced results with scaffolds incorporating nHA and small (250 μm) microchannels, compared to controls without nHA and with large (500 μm) microchannels. Additional *in vitro* analysis with human umbilical vein endothelial cells demonstrated the scaffolds to be effective in supporting and enhancing vascular cell growth and activity, with large channel scaffolds promoting the greatest HUVEC growth. Taking all of the findings together, inclusion of both large and small microchannels and nHA may provide the best overall solution for creating a vascularized, load-bearing, osteogenic scaffold [313].

In a different approach, Ren et al. recently electrospun a blend of PLLA and gelatin to create a nanofibrous mesh designed to aid bone defect repair [314]. The composite mesh was seeded with MSCs, with osteogenic differentiation occurring after 7 days of *in vitro* culture. 3D multi-layered constructs were then built by stacking four mono-layered meshes together. The constructs were incubated *in vitro* for 3 days before being implanted into rat cranial defects. In comparison with a control group, there was significant formation of new calcified bone after 12 weeks. Yao et al. also created nanofibrous composite PLA scaffolds, by electrospinning a blend of PCL and PLA [315]. To improve control over structural properties created by the electrospinning process, an innovative technique of thermally induced nanofiber self-agglomeration (TISA) was developed by the same group [316]. In brief, this involved electrospun nanofibrous mats being converted into tiny nanofibrous pieces, which were then utilised as building materials for making 3D electrospun scaffolds. Grinding, dispersing, agglomerating and freeze-drying processes were involved. The resulting 3D scaffolds had a 96% porosity and possessed interconnected and hierarchically structured pores, including macropores with sizes up to 300 μm. On *in vitro* testing, PCL/PLA-3D blend scaffolds had higher mechanical properties and *in vitro* bioactivity compared to pure PCL-3D scaffolds made by the same process. This was reflected by enhanced hMSC cell viability, osteogenic gene expression and apatite-like deposition in PLA/PCL scaffold compare to pure PCL controls. *In vivo* analysis was then performed, with PCL/PLA-3D scaffolds implanted into mice cranial bone defects. After 6 weeks, histological analysis suggested that PCL/PLA-3D scaffolds provided a more favourable/desired microenvironment for mouse cranial bone formation as compared to the PCL-3D scaffolds, with significantly increased bone formation. Despite this, neither scaffold could bridge the bone defects completely, despite the addition of BMP growth factor supplement.

4.4.8. Poly(lactic-co-glycolic acid)/PLGA – based composite scaffolds

PLGA is a synthetic co-polymer of poly-L-lactic acid (PLLA) and polyglycolic acid (PGA), with US Food and Drug Administration approval for human applications. Degradation rates of PLGA can be customised to range from weeks to months, based on the ratio of PLLA to PGA within the copolymer structure [317]. Other benefits of PLGA over pure PLA and PGA include the range of commonly available solvents that it can be dissolved in and the ease with which it can be manipulated into structures of desired sizes and shapes. Biomolecules such as growth factors can also be easily encapsulated by PLGA.

However, there are some limitations to the use of PLGA within BTE. The amorphous structure of PLGA has a low Young's modulus, resulting in susceptibility to elastic deformation, whilst PLGA is also poorly osteoconductive [318]. In order to address these limitations, PLGA has been combined with ceramics and bioactive glasses to create composite scaffolds [319]. Several groups have combined nano-HA (nHA) with PLGA, hoping to benefit from the osteogenic properties and high modulus of nHA [180,320]. Whilst high concentrations of nHA in a composite can potentially have adverse effects on mechanical properties due to non-uniform distribution, lower concentrations are able to improve tensile and compressive properties of scaffolds [321,322]. When contained within a composite scaffold, nHA has also been shown to help cells and proteins attach to scaffold materials [17]. PLGA also potentially balances the limitations of nHA which include inherent brittleness and slow degradation [318,323]. Several groups have created composite

Please cite this article in press as: G. Turnbull, et al., 3D bioactive composite scaffolds for bone tissue engineering, Bioactive Materials (2017), https://doi.org/10.1016/j.bioactmat.2017.10.001

PLGA-nHA scaffolds using the technique of particulate leaching [324–326]. However, the microarchitecture of scaffolds formed by this method typically have low porosities and interconnectivity. Incomplete solvent removal has been also encountered with this technique, resulting in reduced cell viability. Kim et al. modified the technique of particulate leaching by creating a PLGA-nHA scaffold by gas forming and particulate leaching. This process avoided using organic solvents, eliminating potential issues associated with incomplete solvent evaporation, and resulted in improved scaffold microarchitecture. Higher porosity and improved mechanical characteristics resulted in higher *in vitro* cell growth and mineralization of scaffolds, compared to PLGA-nHA scaffolds formed by solvent casting-particulate leaching [17].

Shaui et al. 3D printed porous PLGA-nHA scaffolds via selective laser sintering. This method allowed formation of well-controlled pore architectures and high scaffold surface bioactive nHA content. The effect of nHA on scaffold mechanical properties was then investigated; although scaffold compressive strength and modulus was improved as nHA content increased from 0 to 20%, nHA content above 20% resulted in worsening, brittle mechanical properties [129]. To re-create bone extracellular matrix (ECM) structure several groups have tried to create nano-fibrous PLGA composite structures via electrospinning; potential benefits of including nanofibers include high surface area per unit mass, increased biodegradability and with the addition of ceramic nanoparticles, improved osteoconductive potential [29,30,128,327]. Jose et al. electrospun nanocomposite scaffolds, adding nHA to PLGA solution before spinning. Like Shaui's findings, nHA content strongly influenced scaffold mechanical properties. Whilst 20% nHA strongly increased the Young's modulus of the electrospun composite meshes, higher concentrations again led to worsening mechanical properties [328]. Yun et al. evaluated the biocompatibility of electrospun PLGA-nHA scaffolds through culturing human primary adipose tissue-derived stem cells (hADSCs) and MSCs on them with promising results. With a nHA content of around 17% (w/w), osteogenic differentiation and mineralization of both MSCs and hADSCs occurred. These results were confirmed by increased expression of osteogenic genes on reverse transcription-polymerase chain reaction (PCR) increased ALP activity and calcium deposition [329]. Haider et al. also evaluated the cell compatibility of PLGA-nHA composite nanofiber scaffolds, by culturing osteoblasts on PLGA and PLGA-nHA scaffolds to allow direct comparison (Fig. 17). In this study, the impact of HA morphology was also examined by comparing spherical and fibre forms of nHA on cell culture results. PLGA-nHA nanofiber scaffolds showed higher cellular adhesion, proliferation, enhanced osteogenesis and increased Ca^{+2} ions release compared to spherical PLGA-nHA and pure PLGA scaffolds. This study re-iterated the beneficial effects of including nHA within scaffolds on osteoblast culture. The enhanced cell proliferation on the fibre PLGA-nHA scaffold compared to scaffolds containing spherical nHA suggested that the morphology of nHA also influences cell behaviour [330].

Whilst the combination of synthetic polymers such as PCL and PLGA with HA has led to successful results, natural polymers such as collagen and chitosan have improved mineralization characteristics compared to synthetic polymers. The presence of numerous ionic molecular groups within natural polymers allows for processes such as calcium chelation to occur and mineralization rates are improved by the negative surface charge. The surfaces of synthetic polymers are also largely hydrophobic, which is less favourable for cell adhesion to occur [331,332]. Attempts have therefore been made to modify the surface of synthetic polymers to increase cell affinity. One approach has been to covalently link arginine-glycine-aspartic acid (RGD) to biomaterials such as PLGA to facilitate cell adhesion. RGD has previously been established as the minimal core peptide recognizable by cell adhesion receptors and is capable of increasing the bioactivity of structures [333]. Shin et al. fabricated biomimetic hybrid nanofiber sheets composed of RGD peptide-decorated PLGA (RGD-PLGA) nanofibers via an electrospinning technique. Cells including the murine preosteoblastic cell line (MC3T3-E1 cell) and the human osteosarcoma cell line (MG-63 cell) were then cultured on the scaffolds. Compared to pure PLGA nanofiber sheets, the initial adhesion and proliferation of cells were significantly enhanced on RGD-PLGA sheets, as found in other studies [201,202,334].

4.5. Hydrogels

Hydrogels are gels constructed from networks of crosslinked, hydrophilic polymer chains. Their hydrophilic nature allows them to absorb copious amounts of water into a three-dimensional network, which is ideal for supporting cell growth. In fact, hydrogels can absorb up to 1000 times their original weight in aqueous medium without dissolving [335]. At the same time, they are highly permeable to oxygen, nutrients and other water-soluble compounds, making them attractive materials for tissue engineering

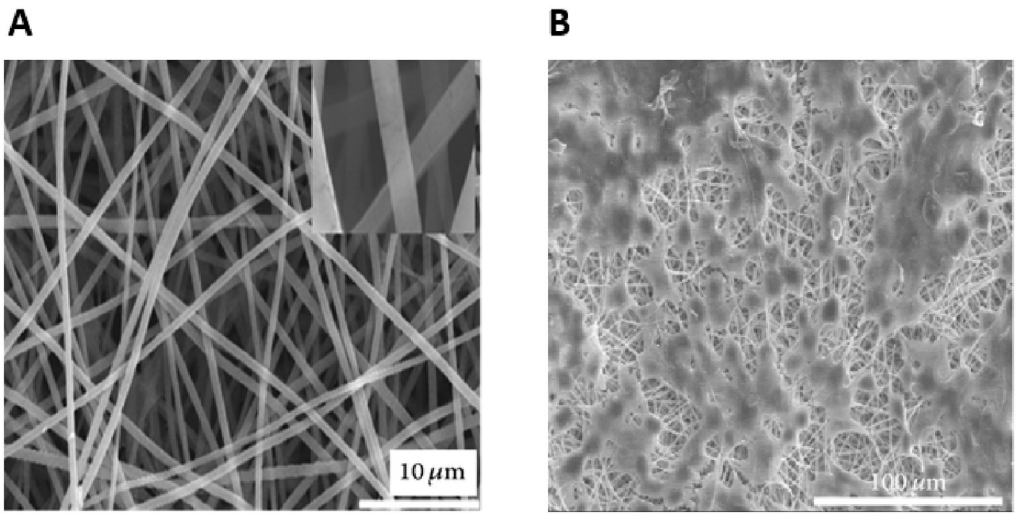

Fig. 17. (A) SEM micrographs of nHA/PLGA composite nanofiber scaffolds, with adherent cells after 24 h incubation also displayed (B).

[182]. Within BTE, they have been shown to facilitate angiogenesis, osteoconductivity, cell adhesion and matrix integration [89,336–338]. Hydrogels can be derived from natural polymers (including collagen, gelatin, alginate, chitosan, hyaluronic acid and agarose) or synthetic materials. Natural polymers are often derived from extracellular matrix components including collagen and hyaluronic acid, and therefore have low toxicity, high biocompatibility and cell affinity [339,340]. However, natural polymers can undergo uncontrolled degradation resulting in compromise of mechanical properties in printed constructs. To help address this issue, synthetic polymers can be used either alone or with natural polymers to create a composite hydrogel, allowing better control over stiffness and elastic modulus of hydrogel constructs [341,342]. Synthetic polymers can also be functionalized with biological molecules, such as RGD, heparin and hyaluronan, to increase bioactivity and cell adhesion in hydrogel composites [202,343]. Growth factors and drugs have also been encapsulated within hydrogels to increase scaffold bioactivity [344–346].

Successful bioprinting relies in part on combining a suitable bioprinting technique with an appropriate bioink. Significant focus within bioprinting has therefore been placed on developing cell-friendly, novel bioinks which can be 3D printed to fabricate tissue constructs. Polymeric hydrogels are usually the main component of bioinks as they have cell-friendly properties whilst being amenable to 3D printing [338]. Hydrogel-based bioinks are often composite materials, containing growth media, cells, biomaterials, added nutrients and growth factors to aid cell proliferation and differentiation [347–349].

4.5.1. Composite bioinks used in bioprinting

Although low-viscosity hydrogels with a high-water content provide a superior environment for cell function and viability, the mechanical integrity and support they provide is often insufficient to allow transfer to *in vivo* analysis. Attempts have therefore been made to create composite bioinks capable of integrating the mechanical strength of viscous hydrogels with the biocompatibility provided by lower-viscosity hydrogels.

Nguyen et al. recently designed bioinks to treat cartilage lesions, containing either nanocellulose with alginate (NFC/A) or nanocellulose with hyaluronic acid (NFC/HLA). NFC was chosen to help mimic the collagen bulk in cartilage matrix [350], alginate used in place of natural proteoglycans, whilst hyaluronic acid was included as a major component in native cartilage. Human-derived induced pluripotent stem cells (iPSCs) and irradiated human chondrocytes were then encapsulated in the bioinks. Utilising a microvalve 3D bioprinter, a grid construct was printed with the two differing bioinks. In the case of NFC/HLA, low proliferation and phenotypic changes away from pluripotency were seen in the iPSCs. However, in the case of the NFC/A (60/40, dry weight % ratio) constructs, hyaline-like cartilaginous tissue with collagen type II expression was seen after 5 weeks. Additionally, a marked increase in cell number within the cartilaginous tissue was detected by 2-photon fluorescence microscopy. The NFC/A bioink therefore appeared suitable for bioprinting iPSCs to support cartilage production in co-culture with chondrocytes. Markestedt et al. also 3D printed a NFC/A bioink containing human chondrocytes. The shear thinning properties of the NFC and the fast crosslinking of alginate allowed microvalve bioprinting to occur with high fidelity and stability. Taking MRI and CT data, they managed to print anatomically accurate scale models of human ears and sheep meniscus (Fig. 18). Chondrocyte viability after printing was approximately 95%, with viability also found of 73% and 86% after 1 and 7 days of 3D culture respectively [351].

Gao et al. used inkjet bioprinting to co-print an acrylated poly(ethylene glycol) (PEG) hydrogel with acrylated peptides. Human MSCs were included in the composite hydrogel, which was exposed to ultraviolet light to initiate simultaneous photopolymerization of the hydrogel during printing. The resulting scaffold demonstrated excellent biocompatibility with a cell viability of 87.9 ± 5.3% 24 h after printing. Printed constructs containing hMSCs were cultured for 21 days in either osteogenic or chondrogenic media. Osteogenic and chondrogenic gene expression was seen to significantly increase from day 7–21, with significant collagen and extracellular matrix deposition seen. Mechanical analysis found modulus increases in PEG-Peptide scaffolds of 100% in osteogenic media and 82% in chondrogenic media from day 7–21. The compressive modulus of the printed PEG-Peptide hydrogel exceeded 500 kPa, which is more than 100

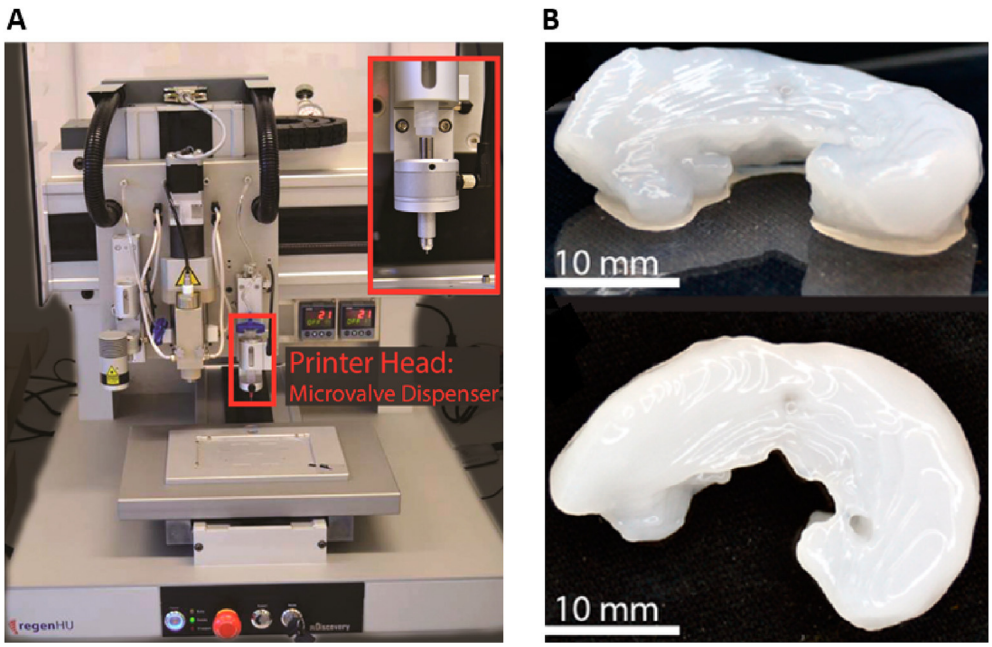

Fig. 18. (A) The 3D Discovery (Switzerland) bioprinter with microvalve print-head shown (B) 3D printed knee meniscus using NFC/A ink. Adapted from Markestedt et al. [351].

Please cite this article in press as: G. Turnbull, et al., 3D bioactive composite scaffolds for bone tissue engineering, Bioactive Materials (2017), https://doi.org/10.1016/j.bioactmat.2017.10.001

times as that reported for some natural hydrogels [352,353]. Overall, the PEG-Peptide hydrogel printed in this study developed into a homogenous tissue with high cell viability and mechanical integrity [354].

Kang et al. used a multi-head bioprinter to create an interwoven scaffold consisting of cell-laden hydrogels, PCL polymer and a sacrificial Pluronic F127 hydrogel [355]. The composite hydrogel consisted of optimised concentrations of gelatin, fibrinogen, hyaluronic acid (HA) and glycerol mixed into cell culture media. Pluronic F127 was printed as a sacrificial outer layer to support the 3D architecture of the composite hydrogel while crosslinking was performed, whilst the PCL provided internal scaffold structural strength. After cross-linking of fibrinogen using thrombin, the uncross-linked components (gelatin, HA, glycerol and Pluronic F127) were washed out. This created microchannels in the tissue constructs, facilitating diffusion of nutrients to printed cells. Tissue models were printed in anatomically relevant shapes through use of clinical imaging data, with constructs created to match skull and mandible defects. The potential of the printing process was demonstrated through fabrication of mandible and calvarial bone, cartilage and skeletal muscle. High cell viability was found post-printing of chondrocytes, amniotic fluid derived stem cells and myoblasts; cell viability in printed structures was typically 91 ± 2% after 24 h of culture.

Pluronic F127 has been adapted into several other composite scaffolds to aid in the creation of temporary structural support or vascular channels [356–359]. Although F127 has poor cell compatibility when used alone, it is easy to print and structurally robust [360–363]. Aqueous F127 solutions undergo thermal gelation at physiological temperatures, but on cooling bellow a critical micellar temperature (CMT) dissociation of the gel occurs. This allows F127 to be printed as a gel into constructs, with secondary cooling of the construct then washing F127 away as a fugitive ink [364,365]. As a result, F127 support structures can be removed post-printing and printed F127 channels left patent for perfusion with media. This approach has proved helpful in attempts to create vascular channels in constructs. Creating a sufficient vascular structure is a major challenge in bioprinting, as in the absence of a vascular network cells are dependent on diffusion for delivery of oxygen and nutrients [361]. Whilst larger vessels have been fabricated, capillaries have yet to be 3D printed, which leaves constructs dependent on infiltration of micro-vessels *in vitro* to ensure cell viability. Unfortunately, microvessel infiltration often lacks depth of penetration, limiting the size of viable bone construct that can be implanted [366,367].

Lewis et all used F127 as a fugitive ink to help create a multi-material 3D construct with vascular channels (Fig. 19) [368].

A silicone ink was first printed and then cured, creating a

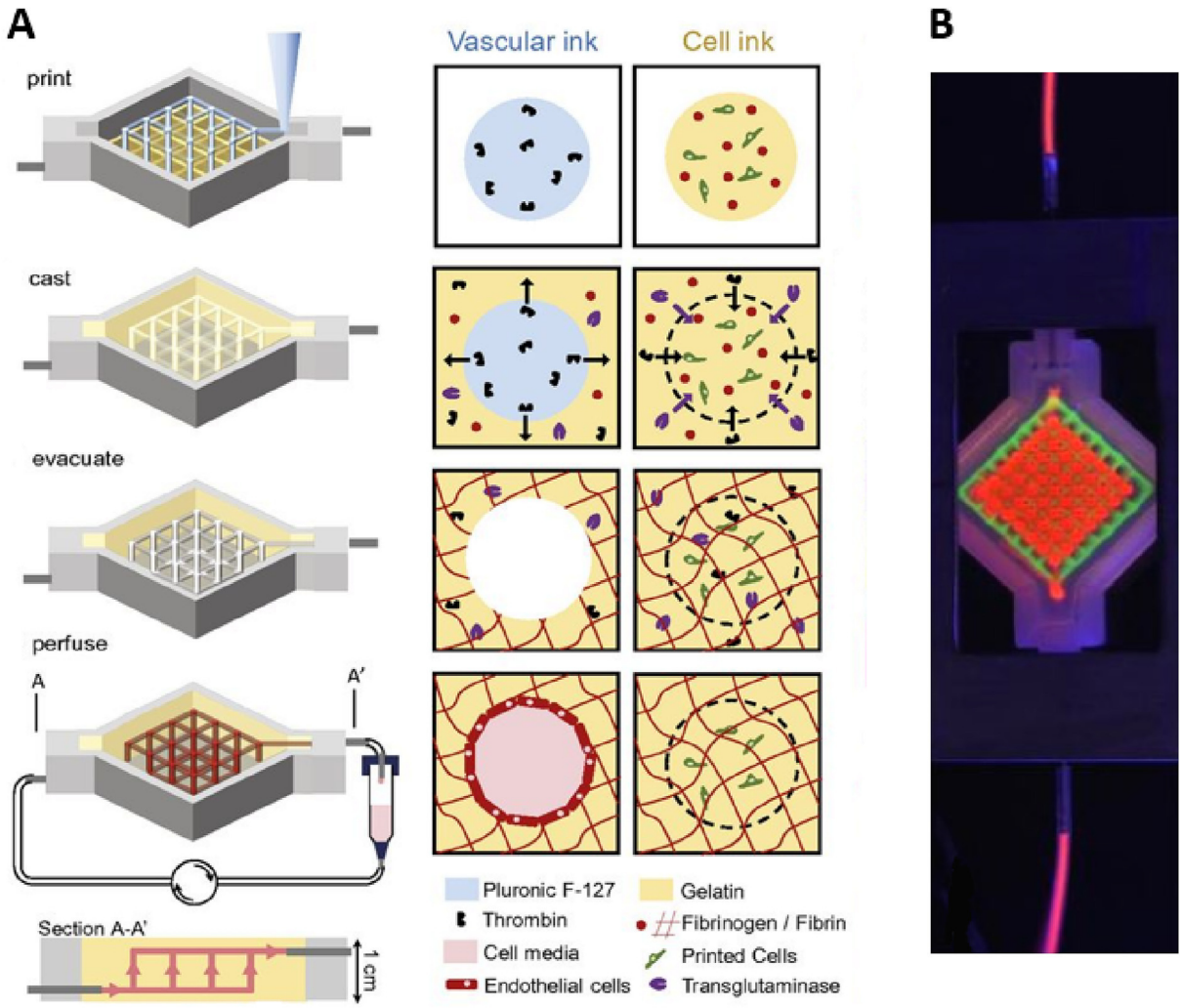

Fig. 19. (A) Illustration of tissue manufacturing process (B) Photograph of a printed tissue construct housed within a perfusion chamber. Perfusion inlet and outlet seen at either end of tissue construct. Adapted from Kolesky et al. [368].

perfusion chip. Fugitive ink, containing F127 and thrombin, and cell-laden inks, containing gelatin, fibrinogen, and hMSC cells, were then printed within the 3D perfusion chip. A composite material containing gelatin, fibrinogen, cells, thrombin and transglutaminase (TG) was then cast over the printed inks, recreating an extracellular matrix. After casting, thrombin converted soluble fibrinogen into insoluble fibrin in the cast matrix. Similarly, TG diffused from the ECM matrix and slowly cross-linked the inner gelatin and fibrin. Upon cooling, the fugitive F127 ink liquefied, leaving behind a pervasive vascular network. This network was seeded with human umbilical vein endothelial cells (HUVECs) to induce endothelialisation and perfused via an external pump. The vascular networks were then perfused with osteogenic media after 6 days of *in vitro* culture. After 30 days, the printed hMSCs expressed osteocalcin in the tissue, with osteocalcin expression found to be highest in areas close to vessels perfused with osteogenic media. Collagen deposition was found within printed filaments and around the circumference of the vasculature. Alizarin staining also revealed a high degree of mineralization within the tissue. In summary, thick (1 cm) vascularized human tissues were created and actively perfused with growth factors to differentiate hMSCs toward an osteogenic lineage in situ over several weeks (>6 weeks).

F127 has also been used in combination with other hydrogels to increase porosity and produce nanostructures. Muller et al. combined diacrylated F127 (F127-DA) with F127 to print chondrocytes, with hyaluronic acid methacrylate (HAMA) added to the bioink to improve mechanical strength [369]. After bioprinting, the F127-DA was UV crosslinked with the acrylate acting as a photocrosslinkable group. This allowed the remaining F127 to be washed out on cooling, subsequently nanostructuring the remaining F127-DA-HAMA network. To increase gel stiffness and to avoid elution of HA during the nanostructuring process, HA was functionalized with methacrylate groups to allow covalent crosslinking between HA and the F127-DA network. Inclusion of 0.5% HAMA increased the compressive modulus from 1.4 kPa in a pure F127-Da scaffold to 5.62 kPa in a F127-DA-HAMA composite. Cell viability was maintained at an elevated level after 14 days in culture in the F127-DA-HAMA composite scaffold, with 79.9% of chondrocytes still alive. Perriman et al. designed a novel pluronic—alginate bioink, which was used in a two-step 3D printing process to engineer bone and cartilage architectures [370]. Specifically, 3D structures containing hMSCs were printed by extruding a shear-thinning, cell-laden F127-alginate composite gel onto a heated stage, resulting in instantaneous solidification via the sol—gel transition of the F127. After printing, $CaCl_2$ crosslinking of alginate and washing steps were performed to allow the F127 to dissolve out of the printed gel structure. The F127 constituent acted as a sacrificial template, creating micron-sized pores and microchannels in the scaffold on dissolution. Optimization experiments found a 13 wt% F127—6 wt% alginate composite hydrogel to have the best print characteristics. MSC-laden 3D printed constructs showed no significant loss in cell viability over 10 days in culture. Encapsulated MSCs were also successfully differentiated into osteoblasts and chondrocytes within the F127-Alginate bioink, with a tracheal ring created.

Byambaa et al. also utilised an extrusion-based bioprinting strategy to fabricate microstructured bone-like tissue constructs, complete with perfusable vascular lumen [371]. To form a perfusable blood vessel in the centre of the construct, a cylinder with 5% gelatin methacryloyl (GelMA) hydrogel at low methacryloyl substitution (GelMALOW) was printed containing HUVECs and hMSCs. The softness of the inner core, prepared with 5% (w/v) GelMALOW, allowed a fast degradation of the hydrogel, leaving an open lumen and a perfusable channel of 500 μm after 12 days of *in vitro* incubation. Three successive layers of cylinders were also initially printed around the soft core using 10% (w/v) high methacryloyl substitution gelatin methacryloyl (GelMAHIGH). The GelMAHIGH was loaded with silicate nanoplatelets to induce osteogenic differentiation of hMSCs into osteoblasts, and contained three different concentrations of covalently conjugated vascular endothelial growth factor (VEGF). The VEGF gradient created different chemical microenvironments, promoting vascular spreading form the central vessel into the surrounding bone niche. Synthetic silicate nanoplatelets were included as bioactive agents that dissociate into products that can trigger osteogenesis (Na^+, Mg^{2+}, $Si(OH)_4$ and Li^+) [372]. It has also been reported that silicate nanoplatelets can induce osteogenic differentiation of encapsulated hMSCs within GelMA hydrogels [373,374]. In this study, it was found that osteogenic differentiation occurred even in the absence of growth factors, with higher concentrations of silicate nanoplatelets resulting in increased calcium deposition after 21 days in culture. Overall, the approach of creating a central lumen and using a composite GelMA-nanoplatelet hydrogel resulted in the creation of a mechanically stable construct. Perfusion with growth media facilitated cell survival, proliferation and osteogenic differentiation over a 21-day period. Compared to conventional approaches such as the use of thermoresponsive hydrogels [15,24] or sacrificial templates [26], this study manged to fabricate a blood vessel through a one-step bioprinting process. Steps such as exposing constructs to temperature changes to remove sacrificial materials were therefore bypassed.

Wang et al. filled a 3D printed bioceramic scaffold with phage nanofibers to try and overcome the challenge of forming vascularized bone tissue [375]. Firstly, a biomimetic bone scaffold, consisting of a biphasic calcium phosphate (BCP) (with a composition of hydroxyapatite (HA) and β-tricalcium phosphate (β-TCP) at a mass ratio of 60/40) was produced via 3D printing. The scaffold showed a uniform structure with interconnected macro-scale pores, and contained micro-scale pores on the scaffold columns. Nanofiber phages expressing RGD (Arg-Gly-Asp) were then combined with chitosan and adhered to the construct pores through electrostatic interactions, with the intention of improving scaffold osteogenesis and vascularisation *in vivo*. The constructs were then implanted in an animal model and native cells invaded the construct to form vasculature, with MSCs undergoing osteogenesis. However, the rate of vascularisation was relatively slow with cell survival within the cell-laden construct impaired as a result.

Costantini et al. printed 3D biomimetic hydrogel scaffolds consisting of differing combinations of gelatin methacrylamide (GelMA), chondroitin sulfate amino ethyl methacrylate (CS-AEMA) and hyaluronic acid methacrylate (HAMA) [376]. Using a two coaxial-needle bioprinting system, they achieved a high cell density (>107 cells ml−1), high cell viability (85 ÷ 90%) and high printing resolution ($\approx$100 μm) post-printing. Bioinks were loaded with MSCs, with addition of 4% alginate and 0.3 M $CaCl_2$ also performed to aid crosslinking. All the employed hydrogels exhibited enhanced chondrogenic differentiation of bone marrow derived-MSCs after 3 weeks of culture in chondrogenic medium. A composite hydrogel of alginate, GelMA and CS-AEMA appeared to be the best candidate for neocartilage formation, as it supported the highest levels of collagen production.

Daly et al. used a novel approach in trying to create bone tissue, by bioprinting a structure more representative of a developmental precursor to adult bone [377]. It was hoped that 3D printing a rudimentary structure would create a template for subsequent organogenesis *in vivo*. An alginate bioink incorporating RGD adhesion peptides was printed along with a network of PCL fibres. Addition of PCL fibres resulted in a near 350-fold increase in construct compressive modulus. The mechanically reinforced template was printed in the geometry of a primitive vertebral body

Please cite this article in press as: G. Turnbull, et al., 3D bioactive composite scaffolds for bone tissue engineering, Bioactive Materials (2017), https://doi.org/10.1016/j.bioactmat.2017.10.001

and implanted *in vivo*. After removal and histological analysis, it was found to support the development of vascularized bone, with trabecular-like endochondral bone and a supporting marrow identified. It was therefore postulated that developmental engineering approaches could be applied to the biofabrication of other solid organs, by bioprinting precursors that have the capacity to mature into their adult counterparts over time *in vivo*.

Silk-based composite hydrogels have also been used in BTE in several forms. Kim et al. fabricated a silk fibroin/hydroxyapatite (SF/HA) composite hydrogel, with hyaluronic acid (HA)-dopamine (DA) surface modification of HA nanoparticles performed to aid distribution of HA content [378]. The composite hydrogel showed excellent cell proliferation, with *in vivo* analysis required to fully examine BTE potential. Park et al. also produced SF composite hydrogels containing HA nanoparticles (NPs) for bone tissue engineering [379]. In this study gamma-ray (γ-ray) irradiation treatment was used to induce rapid chemical crosslinking of a SF solution containing HA NPs, creating a chemically crosslinked SF hydrogel. Compared with compared with the pure SF hydrogels, the SF/HAP composite hydrogels exhibited improved osteogenic differentiation of hMSCs. Ding et al. adapted a hybrid approach, whereby SF hydrogels were used to deliver rat MSCs to a SF scaffold [380]. *In vivo* analysis in a calvarial defect found that encapsulated cells were still viable and actively participating in new bone formation 8 weeks after implantation. The benefits of cell encapsulation were therefore twofold, as both cell viability and cell numbers seeded to the scaffold were increased and maintained *in vivo*.

Within composite hydrogel scaffolds, several studies have examined osteogenic differentiation of MSCs, whilst the potential of human adipose stem cells (hASCs) *in vitro* and *in vivo* has been examined less frequently. Potential benefits of using hASCs over hMSCS include their abundance in adipose tissue and capacity for minimally invasive harvesting [318]. Wang et al. printed a hASC laden 8 wt% alginate and 2 wt% gelatin hydrogel scaffold, with an interwoven grid structure [381]. Cell viability was 90.41% on day 7 of *in vitro* culture, with construct structure maintained. Culture in osteogenic media lead to significant increases in osteogenic gene expression (OSX, RUNX2, and OCN) compared to scaffolds placed in basal media. The hASC laden composite scaffolds were also implanted in mice for 8 weeks. Compared to acellular controls, printed constructs containing cells remained in their original shape, with blood vessels ingrowth into the apertures of the constructs seen. Ectopic bone formation was also seen to occur, with bone matrix seen to replace part of the degraded scaffold material on histology, demonstrating bioactivity within the scaffold. This study therefore showed that 3D bioprinted constructs containing hASCs can promote mineralised bone matrix formation. Maglione et al. demonstrated the osteogenic potential of ASCs further by seeding them onto a chitosan-glycerol phosphate hybrid gel scaffold, which was maintained by in-situ by cross-linking [382]. The scaffolds were implanted into full-thickness mandible defects, with ex vivo histological and micro CT analysis performed after 8 weeks. It was found that ASCs could regenerate bone within the scaffold, with the scaffold able to entrap and maintain cells in situ.

4.5.2. Injectable hydrogels for bone tissue engineering

Injectable hydrogels have attracted significant attention within bone and cartilage tissue-engineering applications. Potential benefits include the ability to perform minimally invasive injections and the capacity to mould hydrogels in situ to match irregular patient defects [383–385].

In one study a chitosan (CS)/β-glycerophosphate (GP)/collagen (Co) injectable scaffold was fabricated by mixing solutions of CS, GP and Co together [386]. SEM found the scaffold to have a porous microstructure, with good biocompatibility and *in vitro* osteogenic differentiation of MSCs also demonstrated. *In vivo* analysis performed in mice found evidence of ectopic bone formation, with neovascularization and differentiation of MSCs toward osteogenic lineage supported after 1 month. The C/GP/Co composite gelled at physiological pH and temperature after 10 min, suggesting this scaffold may be useful as an injectable in situ gel-forming scaffold in bone tissue engineering.

To improve mechanical and osteoinductive properties, bioceramics have also been used in injectable hybrid hydrogels. Dessi et al. included β-tricalcium phosphate (β-TCP) in a β-TCP- chitosan composite hydrogel which was crosslinked with β-glycerophosphate. The hydrogel exhibited a gel-phase transition at body temperature, forming a three-dimensional network with strong rheological properties favouring cellular activity, with enhanced cell adhesion and proliferation demonstrated compared to cells cultured in 12 well-plates [387].

Jiao et al. developed an in situ crosslinkable citric acid-based biodegradable poly (ethylene glycol) maleate citrate (PEGMC)/hydroxyapatite (HA) composite [388]. *In vitro* cell culture with human osteoblast encapsulation was performed, with enhanced DNA content, ALP activity and calcium production found in the hydrogel compared to a control. Ex vivo analysis on a porcine femoral head then demonstrated that PEGMC/HA could be a potentially promising injectable biodegradable bone material for the treatment of femoral head osteonecrosis; in situ crosslinked PEGMC/HA completely filled up and reinforced a femoral head defect (Fig. 20) [389].

Fu et al. created a biomimetic hydrogel composed of triblock PEG-PCL-PEG co-polymer (PECE), collagen and nano-hydroxyapatite (nHA) [390]. SEM demonstrated an interconnected porous structure in the composite. *In vivo* performance was analysed by implantation of the hydrogel in rabbit cranial defects for up to 20 weeks. Compared to self-healing controls, the biodegradable PECE/Collagen/nHA hydrogel had better bone regeneration in addition to good biocompatibility and biodegradability. Huang et al. fabricated an injectable nano-hydroxyapatite (nHA)/glycol chitosan (G-CS)/hyaluronic acid (HLA) composite hydrogel [391]. SEM found the composite hydrogels to exhibit a porous structure (pore size: 100–350 μm) ideal for BTE. *In vitro* culture of osteoblast like cells (MC-3T3-E1) in the hydrogel confirmed cytocompatibility, with cells found to be attached and well spread out after 7 days in culture. Yan et al. produced an injectable and biodegradable composite gel containing hydroxyapatite (HA), gelatin microspheres (GMs) and alginate [392]. This composite hydrogel was calcium-crosslinked in-situ by a previously developed technique [393]; crosslinking relied on gradual release of calcium cations from $CaCO_3$, caused by reaction with glucono-d-lactone (GDL) included in the composite. It was found that inclusion of HA and GMs successfully improved the mechanical properties of the scaffold, with cell viability in the alginate/HA/GMs gel scaffolds also increased compared to alginate controls. The scaffold could elute an embedded anti-biotic, tetracycline hydrochloride, over a 21-day period. However, over 40% of the drug was trapped in the scaffold, perhaps due to the cross-linking processes and resulting structural changes. Nevertheless, the composite seemed promising for local treatment of bone pathologies.

A further study utilised GDL, with an injectable calcium silicate (CS)/sodium alginate (SA) hybrid hydrogel prepared [394]. Once again in situ cross-linking was induced by calcium ions directly released from CS through the addition of GDL. SEM found the scaffolds to have an interconnected porous structure, with pore sizes ranging between 50 and 200 μm. Rat bone mesenchymal stem cells (rtBMSCs) cultured in the hydrogels proliferated well, with hydroxyapatite deposition and ALP activity found, suggesting

Please cite this article in press as: G. Turnbull, et al., 3D bioactive composite scaffolds for bone tissue engineering, Bioactive Materials (2017), https://doi.org/10.1016/j.bioactmat.2017.10.001

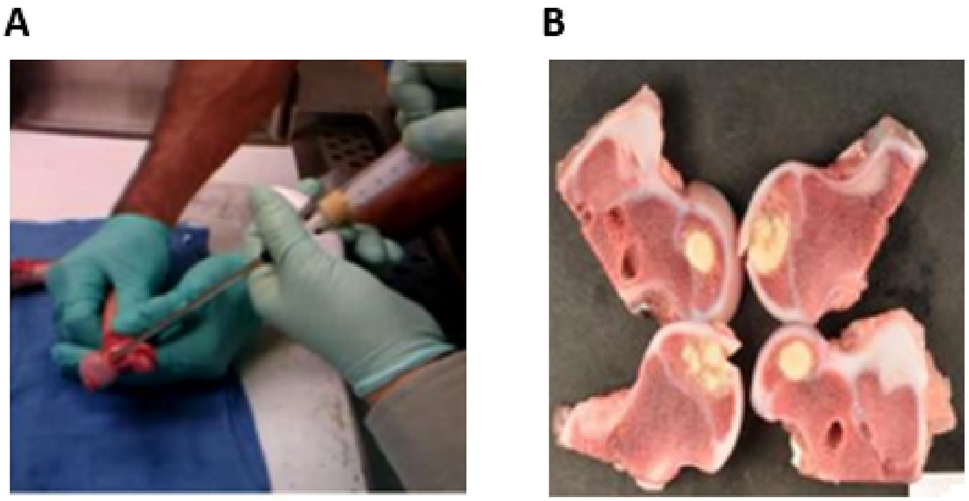

Fig. 20. (A) PEGMC/HA composite being injected into collapsed femoral head; and (B)) Cross-sectional view of femoral head with injected composite visible. Crosslinking was achieved within 5 min of injection. Adapted from Jiao et al. [388].

osteogenic potential. The hydrogel was also able to promote angiogenesis of human umbilical vein endothelial cells. The CS/SA composite hydrogel seemed well suited to BTE applications, due to a porous 3D-structure, injectable properties and a capability to support osteogenesis and angiogenesis.

Zhao et al. created an injectable calcium phosphate-alginate hydrogel composite with mechanical properties matching cancellous bone [395]. This was achieved through mixing a calcium phosphate cement (CPC) paste with hydrogel microbeads encapsulating human umbilical cord mesenchymal stem cells (hUCMSCs). The composite seemed cell-friendly, with viability after injection matching that in pure alginate and prior to injection. Mechanical properties including elastic modulus, work of fracture and flexural strength of the construct matched the reported values of cancellous bone, and were much higher than many previous injectable polymeric and hydrogel carriers. hUCMSCs in the injectable constructs also osteodifferentiated, with high ALP, osteocalcin and collagen type I expression found after 7 days in culture. In fact, mineralization by hUCMSCs after 14 days was 100-fold that found after 1 day *in vitro*. In conclusion, a fully-injectable, mechanically-strong, stem cell-CPC scaffold construct was developed.

A further study produced an injectable thermosensitive hydrogel containing zinc-doped chitosan/nanohydroxyapatite/beta-glycerophosphate (Zn-CS/nHA/β-GP) for bone tissue repair *in vitro* and *in vivo* [396]. The hydrogels exhibited sol-gel transition at 37 °C, ideal for use in clinical interventions. The presence of nHA in the Zn-CS/nHA/β-GP hydrogel enhanced swelling, protein adsorption, and exogenous biomineralization. Osteoblast differentiation under osteogenic conditions *in vitro* and bone formation *in vivo* in a rat bone defect was also accelerated by the presence of nHA, with increased deposition of apatite and collagen found. This study therefore further underlined the importance of nHA in composite hydrogels for BTE.

Further studies have taken advantage of nanocomposite hydrogels [397,398], with one in particular developing an injectable hydrogel composed of chitin, poly (butylene succinate) (PBSu), fibrin nanoparticles (FNPs) and magnesium-doped bioglass (MBG) [399]. Composite gels with 2% FNPs and 2% MBG were found to be non-toxic to cells, leading to *in vitro* analysis. Delivery of the composite gel to aortic tissue lead to enhanced sprouting of blood vessels, with osteoblastic differentiation, expression of ALP and osteocalcin confirming the osteoinductive property of MBG. The osteogenic and vasculogenic potential of this composite hydrogel would therefore seem promising for bone regeneration. Miri et al. also incorporated bioactive glass into a composite scaffold, creating an injectable dense collagen (IDC)- Bioglass) (IDC-BG) hybrid gel scaffold [400]. *In vitro* mineralization of IDC-BG gels was confirmed as early as day 1 in simulated body fluid, which progressively increased up to day 14. Implantation in adult rats found mineralization, neovascularization and cell infiltration into the scaffolds was enhanced by the addition of BG. After 21 days *in vivo*, there was evidence of remodelling of granulation tissue into woven bone-like tissue in IDC-BG scaffolds in ectopic sites. The IDC-BG composite therefore appeared to be a malleable and osteoinductive bone graft that mineralizes under physiological conditions.

4.5.3. Injectable hydrogels for cartilage regeneration

Several natural and synthetic bioactive materials have been used to create injectable hydrogel scaffolds for cartilage regeneration. Examples that have been used successfully include hyaluronic acid, chitosan, collagen, elastin, alginate, glycopeptides [401–407] and synthetic polymers [408,409].

Hyaluronic acid has a known ability to aid chondrocyte differentiation, ECM deposition and proliferation [410–413]. These effects are at least partly achieved by the presence of chondrocyte surface receptors including CD44, which directly bind to hyaluronic acid and internalize it via endocytosis [414–416]. Park et al. created an injectable hyaluronic acid (HLA) and methacrylated glycol chitosan (MeGC) hydrogel by photo-crosslinking with a riboflavin photoinitiator under visible light [417]. Increasing the crosslinking time from 40 to 600 s significantly enhanced the compressive modulus of the hydrogels from 11 to 17 kPa; however, encapsulated cell viability also reduced to 60–65% (from 90% after 120 s) with prolonged crosslinking. Compared to MeGC controls, incorporation of HLA in MeGC hydrogels increased the proliferation and deposition of cartilaginous extracellular matrix by encapsulated chondrocytes, with high cell viability of ~80–87% over a 21-day culture period seen. Given these results, this hydrogel would appear to have exciting potential for cartilage regeneration.

Guo et al. prepared hydrogels of collagen/chondroitin sulfate/HLA for cartilage regeneration [418]. This was achieved via two simultaneous processes of collagen self-assembly and crosslinking polymerization of chondroitin sulfate-methacrylate (CSMA) and

hyaluronic acid-methacrylate. An interpenetrating polymeric network (IPN) structure was achieved through this process, partly replicating the structure of native cartilage extracellular matrix. The composite hydrogel was found *in vitro* to upregulate cartilage-specific gene expression and promote chondrocyte secretion of glycosaminoglycans and type II collagen.

Yu et al. created an injectable hyaluronic acid/PEG (HLA/PEG) hydrogel through integrating two cross-linking processes, including firstly enzymatic crosslinking and subsequent Diels–Alder click chemistry [419]. Enzymatic crosslinking resulted in fast gelation of the HLA/PEG hydrogel in 5 min, leading to the formation of an injectable material. ATDC-5 chondrocytes encapsulated in the hydrogel showed high metabolic viability and proliferation. From a mechanical point of view, the hydrogel could recover from repeated compression to restore initial shape. Taking the cell-friendly and anti-fatigue properties together, this composite could have potential for cartilage regeneration with further *in vitro* analysis required.

Chen et al. recently developed an injectable HLA/RGD-functionalized pectin hydrogel for cartilage tissue engineering [420]. Pectins are natural polysaccharides found in most primary cell walls and have excellent hydrophilic properties. They have been used within bone and cartilage regeneration to act an ECM alternative, helping to immobilize cells [421,422]. *In vitro* analysis found significant production of collagen, glycosaminoglycans and aggrecans with high cell viability after encapsulation in the HLA/RGD hydrogel. After 8 weeks of implantation in mice, the scaffold was well tolerated, with minimal inflammation and integration with surrounding subcutaneous tissues seen.

Choi et al. created an injectable type-II collagen (Col II) and chondroitin sulfate (CS) composite hydrogel for cartilage regeneration [423]. The composite gel was crosslinked by exposure to visible blue light (VBL) in the presence of riboflavin. Whilst unmodified chitosan hydrogel supported proliferation and deposition of cartilaginous ECM by encapsulated chondrocytes and mesenchymal stem cells, incorporation of Col II or CS into chitosan hydrogels further increased chondrogenesis. Col II was found have the biggest impact on chondrogenesis and cell proliferation *in vitro*, thought to be related to integrin α10 binding to Col II, increasing cell-matrix adhesion.

Alginate has also been utilised in composite hydrogels for cartilage regeneration with some success. One study combined oxidized alginate and hyaluronic acid in a composite hydrogel (Al/HLA), with *in vivo* analysis in mice performed [424]. Six weeks after chondrocyte-loaded AL/HLA gels were injected subcutaneously into mice, effective cartilage regeneration was observed on histological analysis. Moreover, substantial secretion of sulphated glycosaminoglycans and expression of chondrogenic marker genes was found, with significantly better results demonstrated compared to control scaffolds. A similar scaffold composed of alginate and low molecular weight hyaluronic acid was produced by Park et al., with calcium crosslinking also performed [425]. Once again, hyaluronic acid bound to alginate triggered chondrocyte differentiation to a much higher degree than found in pure alginate scaffolds. Scaffold stiffness was also found to be critical in triggering chondrocyte differentiation, with low scaffold stiffness leading to diminished chondrocyte differentiation. It was therefore concluded that hydrogels require defined polymer compositions and mechanical properties, to best regulate chondrocyte differentiation and phenotype.

Lee et al. created an injectable collagen/hyaluronic acid/fibrinogen composite gel, which they inserted into rabbit osteochondral knee defects along with MSCs. Histological analysis of the scaffolds found glycosaminoglycans and type II collagen production within the extracellular matrix. After twenty-four weeks, the defects had been repaired with hyaline-like cartilage, demonstrating the strong therapeutic potential of this composite hydrogel [426].

Composite scaffolds for cartilage regeneration have also been produced from degradable synthetic polymers such as polyethylene glycol (PEG) and poly(L-glutamic acid) [408,427–430]. Hyaluronic acid/PEG-based injectable hydrogels were prepared via a dual cross-linking by Dubbini et al., with thermal gelation at occurring at 37 °C [431]. Through altering polymer content, degree of vinyl sulfonation and degree of thiolation it was possible to alter the gelation kinetics, mechanical properties, swelling and degradation times of the scaffolds. The composite hydrogels also supported MSC and fibroblast growth *in vitro* over 21 days.

5. Barriers to clinical translation

Despite extensive research and several thousand papers published on bone and cartilage tissue regeneration, autologous bone grafts continue to represent the gold standard treatment for critical-sized bone defects. Several factors have contributed to the slow translation of research from the bench side to the bedside, including technical, collaborative and regulatory issues [192,432,433].

5.1. Scientific and technological challenges

Addressing all the technical demands faced by a BTE scaffold is a complex task, with success in one design aspect often coming at the expense of performance in another area. Current technical challenges include:

- Choice of scaffold cell content [434,435]. Whilst inclusion of cells in bone and cartilage regenerative therapies is undoubtedly beneficial, the most effective cell type remains unclear. Mesenchymal stem cells have frequently been used clinically and experimentally with varying degrees of success depending on method of delivery. However, there is potential risk of morbidity associated with their collection from bone marrow, and their regenerative capacity decreases with patient age [436,437]. Embryonic (ESCs) and induced-pluripotent stem cells (iPSCs) have also been investigated. These cells are not ordinarily involved in adult tissue repair and can require significant laboratory manipulation. Further limitations include teratoma risk and ethical considerations [438,439].
- Introducing sufficient scaffold vascularisation [13,302,368,371]. In the absence of a vascular network, cells are dependent on diffusion for survival [361]. Whilst larger vessels have been fabricated, capillaries have yet to be 3D printed, which leaves constructs dependent on infiltration of micro-vessels *in vitro* to ensure cell viability. Unfortunately, infiltration of microvessels often lacks depth of penetration, limiting the size of viable bone construct that can be implanted [366,367].
- Achieving precise control over scaffold degradation [132,251,440]. If a scaffold degrades too quickly, mechanical failure can occur. Similarly, if a scaffold does not degrade sufficiently quickly, an inflammatory response could be triggered, impairing tissue regeneration. Balancing degradation levels with new host tissue formation has so far proved challenging [26].
- Improving structural biomimetic properties [277,334,374,387,441,442]. Although gross 3D scaffold geometry for individual patient defects can be identified by magnetic resonance or computed tomography imaging, successful replication of anatomy at the microscale remains challenging with current fabrication methods. The current standard STL file

Please cite this article in press as: G. Turnbull, et al., 3D bioactive composite scaffolds for bone tissue engineering, Bioactive Materials (2017), https://doi.org/10.1016/j.bioactmat.2017.10.001

format used to control 3D bioprinters faces limitations in ability to describe internal pore architecture [443].
- Improving scaffold mechanical properties [313,355,442]. Tailoring scaffold mechanical performance to individual defects remains difficult, as anatomical loading conditions for individual defects are difficult to quantify. Achieving satisfactory mechanical performance requires a range of properties to be addressed during scaffold fabrication, including compressive, tensile, elastic and fatigue resistance, and successful replication of these properties can help stimulate osteogenesis and perhaps facilitate degrees of load bearing to occur [55,80,169,440,442].
- Scaling up biofabrication and scaffold production to treat large scale defects and a potentially high number of patients [432,444]. High resolution bioprinting methods including laser-assisted and inkjet techniques currently provide low volume, smaller-scale manufacturing solutions. However, extrusion bioprinting may offer a larger scale method for producing structures suitable for clinical use [445].

Selection of the optimum scaffold fabrication method therefore remains challenging, due to the extensive variety of manufacturing methods, biomaterials, cell types and growth factors that have been investigated, with conflicting data available in some cases. Producing a scaffold that can address all technical requirements is also extremely challenging. For example, as scaffold porosity is increased to improve cell migration and diffusion of nutrients, scaffold mechanical strength is often reduced [445].

5.2. Translational challenges

In addition to technological and scientific challenges, significant research and development barriers to translation also exist.

- Obtaining external funding and grants for product development represents a significant hurdle. The cost of performing preclinical and human clinical trials is substantial, and can extend to hundreds of millions of dollars [446,447]. Despite considerable time and financial investment, there are also no guarantees of product approval. A trail of bone graft material containing BMP for spinal fusion was ultimately rejected, despite 5 year follow up of nearly 500 patients [448]. Following significant cost and time investment in clinical trials, approval is only given for a specific scaffold composition to be used for a specific clinical indication. Therefore, if an individual scaffold is to be licenced for use in both tibial non-union and lumbar spine fusion, it may have to undergo separate clinical trials despite potentially being unchanged as a product. The inclusion of a drug in a scaffold will also necessitate further human clinical trials, with further regulatory and financial challenges associated. As a result, some 20–50% of drug candidates fail to translate from preclinical trials to human clinical trials, potentially costing hundreds of millions of dollars [449,450].
- The time and cost of meeting complex regulation has also increased substantially in recent decades. The resources of large multinational firms are often required to deliver new products to large patient populations as a result [451].
- There is therefore a potential lack of “first mover advantage” in that research pioneers can be faced simultaneously with regulatory and funding challenges, at the same time as attempting to resolve scientific and technical problems that emerge [451].

There are further constraints faced by researchers undertaking collaborative, translational research. Through close collaboration with orthopaedic clinicians, as the end users of BTE constructs, it is hoped that 3D bioprinting and biofabrication strategies can undergo clinical translation in a streamlined manner from the “bench to the bedside”. However, it can be difficult for surgeons to spend quality time in the laboratory as an ageing population is leading to rising clinical demand and health service financial pressures. In general, as research translational potential increases, costs increase and progress slows. This also has challenges for academics, who may have to produce a steady stream of data and publications as evidence of productivity to maintain job security and career progression [192,449].

5.3. Ethical issues

Whilst biofabrication approaches including 3D bioprinting offer great hope for the future, many of the technologies in use are expensive and ethical issues may be associated with their future implementation.

- Despite the promise and hype of tissue and organs being printed on-demand for specific indications, the cost of implementing the technology may lead to only those who can afford to pay for their ‘own’ tissue or organs benefitting. As a result, biofabrication therapies may initially face limited translation into wider medical practice, with usage determined by individual patient access to funding [452,453].
- The risks associated with placing bioprinted cells into the human body are currently difficult to quantify due to a lack of long-term *in vivo* studies. Potential for teratoma formation and dislodgement and migration of cells from implanted constructs could exist depending on cell types used. Further questions remain to be addressed, such as long term biomaterial degradation, tissue integration and biocompatibility [454].
- Stratifying the clinical risk of using a technology developed from personalized cell sources and biomaterials to the entire population could be difficult to achieve.
- Not all patients will find it acceptable for their cells to be mixed with biomaterials that may be animal derived.
- As the technology develops, the boundaries of what can be achieved may advance such that new types of tissues and organs can be produced with superior functionality to the human body. Robust regulation and governance will need to develop to ensure responsible, safe and ethical use of the technology [452].

5.4. Future perspectives

It has been suggested by Mironov et al. that the remaining challenges faced in creating complex tissue and organ constructs include “achieving the desired level of cell density, effective vascularisation and accelerated tissue maturation” [455]. A number of developments would be beneficial in helping work towards these challenges:

- A scalable method of directing osteogenic differentiation would be advantageous, potentially reducing reliance on differentiating media and increasing cost—effectiveness. As an example, Dalby's team in Glasgow used nanoscale vibrations delivered by a nanovibrational bioreactor to differentiate MSCs seeded in collagen gels into mineralised tissue in 3D. This technology would appear to be readily scalable, compatible with 3D scaffolds, easy to maintain compared to rotary/perfusion chamber bioreactors and could be used “off the shelf” [456].
- It is already well demonstrated that MSC spheroids exhibit enhanced *in vitro* and *in vivo* osteoregenerative potential compared to MSCs cultured in monolayer. Increasing incorporation of organoids and spheroids into bioprinting could help

Please cite this article in press as: G. Turnbull, et al., 3D bioactive composite scaffolds for bone tissue engineering, Bioactive Materials (2017), https://doi.org/10.1016/j.bioactmat.2017.10.001

accelerate the growth of printed constructs towards clinically relevant, functional tissue [86,367,455,457,458].

- Development of smart hydrogels, with tailored and tuneable properties such as mechanical stiffness, degradation rates and increased bioactivity could help expedite maturation of 3D constructs [459].
- Increasingly biomimetic construct microarchitectures may be produced by incorporating approaches such as sophisticated clinical imaging and mathematical modelling into manufacturing of scaffolds [460].
- Inclusion of increasingly novel biological cues into bioprinted constructs could also help expedite their maturation towards complex, biologically functional tissue. In addition to growth factors, microRNAs could have a role to play in this area. These small encoding RNAs have been shown to be capable of differentiating MSCs into osteoblasts and chondrocytes by regulating post-transcription gene expression. Although understanding is developing, spatially 3D printing miRNAs into constructs could be used to help drive vascularisation and formation of osteochondral tissue in 3D constructs [461,462].
- Surface modification also has a significant role to play in the future development of biomaterials and tissue engineering scaffolds for bone and cartilage tissue repair and regeneration. We have already seen beneficial effects on osteogenic differentiation caused by immobilisation of biological factors such as BMP, collagen, apatite and polydopamine on scaffold surfaces [121,282,303,306,463]. Engineering micro- and nanometre surface topography into scaffolds is also critical for promoting osteoinduction and directing cellular adhesion, spreading, and proliferation. Nano-topography significantly influences osteoconductivity and osseointegration of BTE constructs. It has also been found that osteoblasts demonstrate increased cell adhesion and proliferation, ALP activity, and enhanced expression of osteoblast differentiation markers including RunX2, osteocalcin, and bone sialoprotein (BSP) on nano-featured biomaterials [464–466].
- Biomaterial surface topography and micro/nano-scale architecture has also been found to play a significant role in modulating and activating the immune system. Cao et al. demonstrated increased tissue regeneration and decreased inflammatory reaction in scaffolds with aligned fibre topography compared to scaffolds with randomly aligned fibres [467]. Biomaterial surface treatments may also be used to reduce local degradation or to deliver bioactive molecules [468].
- Scaffold-induced cell homing is a further approach that may benefit bone and cartilage regeneration in future. Various methods have been investigated to achieve enhanced cell homing to defect sites. Through controlled release of chemokines responsible for MSC homing, it is possible that bioprinted scaffolds placed into defects will be able to better recruit local cells for tissue regeneration. Although the mechanisms of cell mobilization have yet to be fully understood, several key molecules have been identified as important factors in attracting MSCs, including specific chemokine receptors (e.g., CCR1, CXCR4, CXCR5 and CXCR6) [468,469].
- Ultimately, increasing biofabrication scalability will require development of an integrated, standardized biofabrication line. Mironov et al. suggest that “It is not sufficient to develop just one robotic device—a bioprinter … [it] will require the development of series of integrated automated robotic devices, or an organ biofabrication line” [455]. It will therefore be necessary to develop current biofabrication platforms from novel and bespoke systems towards high throughput, standardized systems suitable for clinical practice. This remains a significant challenge that will have to be surmounted to allow biofabrication to be adapted into larger scale clinical practice.
- Finally, to advance and scale-up bioprinting-based technologies and models, long-term, cross-discipline collaboration is necessary to enable sharing of expertise and increase research efficiency.

6. Conclusions

Critical-sized bone defects have increasing prevalence and remain a great challenge for both tissue engineers and orthopaedic surgeons to repair, despite substantial and novel research into their treatment. Current challenges include tailoring scaffold degradation, improving structural biomimicry, incorporating sufficient vascularisation and scaling up of scaffold production to treat large scale defects in a potentially high number of patients.

As scaffold manufacture has increasingly looked to include composite materials with increased bioactivity, we have seen desirable mechanical and cell-friendly properties combined into single tissue-engineered constructs. Several examples of successful bone and cartilage constructs with clinical translation have been developed as a result, with ceramic and polymer composites perhaps having the greatest success. To maximise osteogenesis and chondrogenesis in future, it will be necessary to achieve yet closer replication of natural mechanical and biochemical stimuli that cells are exposed to, in addition to increasing construct vascularisation. This may be achieved in part through advances in biomaterials, scaffold manufacturing techniques and computational modelling. More effective methods are also required to streamline the process of cell isolation, culturing and seeding into constructs. This is a labour and time intensive process at present, although advances in bioreactor technology may increase efficiency. However, the quickest route to success may be to utilise the natural bioreactor provided by native bone tissue, which has extraordinary regenerative capacity. In this way, *in vivo* bone and cartilage tissue regeneration may be maximised when combined with increasingly bioactive, anatomically sophisticated scaffolds capable of recruiting host cells.

3D biofabrication and bioprinting technologies offer increasingly precise control over construct microarchitecture and spatial content. When combined with the developing array of available bioactive materials, growth factors, functionalization techniques and biomimetic scaffold designs, the potential for creating complex BTE scaffolds tailored to patient-specific applications in the future is vast. This also offers hope for the treatment of a variety of challenging conditions, including osteonecorosis, osteoporosis and critical bone defects. As scalability and manufacturing methods continue to develop, it is hoped that treatment tailored to the individual patient can be produced in an increasingly cost effective, efficient and reproducible manner in the future.

Declaration of conflicting interests

The authors declare no potential conflicts of interest with respect to the research, authorship, and/or publication of this article.

Funding

The authors received no financial support for the research, authorship, and/or publication of this article.

References

[1] R. Kapferer, Hippocrates, the Nature of Bones, 1938.

[2] O. Ashman, A.M. Phillips, Treatment of non-unions with bone defects: which option and why? Injury 44 (Suppl 1) (2013) S43–S45.
[3] P.H. Thaller, et al., Limb lengthening with fully implantable magnetically actuated mechanical nails (PHENIX((R)))-preliminary results, Injury 45 (Suppl 1) (2014) S60–S65.
[4] A.S. Greenwald, et al., Bone-graft substitutes: facts, fictions, and applications, J. Bone Jt. Surg. Am. 83-A (Suppl 2 Pt 2) (2001) 98–103.
[5] O. Faour, et al., The use of bone graft substitutes in large cancellous voids: any specific needs? Injury 42 (Suppl 2) (2011) S87–S90.
[6] A.S. Brydone, D. Meek, S. Maclaine, Bone grafting, orthopaedic biomaterials, and the clinical need for bone engineering, Proc. Inst. Mech. Eng. H. 224 (12) (2010) 1329–1343.
[7] S.J. Hollister, Porous scaffold design for tissue engineering, Nat. Mater 4 (7) (2005) 518–524.
[8] E. Garcia-Gareta, M.J. Coathup, G.W. Blunn, Osteoinduction of bone grafting materials for bone repair and regeneration, Bone 81 (2015) 112–121.
[9] A. Higgins, et al., EXOGEN ultrasound bone healing system for long bone fractures with non-union or delayed healing: a NICE medical technology guidance, Appl. Health Econ. Health Policy 12 (5) (2014) 477–484.
[10] R.J. O'Keefe, J. Mao, Bone tissue engineering and regeneration: from discovery to the clinic–an overview, Tissue Eng. Part B Rev. 17 (6) (2011) 389–392.
[11] S. Bose, M. Roy, A. Bandyopadhyay, Recent advances in bone tissue engineering scaffolds, Trends Biotechnol. 30 (10) (2012) 546–554.
[12] S. Wu, et al., Biomimetic porous scaffolds for bone tissue engineering, Mater. Sci. Eng. R Rep. 80 (2014) 1–36.
[13] M.J. Webber, et al., A perspective on the clinical translation of scaffolds for tissue engineering, Ann. Biomed. Eng. 43 (3) (2015) 641–656.
[14] A.L. Boskey, R. Roy, Cell culture systems for studies of bone and tooth mineralization, Chem. Rev. 108 (11) (2008) 4716–4733.
[15] M.F. Young, Bone matrix proteins: their function, regulation, and relationship to osteoporosis, Osteoporos. Int. 14 (Suppl 3) (2003) S35–S42.
[16] A.L. Boskey, Bone composition: relationship to bone fragility and antiosteoporotic drug effects, BoneKEy Rep. 2 (2013).
[17] S.S. Kim, et al., Poly(lactide-co-glycolide)/hydroxyapatite composite scaffolds for bone tissue engineering, Biomaterials 27 (8) (2006) 1399–1409.
[18] L. Hench, Opening paper 2015- some comments on Bioglass: four eras of discovery and development, Biomed. glasses 1 (1) (2015), https://doi.org/10.1515/bglass-2015-0001. Retrieved 10 Nov. 2017.
[19] T. Albrektsson, C. Johansson, Osteoinduction, osteoconduction and osseointegration, Eur. Spine J. 10 (Suppl 2) (2001) S96–S101.
[20] A.R. Vaccaro, The role of the osteoconductive scaffold in synthetic bone graft, Orthopedics 25 (5 Suppl) (2002) s571–s578.
[21] D.W. Hutmacher, Scaffolds in tissue engineering bone and cartilage, Biomaterials 21 (24) (2000) 2529–2543.
[22] C. Gao, et al., Current progress in bioactive ceramic scaffolds for bone repair and regeneration, Int. J. Mol. Sci. 15 (3) (2014) 4714–4732.
[23] Q.L. Loh, C. Choong, Three-dimensional scaffolds for tissue engineering applications: role of porosity and pore size, Tissue Eng. Part B Rev. 19 (6) (2013) 485–502.
[24] A.W. Lloyd, Interfacial bioengineering to enhance surface biocompatibility, Med. device Technol. 13 (1) (2001) 18–21.
[25] Z. Dong, Y. Li, Q. Zou, Degradation and biocompatibility of porous nano-hydroxyapatite/polyurethane composite scaffold for bone tissue engineering, Appl. Surf. Sci. 255 (12) (2009) 6087–6091.
[26] P.M. Mountziaris, A.G. Mikos, Modulation of the inflammatory response for enhanced bone tissue regeneration, Tissue Eng. Part B Rev. 14 (2) (2008) 179–186.
[27] X. Cao, D. Chen, The BMP signaling and in vivo bone formation, Gene 357 (1) (2005) 1–8.
[28] E. Leblanc, et al., BMP-9-induced muscle heterotopic ossification requires changes to the skeletal muscle microenvironment, J. Bone Min. Res. 26 (6) (2011) 1166–1177.
[29] C. Li, et al., Electrospun silk-BMP-2 scaffolds for bone tissue engineering, Biomaterials 27 (16) (2006) 3115–3124.
[30] H. Nie, C.H. Wang, Fabrication and characterization of PLGA/HAp composite scaffolds for delivery of BMP-2 plasmid DNA, J. Control Release 120 (1–2) (2007) 111–121.
[31] S. Shi, et al., RhBMP-2 microspheres-loaded chitosan/collagen scaffold enhanced osseointegration: an experiment in dog, J. Biomater. Appl. 23 (4) (2009) 331–346.
[32] A. Cipitria, et al., BMP delivery complements the guiding effect of scaffold architecture without altering bone microstructure in critical-sized long bone defects: a multiscale analysis, Acta Biomater. 23 (2015) 282–294.
[33] J.T. Schantz, H. Chim, M. Whiteman, Cell guidance in tissue engineering: SDF-1 mediates site-directed homing of mesenchymal stem cells within three-dimensional polycaprolactone scaffolds, Tissue Eng. 13 (11) (2007) 2615–2624.
[34] E. Wernike, et al., VEGF incorporated into calcium phosphate ceramics promotes vascularisation and bone formation in vivo, Eur. Cell Mater. 19 (2010) 30–40.
[35] D. Kaigler, et al., VEGF scaffolds enhance angiogenesis and bone regeneration in irradiated osseous defects, J. Bone Min. Res. 21 (5) (2006) 735–744.
[36] R. Dimitriou, E. Tsiridis, P.V. Giannoudis, Current concepts of molecular aspects of bone healing, Injury 36 (12) (2005) 1392–1404.
[37] A.J. Salgado, O.P. Coutinho, R.L. Reis, Bone tissue engineering: state of the art and future trends, Macromol. Biosci. 4 (8) (2004) 743–765.
[38] C. Zhang, et al., A study on a tissue-engineered bone using rhBMP-2 induced periosteal cells with a porous nano-hydroxyapatite/collagen/poly(L-lactic acid) scaffold, Biomed. Mater. 1 (2) (2006) 56–62.
[39] K.A. Hing, et al., Mediation of bone ingrowth in porous hydroxyapatite bone graft substitutes, J. Biomed. Mater. Res. A 68 (1) (2004) 187–200.
[40] F. Barrere, et al., Advanced biomaterials for skeletal tissue regeneration: instructive and smart functions, Mater. Sci. Eng. R Rep. 59 (1) (2008) 38–71.
[41] J. Zeltinger, et al., Effect of pore size and void fraction on cellular adhesion, proliferation, and matrix deposition, Tissue Eng. 7 (5) (2001) 557–572.
[42] F.J. O'Brien, et al., The effect of pore size on cell adhesion in collagen-GAG scaffolds, Biomaterials 26 (4) (2005) 433–441.
[43] S. Hulbert, et al., Potential of ceramic materials as permanently implantable skeletal prostheses, J. Biomed. Mater. Res. 4 (3) (1970) 433–456.
[44] Y. Kuboki, Q. Jin, H. Takita, Geometry of carriers controlling phenotypic expression in BMP-induced osteogenesis and chondrogenesis, J. Bone Jt. Surg. Am. 83-A (Suppl 1(Pt 2)) (2001) S105–S115.
[45] E. Tsuruga, et al., Pore size of porous hydroxyapatite as the cell-substratum controls BMP-induced osteogenesis, J. Biochem. 121 (2) (1997) 317–324.
[46] C.M. Walthers, et al., The effect of scaffold macroporosity on angiogenesis and cell survival in tissue-engineered smooth muscle, Biomaterials 35 (19) (2014) 5129–5137.
[47] M. Rouahi, et al., Influence of hydroxyapatite microstructure on human bone cell response, J. Biomed. Mater. Res. A 78 (2) (2006) 222–235.
[48] A.L. Rosa, M.M. Beloti, R. van Noort, Osteoblastic differentiation of cultured rat bone marrow cells on hydroxyapatite with different surface topography, Dent. Mater. 19 (8) (2003) 768–772.
[49] P. Habibovic, et al., 3D microenvironment as essential element for osteoinduction by biomaterials, Biomaterials 26 (17) (2005) 3565–3575.
[50] K. Whang, et al., Engineering bone regeneration with bioabsorbable scaffolds with novel microarchitecture, Tissue Eng. 5 (1) (1999) 35–51.
[51] K. Doi, et al., Development of implant/interconnected porous hydroxyapatite complex as new concept graft material, PLoS One 7 (11) (2012) e49051.
[52] A. Boccaccio, et al., Finite element method (FEM), mechanobiology and biomimetic scaffolds in bone tissue engineering, Int. J. Biol. Sci. 7 (1) (2011) 112–132.
[53] D.J. Kelly, P.J. Prendergast, Prediction of the optimal mechanical properties for a scaffold used in osteochondral defect repair, Tissue Eng. 12 (9) (2006) 2509–2519.
[54] C. Sandino, D. Lacroix, A dynamical study of the mechanical stimuli and tissue differentiation within a CaP scaffold based on micro-CT finite element models, Biomech. Model Mechanobiol. 10 (4) (2011) 565–576.
[55] G. Chen, et al., 3D scaffolds with different stiffness but the same microstructure for bone tissue engineering, ACS Appl. Mater. Interfaces 7 (29) (2015) 15790–15802.
[56] R.G.M. Breuls, T.U. Jiya, T.H. Smit, Scaffold stiffness influences cell behavior: opportunities for skeletal tissue engineering, Open Orthop. J. 2 (2008) 103–109.
[57] L. Polo-Corrales, M. Latorre-Esteves, J.E. Ramirez-Vick, Scaffold design for bone regeneration, J. Nanosci. Nanotechnol. 14 (1) (2014) 15–56.
[58] D. Howk, T.M. Chu, Design variables for mechanical properties of bone tissue scaffolds, Biomed. Sci. Instrum. 42 (2006) 278–283.
[59] D.W. Hutmacher, et al., State of the art and future directions of scaffold-based bone engineering from a biomaterials perspective, J. Tissue Eng. Regen. Med. 1 (4) (2007) 245–260.
[60] T. Kokubo, H.M. Kim, M. Kawashita, Novel bioactive materials with different mechanical properties, Biomaterials 24 (13) (2003) 2161–2175.
[61] M. Amaral, et al., Densification route and mechanical properties of Si3N4-bioglass biocomposites, Biomaterials 23 (3) (2002) 857–862.
[62] Q. Chen, C. Zhu, G.A. Thouas, Progress and challenges in biomaterials used for bone tissue engineering: bioactive glasses and elastomeric composites, Prog. Biomater. 1 (1) (2012) 2.
[63] A. Manke, L. Wang, Y. Rojanasakul, Mechanisms of nanoparticle-induced oxidative stress and toxicity, BioMed Res. Int. 2013 (2013) 15.
[64] M. Mastrogiacomo, et al., Tissue engineering of bone: search for a better scaffold, Orthod. Craniofac Res. 8 (4) (2005) 277–284.
[65] B.P. Chan, K.W. Leong, Scaffolding in tissue engineering: general approaches and tissue-specific considerations, Eur. Spine J. 17 (Suppl 4) (2008) 467–479.
[66] S.J. Hollister, R.D. Maddox, J.M. Taboas, Optimal design and fabrication of scaffolds to mimic tissue properties and satisfy biological constraints, Biomaterials 23 (20) (2002) 4095–4103.
[67] T. Johnson, et al., Fabrication of highly porous tissue-engineering scaffolds using selective spherical porogens, Biomed. Mater Eng. 20 (2) (2010) 107–118.
[68] C.-J. Liao, et al., Fabrication of porous biodegradable polymer scaffolds using a solvent merging/particulate leaching method, J. Biomed. Mater. Res. 59 (4) (2002) 676–681.
[69] D.J. Mooney, et al., Novel approach to fabricate porous sponges of poly(d,l-lactic-co-glycolic acid) without the use of organic solvents, Biomaterials 17 (14) (1996) 1417–1422.
[70] F. Dehghani, N. Annabi, Engineering porous scaffolds using gas-based techniques, Curr. Opin. Biotechnol. 22 (5) (2011) 661–666.
[71] D. Puppi, et al., Polymeric materials for bone and cartilage repair, Prog. Polym. Sci. 35 (4) (2010) 403–440.

Please cite this article in press as: G. Turnbull, et al., 3D bioactive composite scaffolds for bone tissue engineering, Bioactive Materials (2017), https://doi.org/10.1016/j.bioactmat.2017.10.001

[72] K. Whang, et al., A novel method to fabricate bioabsorbable scaffolds, Polymer 36 (4) (1995) 837–842.
[73] J.A. Matthews, et al., Electrospinning of collagen nanofibers, Biomacromolecules 3 (2) (2002) 232–238.
[74] W.J. Li, et al., Electrospun nanofibrous structure: a novel scaffold for tissue engineering, J. Biomed. Mater. Res. 60 (4) (2002) 613–621.
[75] Y. Huang, et al., Electrodeposition of porous hydroxyapatite/calcium silicate composite coating on titanium for biomedical applications, Appl. Surf. Sci. 271 (2013) 299–302.
[76] Z.-M. Huang, et al., A review on polymer nanofibers by electrospinning and their applications in nanocomposites, Compos. Sci. Technol. 63 (15) (2003) 2223–2253.
[77] L, J. Primary 3D Printing Processes. [cited 2017 29/07/2017]; Available from: https://www.printspace3d.com/3d-printing-processes/.
[78] K. Kim, et al., Stereolithographic bone scaffold design parameters: osteogenic differentiation and signal expression, Tissue Eng. Part B Rev. 16 (5) (2010) 523–539.
[79] I. Zein, et al., Fused deposition modeling of novel scaffold architectures for tissue engineering applications, Biomaterials 23 (4) (2002) 1169–1185.
[80] A.-V. Do, et al., 3D printing of scaffolds for tissue regeneration applications, Adv. Healthc. Mater. 4 (12) (2015) 1742–1762.
[81] J.M. Williams, et al., Bone tissue engineering using polycaprolactone scaffolds fabricated via selective laser sintering, Biomaterials 26 (23) (2005) 4817–4827.
[82] Y. Xia, et al., Selective laser sintering fabrication of nano-hydroxyapatite/poly-ε-caprolactone scaffolds for bone tissue engineering applications, Int. J. Nanomed. 8 (2013) 4197–4213.
[83] S.V. Murphy, A. Atala, 3D bioprinting of tissues and organs, Nat. Biotechnol. 32 (8) (2014) 773–785.
[84] A. Shafiee, A. Atala, Printing technologies for medical applications, Trends Mol. Med. 22 (3) (2016) 254–265.
[85] E. Fennema, et al., Spheroid culture as a tool for creating 3D complex tissues, Trends Biotechnol. 31 (2) (2013) 108–115.
[86] Y. Yamaguchi, et al., Mesenchymal stem cell spheroids exhibit enhanced in-vitro and in-vivo osteoregenerative potential, BMC Biotechnol. 14 (1) (2014) 105.
[87] J.G.K. Handschel, et al., Prospects of micromass culture technology in tissue engineering, Head Face Med. 3 (2007), 4–4.
[88] C.L. Ventola, Medical applications for 3D printing: current and projected uses, Pharm. Ther. 39 (10) (2014) 704–711.
[89] J. Li, et al., Recent advances in bioprinting techniques: approaches, applications and future prospects, J. Transl. Med. 14 (2016) 271.
[90] X. Cui, et al., Thermal inkjet printing in tissue engineering and regenerative medicine, Recent Pat. drug Deliv. Formulation 6 (2) (2012) 149–155.
[91] R.E. Saunders, B. Derby, Inkjet printing biomaterials for tissue engineering: bioprinting, Int. Mater. Rev. 59 (8) (2014) 430–448.
[92] S. Bose, S. Vahabzadeh, A. Bandyopadhyay, Bone tissue engineering using 3D printing, Mater. Today 16 (12) (2013) 496–504.
[93] V. Keriquel, et al., In situ printing of mesenchymal stromal cells, by laser-assisted bioprinting, for in vivo bone regeneration applications, Sci. Rep. 7 (1) (2017) 1778.
[94] L. Koch, et al., Laser assisted cell printing, Curr. Pharm. Biotechnol. 14 (1) (2013) 91–97.
[95] F.-J. Alan, et al., Bioprinting of human pluripotent stem cells and their directed differentiation into hepatocyte-like cells for the generation of mini-livers in 3D, Biofabrication 7 (4) (2015) 044102.
[96] A. Faulkner-Jones, et al., Development of a valve-based cell printer for the formation of human embryonic stem cell spheroid aggregates, Biofabrication 5 (1) (2013) 015013.
[97] U.A. Gurkan, et al., Engineering anisotropic biomimetic fibrocartilage microenvironment by bioprinting mesenchymal stem cells in nanoliter gel droplets, Mol. Pharm. 11 (7) (2014) 2151–2159.
[98] Y. Yu, et al., Three-dimensional bioprinting using self-assembling scalable scaffold-free “tissue strands” as a new bioink 6 (2016) 28714.
[99] I.T. Ozbolat, M. Hospodiuk, Current advances and future perspectives in extrusion-based bioprinting, Biomaterials 76 (2016) 321–343.
[100] G. Hunter, et al., Creation of Oxidized Zirconium Orthopaedic Implants, 2005.
[101] M.P. Staiger, et al., Magnesium and its alloys as orthopedic biomaterials: a review, Biomaterials 27 (9) (2006) 1728–1734.
[102] M.A. Lopez-Heredia, et al., Rapid prototyped porous titanium coated with calcium phosphate as a scaffold for bone tissue engineering, Biomaterials 29 (17) (2008) 2608–2615.
[103] R. Huiskes, H. Weinans, B. van Rietbergen, The relationship between stress shielding and bone resorption around total hip stems and the effects of flexible materials, Clin. Orthop. Relat. Res. (274) (1992) 124–134.
[104] Y. Lei, et al., Strontium hydroxyapatite/chitosan nanohybrid scaffolds with enhanced osteoinductivity for bone tissue engineering, Mater Sci. Eng. C Mater Biol. Appl. 72 (2017) 134–142.
[105] S. Wu, et al., A biomimetic hierarchical scaffold: natural growth of nanotitanates on three-dimensional microporous Ti-Based metals, Nano Lett. 8 (11) (2008) 3803–3808.
[106] H. Chen, et al., Fabrication of porous titanium scaffolds by stack sintering of microporous titanium spheres produced with centrifugal granulation technology, Mater. Sci. Eng. C 43 (2014) 182–188.
[107] D.T. Chou, et al., Novel processing of iron-manganese alloy-based biomaterials by inkjet 3-D printing, Acta Biomater. 9 (10) (2013) 8593–8603.
[108] F.-H. Liu, et al., Selective laser sintering of bio-metal scaffold, Procedia CIRP 5 (2013) 83–87.
[109] J. Vaithilingam, et al., Functionalisation of Ti6Al4V components fabricated using selective laser melting with a bioactive compound, Mater. Sci. Eng. C 46 (2015) 52–61.
[110] J.P. Kruth, et al., Binding mechanisms in selective laser sintering and selective laser melting, Rapid Prototyp. J. 11 (1) (2005) 26–36.
[111] W. Bonfield, et al., Hydroxyapatite reinforced polyethylene–a mechanically compatible implant material for bone replacement, Biomaterials 2 (3) (1981) 185–186.
[112] G.W. Ho, J.P. Matinlinna, Insights on ceramics as dental materials. Part I: ceramic material types in Dentistry, Silicon 3 (3) (2011) 109–115.
[113] J.P. Bonjour, Calcium and phosphate: a duet of ions playing for bone health, J. Am. Coll. Nutr. 30 (5 Suppl 1) (2011), 438s-48s.
[114] M. Bohner, L. Galea, N. Doebelin, Calcium phosphate bone graft substitutes: failures and hopes, J. Eur. Ceram. Soc. 32 (11) (2012) 2663–2671.
[115] M. Bohner, Resorbable biomaterials as bone graft substitutes, Mater. Today 13 (1–2) (2010) 24–30.
[116] R.Z. LeGeros, Properties of osteoconductive biomaterials: calcium phosphates, Clin. Orthop. Relat. Res. (395) (2002) 81–98.
[117] C.L. Ko, et al., Properties of osteoconductive biomaterials: calcium phosphate cement with different ratios of platelet-rich plasma as identifiers, Mater Sci. Eng. C Mater Biol. Appl. 33 (6) (2013) 3537–3544.
[118] S. Bose, S. Tarafder, Calcium phosphate ceramic systems in growth factor and drug delivery for bone tissue engineering: a review, Acta Biomater. 8 (4) (2012) 1401–1421.
[119] U. Gbureck, et al., Resorbable dicalcium phosphate bone substitutes prepared by 3D powder printing, Adv. Funct. Mater. 17 (18) (2007) 3940–3945.
[120] T. Tian, C. Wu, J. Chang, Preparation and in vitro osteogenic, angiogenic and antibacterial properties of cuprorivaite (CaCuSi4O10, Cup) bioceramics, RSC Adv. 6 (51) (2016) 45840–45849.
[121] J. Cui, et al., Polydopamine-functionalized polymer particles as templates for mineralization of hydroxyapatite: biomimetic and in vitro bioactivity, RSC Adv. 6 (8) (2016) 6747–6755.
[122] M.-Y. Shie, S.-J. Ding, H.-C. Chang, The role of silicon in osteoblast-like cell proliferation and apoptosis, Acta Biomater. 7 (6) (2011) 2604–2614.
[123] G. Calabrese, et al., Collagen-hydroxyapatite scaffolds induce human adipose derived stem cells osteogenic differentiation in vitro, PLoS One 11 (3) (2016).
[124] E.M. Goncalves, et al., Three-dimensional printed PCL-hydroxyapatite scaffolds filled with CNTs for bone cell growth stimulation, J. Biomed. Mater Res. B Appl. Biomater. 104 (6) (2016) 1210–1219.
[125] E.M. Gonçalves, et al., Three-dimensional printed PCL-hydroxyapatite scaffolds filled with CNTs for bone cell growth stimulation, J. Biomed. Mater. Res. Part B Appl. Biomater. 104 (6) (2016) 1210–1219.
[126] R.J. Kane, et al., Hydroxyapatite reinforced collagen scaffolds with improved architecture and mechanical properties, Acta Biomater. 17 (2015) 16–25.
[127] C. Li, et al., Electrospun silk-BMP-2 scaffolds for bone tissue engineering, Biomaterials 27 (16) (2006) 3115–3124.
[128] F. Peng, X. Yu, M. Wei, In vitro cell performance on hydroxyapatite particles/poly(L-lactic acid) nanofibrous scaffolds with an excellent particle along nanofiber orientation, Acta Biomater. 7 (6) (2011) 2585–2592.
[129] C. Shuai, et al., Development of composite porous scaffolds based on poly(lactide-co-glycolide)/nano-hydroxyapatite via selective laser sintering, Int. J. Adv. Manuf. Technol. 69 (1) (2013) 51–57.
[130] D.L. Alge, et al., Poly(propylene fumarate) reinforced dicalcium phosphate dihydrate cement composites for bone tissue engineering, J. Biomed. Mater. Res. Part A 100A (7) (2012) 1792–1802.
[131] N. Tanataweethum, et al., Fabrication of poly-l-lactic acid/dicalcium phosphate dihydrate composite scaffolds with high mechanical strength-implications for bone tissue engineering, J. Funct. Biomater. 6 (4) (2015) 1036–1053.
[132] P. Wang, P. Liu, F. Xu, X. Fan, H. Yuan, H. Li, Y. Yan, Controlling the degradation of dicalcium phosphate/calcium sulfate/poly(amino acid) biocomposites for bone regeneration, Polym Compos. (2016), https://doi.org/10.1002/pc.24049.
[133] T. Matsuno, et al., Preparation of injectable 3D-formed beta-tricalcium phosphate bead/alginate composite for bone tissue engineering, Dent. Mater. J. 27 (6) (2008) 827–834.
[134] T. Kurien, R.G. Pearson, B.E. Scammell, Bone graft substitutes currently available in orthopaedic practice, The evidence for their use 95-B (5) (2013) 583–597.
[135] M. Mohseni, et al., Assessment of tricalcium phosphate/collagen (TCP/collagene)nanocomposite scaffold compared with hydroxyapatite (HA) on healing of segmental femur bone defect in rabbits, Artif. Cells Nanomed. Biotechnol. (2017) 1–8.
[136] S. Tarafder, S. Bose, Polycaprolactone-coated 3D printed tricalcium phosphate scaffolds for bone tissue engineering: in vitro alendronate release behavior and local delivery effect on in vivo osteogenesis, ACS Appl. Mater. Interfaces 6 (13) (2014) 9955–9965.
[137] S. Bose, S. Tarafder, A. Bandyopadhyay, Effect of chemistry on osteogenesis and angiogenesis towards bone tissue engineering using 3D printed scaffolds, Ann. Biomed. Eng. 45 (1) (2017) 261–272.
[138] A. Rakovsky, et al., beta-TCP-polylactide composite scaffolds with high strength and enhanced permeability prepared by a modified salt leaching

Please cite this article in press as: G. Turnbull, et al., 3D bioactive composite scaffolds for bone tissue engineering, Bioactive Materials (2017), https://doi.org/10.1016/j.bioactmat.2017.10.001

method, J. Mech. Behav. Biomed. Mater. 32 (2014) 89–98.
[139] C. Wu, et al., Improvement of mechanical and biological properties of porous CaSiO3 scaffolds by poly(d,l-lactic acid) modification, Acta Biomater. 4 (2) (2008) 343–353.
[140] Z. Gou, J. Chang, W. Zhai, Preparation and characterization of novel bioactive dicalcium silicate ceramics, J. Eur. Ceram. Soc. 25 (9) (2005) 1507–1514.
[141] Y. Ramaswamy, et al., Biological response of human bone cells to zinc-modified Ca–Si-based ceramics, Acta Biomater. 4 (5) (2008) 1487–1497.
[142] W. Xue, et al., In vivo evaluation of plasma-sprayed wollastonite coating, Biomaterials 26 (17) (2005) 3455–3460.
[143] P. Feng, et al., Calcium silicate ceramic scaffolds toughened with hydroxyapatite whiskers for bone tissue engineering, Mater. Charact. 97 (2014) 47–56.
[144] Y. Dai, et al., Porous β-Ca2SiO4 ceramic scaffolds for bone tissue engineering: in vitro and in vivo characterization, Ceram. Int. 41 (4) (2015) 5894–5902.
[145] P. Feng, et al., Toughening and strengthening mechanisms of porous akermanite scaffolds reinforced with nano-titania, RSC Adv. 5 (5) (2015) 3498–3507.
[146] J. Pasold, et al., Direct influence of titanium and zirconia particles on the morphology and functionality of mature human osteoclasts, J. Biomed. Mater. Res. A 105A (2017) 2608–2615.
[147] S. Kurtz, et al., Projections of primary and revision hip and knee arthroplasty in the United States from 2005–2030, J. Bone Jt. Surg. Am. 89 (2007).
[148] L.L. Hench, The story of Bioglass®, J. Mater. Sci. Mater. Med. 17 (11) (2006) 967–978.
[149] L.L. Hench, et al., Bonding mechanisms at the interface of ceramic prosthetic materials, J. Biomed. Mater. Res. 5 (6) (1971) 117–141.
[150] L.L. Hench, J.M. Polak, Third-generation biomedical materials, Science 295 (5557) (2002), 1014+1016-1017.
[151] M. Aebi, P. Regazzoni, O. Schwarzenbach, Segmental bone grafting, Int. Orthop. 13 (2) (1989) 101–111.
[152] D.F. Williams, Titanium: epitome of biocompatibility or cause for concern, J. Bone Jt. Surg. Br. 76 (3) (1994) 348–349.
[153] J.R. Jones, Review of bioactive glass: from Hench to hybrids, Acta Biomater. 9 (1) (2013) 4457–4486.
[154] D. Beutner, K.-B. Hüttenbrink, Passive and active middle ear implants. GMS Current Topics in Otorhinolaryngology, Head Neck Surg. 8 (2009) Doc09.
[155] M.N. Rahaman, et al., Bioactive glass in tissue engineering, Acta Biomater. 7 (6) (2011) 2355–2373.
[156] V. Miguez-Pacheco, L.L. Hench, A.R. Boccaccini, Bioactive glasses beyond bone and teeth: emerging applications in contact with soft tissues, Acta Biomater. 13 (2015) 1–15.
[157] B. Ilharreborde, et al., Bioactive glass as a bone substitute for spinal fusion in adolescent idiopathic scoliosis: a comparative study with iliac crest autograft, J. Pediatr. Orthop. 28 (3) (2008) 347–351.
[158] V. Maquet, et al., Porous poly(alpha-hydroxyacid)/Bioglass composite scaffolds for bone tissue engineering. I Preparation and in vitro characterisation, Biomaterials 25 (18) (2004) 4185–4194.
[159] W.J. Habraken, J.G. Wolke, J.A. Jansen, Ceramic composites as matrices and scaffolds for drug delivery in tissue engineering, Adv. Drug Deliv. Rev. 59 (4–5) (2007) 234–248.
[160] V. Karageorgiou, D. Kaplan, Porosity of 3D biomaterial scaffolds and osteogenesis, Biomaterials 26 (27) (2005) 5474–5491.
[161] D. Ishii, et al., In vivo tissue response and degradation behavior of PLLA and stereocomplexed PLA nanofibers, Biomacromolecules 10 (2) (2009) 237–242.
[162] C.C. Verheyen, et al., Evaluation of hydroxylapatite/poly(L-lactide) composites: mechanical behavior, J. Biomed. Mater. Res. 26 (10) (1992) 1277–1296.
[163] T. Furukawa, et al., Histomorphometric study on high-strength hydroxyapatite/poly(L-lactide) composite rods for internal fixation of bone fractures, J. Biomed. Mater. Res. 50 (3) (2000) 410–419.
[164] Y. Shikinami, Y. Matsusue, T. Nakamura, The complete process of bioresorption and bone replacement using devices made of forged composites of raw hydroxyapatite particles/poly l-lactide (F-u-HA/PLLA), Biomaterials 26 (27) (2005) 5542–5551.
[165] C.C. Verheyen, et al., Hydroxylapatite/poly(L-lactide) composites: an animal study on push-out strengths and interface histology, J. Biomed. Mater. Res. 27 (4) (1993) 433–444.
[166] F. Westhauser, et al., Three-dimensional polymer coated 45S5-type bioactive glass scaffolds seeded with human mesenchymal stem cells show bone formation in vivo, J. Mater. Sci. Mater. Med. 27 (7) (2016) 119.
[167] C. Murphy, et al., 3D Printing of a Polymer Bioactive Glass Composite for Bone Repair, 2016.
[168] F. Baino, C. Vitale-Brovarone, Mechanical properties and reliability of glass–ceramic foam scaffolds for bone repair, Mater. Lett. 118 (2014) 27–30.
[169] S. Eqtesadi, et al., Improving mechanical properties of 13–93 bioactive glass robocast scaffold by poly (lactic acid) and poly (ε-caprolactone) melt infiltration, J. Non-Cryst. Solids 432 (Part A) (2016) 111–119.
[170] X. Zhang, et al., Functionalized mesoporous bioactive glass scaffolds for enhanced bone tissue regeneration, Sci. Rep. 6 (2016) 19361.
[171] D. Arcos, M. Vallet-Regí, Bioceramics for drug delivery, Acta Mater. 61 (3) (2013) 890–911.
[172] J. Shengxiang, et al., Amino-functionalized mesoporous bioactive glass for drug delivery, Biomed. Mater. 12 (2) (2017) 025017.
[173] C. Wu, J. Chang, Y. Xiao, Mesoporous bioactive glasses as drug delivery and bone tissue regeneration platforms, Ther. Deliv. 2 (9) (2011) 1189–1198.
[174] B. Sui, G. Zhong, J. Sun, Drug-loadable mesoporous bioactive glass nanospheres: biodistribution, clearance, BRL cellular location and systemic risk assessment via 45Ca labelling and histological analysis, Sci. Rep. 6 (2016) 33443.
[175] Y. Li, et al., Mesoporous bioactive glass as a drug delivery system: fabrication, bactericidal properties and biocompatibility, J. Mater. Sci. Mater. Med. 24 (8) (2013) 1951–1961.
[176] H. Ding, et al., A novel injectable borate bioactive glass cement as an antibiotic delivery vehicle for treating osteomyelitis, PLoS One 9 (1) (2014) e85472.
[177] X. Cui, et al., An injectable borate bioactive glass cement for bone repair: preparation, bioactivity and setting mechanism, J. Non-Cryst. Solids 432 (2016) 150–157.
[178] A.J. Aho, et al., Injectable bioactive glass/biodegradable polymer composite for bone and cartilage reconstruction: concept and experimental outcome with thermoplastic composites of poly(ε-caprolactone-co-D,L-lactide) and bioactive glass S53P4, J. Mater. Sci. Mater. Med. 15 (10) (2004) 1165–1173.
[179] Y. Zhang, et al., Evaluation of injectable strontium-containing borate bioactive glass cement with enhanced osteogenic capacity in a critical-sized rabbit femoral condyle defect model, ACS Appl. Mater. Interfaces 7 (4) (2015) 2393–2403.
[180] X. Liu, P.X. Ma, Polymeric scaffolds for bone tissue engineering, Ann. Biomed. Eng. 32 (3) (2004) 477–486.
[181] S. Ravi, E.L. Chaikof, Biomaterials for vascular tissue engineering, Regen. Med. 5 (1) (2010) 107.
[182] J. Zhu, R.E. Marchant, Design properties of hydrogel tissue-engineering scaffolds, Expert Rev. Med. Devices 8 (5) (2011) 607–626.
[183] D.M. Yoon, J.P. Fisher, Natural and synthetic polymeric scaffolds, in: R. Narayan (Ed.), Biomedical Materials, Springer, US: Boston, MA, 2009, pp. 415–442.
[184] F.A. Sheikh, et al., Hybrid scaffolds based on PLGA and silk for bone tissue engineering, J. Tissue Eng. Regen. Med. 10 (3) (2016) 209–221.
[185] M.J. Yaszemski, et al., Evolution of bone transplantation: molecular, cellular and tissue strategies to engineer human bone, Biomaterials 17 (2) (1996) 175–185.
[186] Y. Hu, et al., Fabrication of poly(α-hydroxy acid) foam scaffolds using multiple solvent systems, J. Biomed. Mater. Res. 59 (3) (2002) 563–572.
[187] S.H. Oh, et al., Fabrication and characterization of hydrophilic poly(lactic-co-glycolic acid)/poly(vinyl alcohol) blend cell scaffolds by melt-molding particulate-leaching method, Biomaterials 24 (22) (2003) 4011–4021.
[188] M. Tallawi, et al., Strategies for the chemical and biological functionalization of scaffolds for cardiac tissue engineering: a review, J. R. Soc. Interface 12 (108) (2015) 20150254.
[189] J. Wang, et al., Biodegradable polymer membranes applied in guided bone/tissue regeneration: a review, Polymers 8 (4) (2016) 115.
[190] P.X. Ma, J.W. Choi, Biodegradable polymer scaffolds with well-defined interconnected spherical pore network, Tissue Eng. 7 (1) (2001) 23–33.
[191] M.A. Woodruff, D.W. Hutmacher, The return of a forgotten polymer—polycaprolactone in the 21st century, Prog. Polym. Sci. 35 (10) (2010) 1217–1256.
[192] S.J. Hollister, W.L. Murphy, Scaffold translation: barriers between concept and clinic, Tissue Eng. Part B Rev. 17 (6) (2011) 459–474.
[193] K. Rezwan, et al., Biodegradable and bioactive porous polymer/inorganic composite scaffolds for bone tissue engineering, Biomaterials 27 (18) (2006) 3413–3431.
[194] A. Gloria, R. De Santis, L. Ambrosio, Polymer-based composite scaffolds for tissue engineering, J. Appl. Biomater. Biomech. 8 (2) (2010) 57–67.
[195] M.P. Prabhakaran, J. Venugopal, S. Ramakrishna, Electrospun nanostructured scaffolds for bone tissue engineering, Acta Biomater. 5 (8) (2009) 2884–2893.
[196] Q. Tan, et al., Fabrication of porous scaffolds with a controllable microstructure and mechanical properties by porogen fusion technique, Int. J. Mol. Sci. 12 (2) (2011) 890–904.
[197] A. Salerno, et al., Bio-safe fabrication of PLA scaffolds for bone tissue engineering by combining phase separation, porogen leaching and scCO2 drying, J. Supercrit. Fluids 97 (2015) 238–246.
[198] M.J. Mondrinos, et al., Porogen-based solid freeform fabrication of polycaprolactone–calcium phosphate scaffolds for tissue engineering, Biomaterials 27 (25) (2006) 4399–4408.
[199] N. Thadavirul, P. Pavasant, P. Supaphol, Development of polycaprolactone porous scaffolds by combining solvent casting, particulate leaching, and polymer leaching techniques for bone tissue engineering, J. Biomed. Mater. Res. A 102 (10) (2014) 3379–3392.
[200] F. Intranuovo, et al., Plasma modification of PCL porous scaffolds fabricated by solvent-casting/particulate-leaching for tissue engineering, Plasma Process. Polym. 11 (2) (2014) 184–195.
[201] S.L. Bellis, Advantages of RGD peptides for directing cell association with biomaterials, Biomaterials 32 (18) (2011) 4205–4210.
[202] U. Hersel, C. Dahmen, H. Kessler, RGD modified polymers: biomaterials for stimulated cell adhesion and beyond, Biomaterials 24 (24) (2003) 4385–4415.
[203] C.T. Kao, et al., Poly(dopamine) coating of 3D printed poly(lactic acid) scaffolds for bone tissue engineering, Mater. Sci. Eng. C Mater Biol. Appl. 56 (2015) 165–173.

Please cite this article in press as: G. Turnbull, et al., 3D bioactive composite scaffolds for bone tissue engineering, Bioactive Materials (2017), https://doi.org/10.1016/j.bioactmat.2017.10.001

[204] R. Parenteau-Bareil, R. Gauvin, F. Berthod, Collagen-based biomaterials for tissue engineering applications, Materials 3 (3) (2010) 1863.
[205] Y. Hiraoka, et al., Fabrication and biocompatibility of collagen sponge reinforced with poly(glycolic acid) fiber, Tissue Eng. 9 (6) (2003) 1101–1112.
[206] A. Aravamudhan, et al., Cellulose and collagen derived micro-nano structured scaffolds for bone tissue engineering, J. Biomed. Nanotechnol. 9 (4) (2013) 719–731.
[207] C.P. Barnes, et al., Cross-linking electrospun type II collagen tissue engineering scaffolds with carbodiimide in ethanol, Tissue Eng. 13 (7) (2007) 1593–1605.
[208] B.A. Harley, et al., Mechanical characterization of collagen-glycosaminoglycan scaffolds, Acta Biomater. 3 (4) (2007) 463–474.
[209] M.M. Villa, et al., Bone tissue engineering with a collagen-hydroxyapatite scaffold and culture expanded bone marrow stromal cells, J. Biomed. Mater. Res. B Appl. Biomater. 103 (2) (2015) 243–253.
[210] M. Marcacci, et al., Stem cells associated with macroporous bioceramics for long bone repair: 6- to 7-year outcome of a pilot clinical study, Tissue Eng. 13 (5) (2007) 947–955.
[211] H. Babiker, Bone graft materials in fixation of orthopaedic implants in sheep, Dan. Med. J. 60 (7) (2013) B4680.
[212] G. Calabrese, et al., Bone augmentation after ectopic implantation of a cell-free collagen-hydroxyapatite scaffold in the mouse, Sci. Rep. (2016) 6.
[213] A. Tampieri, et al., Design of graded biomimetic osteochondral composite scaffolds, Biomaterials 29 (26) (2008) 3539–3546.
[214] J.M. Oliveira, et al., Novel hydroxyapatite/chitosan bilayered scaffold for osteochondral tissue-engineering applications: scaffold design and its performance when seeded with goat bone marrow stromal cells, Biomaterials 27 (36) (2006) 6123–6137.
[215] B. Grigolo, et al., Novel nano-composite biomimetic biomaterial allows chondrogenic and osteogenic differentiation of bone marrow concentrate derived cells, J. Mater Sci. Mater. Med. 26 (4) (2015) 173.
[216] C. Manferdini, et al., Specific inductive potential of a novel nanocomposite biomimetic biomaterial for osteochondral tissue regeneration, J. Tissue Eng. Regen. Med. 10 (5) (2016) 374–391.
[217] G.L. Jones, et al., Primary human osteoblast culture on 3D porous collagen-hydroxyapatite scaffolds, J. Biomed. Mater. Res. - Part A 94 (4) (2010) 1244–1250.
[218] J.P. Gleeson, N.A. Plunkett, F.J. O'Brien, Addition of hydroxyapatite improves stiffness, interconnectivity and osteogenic potential of a highly porous collagen-based scaffold for bone tissue regeneration, Eur. Cells Mater. 20 (2010) 218–230.
[219] F.G. Lyons, et al., The healing of bony defects by cell-free collagen-based scaffolds compared to stem cell-seeded tissue engineered constructs, Biomaterials 31 (35) (2010) 9232–9243.
[220] G.L. Jones, et al., Primary human osteoblast culture on 3D porous collagen-hydroxyapatite scaffolds, J. Biomed. Mater. Res. Part A 94A (4) (2010) 1244–1250.
[221] F.G. Lyons, et al., The healing of bony defects by cell-free collagen-based scaffolds compared to stem cell-seeded tissue engineered constructs, Biomaterials 31 (35) (2010) 9232–9243.
[222] M.J. Meagher, et al., Acellular hydroxyapatite-collagen scaffolds support angiogenesis and osteogenic gene expression in an ectopic murine model: effects of hydroxyapatite volume fraction, J. Biomed. Mater. Res. Part A 104 (9) (2016) 2178–2188.
[223] Perdisa, F., et al., One-step treatment for patellar cartilage defects with a cell-free osteochondral scaffold. Am. J. Sports Med.. 0(0): p. 0363546517694159.
[224] A.R. Costa-Pinto, et al., Osteogenic differentiation of human bone marrow mesenchymal stem cells seeded on melt based chitosan scaffolds for bone tissue engineering applications, Biomacromolecules 10 (8) (2009) 2067–2073.
[225] A.R. Costa-Pinto, R.L. Reis, N.M. Neves, Scaffolds based bone tissue engineering: the role of chitosan, Tissue Eng. Part B Rev. 17 (5) (2011) 331–347.
[226] K. Dahlan, et al., Synthesis and characterization of calcium phosphate/chitosan composites, Int. J. Basic & Appl. Sci. 12 (1) (2012) 50–57.
[227] J.G. Saltarrelli Jr., D.P. Mukherjee, In vivo testing of a bone graft containing chitosan, calcium sulfate and osteoblasts in a paste form in a critical size defect model in rats, J. Biomed. Sci. Eng. 2 (01) (2009) 24.
[228] J. Zhang, et al., Novel mesoporous hydroxyapatite/chitosan composite for bone repair, J. Bionic Eng. 9 (2) (2012) 243–251.
[229] G.-J. Lai, et al., Composite chitosan/silk fibroin nanofibers for modulation of osteogenic differentiation and proliferation of human mesenchymal stem cells, Carbohydr. Polym. 111 (2014) 288–297.
[230] A. Anitha, et al., Chitin and chitosan in selected biomedical applications, Prog. Polym. Sci. 39 (9) (2014) 1644–1667.
[231] J.H. Lee, B.O. Jeong, The effect of hyaluronate-carboxymethyl cellulose on bone graft substitute healing in a rat spinal fusion model, J. Korean Neurosurg. Soc. 50 (5) (2011) 409–414.
[232] B.M. Chesnutt, et al., Design and characterization of a novel chitosan/nanocrystalline calcium phosphate composite scaffold for bone regeneration, J. Biomed. Mater. Res. A 88 (2) (2009) 491–502.
[233] T. Jiang, W.I. Abdel-Fattah, C.T. Laurencin, In vitro evaluation of chitosan/poly(lactic acid-glycolic acid) sintered microsphere scaffolds for bone tissue engineering, Biomaterials 27 (28) (2006) 4894–4903.
[234] P.B. Malafaya, J.T. Oliveira, R.L. Reis, The effect of insulin-loaded chitosan particle-aggregated scaffolds in chondrogenic differentiation, Tissue Eng. Part A 16 (2) (2010) 735–747.
[235] T. Jiang, et al., Functionalization of chitosan/poly(lactic acid-glycolic acid) sintered microsphere scaffolds via surface heparinization for bone tissue engineering, J. Biomed. Mater. Res. A 93 (3) (2010) 1193–1208.
[236] F. Pati, B. Adhikari, S. Dhara, Development of chitosan-tripolyphosphate fibers through pH dependent ionotropic gelation, Carbohydr. Res. 346 (16) (2011) 2582–2588.
[237] S.L. Levengood, M. Zhang, Chitosan-based scaffolds for bone tissue engineering, J. Mater. Chem. B Mater. Biol. Med. 2 (21) (2014) 3161–3184.
[238] X. Geng, O.H. Kwon, J. Jang, Electrospinning of chitosan dissolved in concentrated acetic acid solution, Biomaterials 26 (27) (2005) 5427–5432.
[239] K.C. Kavya, et al., Fabrication and characterization of chitosan/gelatin/nSiO2 composite scaffold for bone tissue engineering, Int. J. Biol. Macromol. 59 (2013) 255–263.
[240] W.W. Thein-Han, R.D.K. Misra, Biomimetic chitosan–nanohydroxyapatite composite scaffolds for bone tissue engineering, Acta Biomater. 5 (4) (2009) 1182–1197.
[241] S. Saravanan, R.S. Leena, N. Selvamurugan, Chitosan based biocomposite scaffolds for bone tissue engineering, Int. J. Biol. Macromol. 93 (2016) 1354–1365.
[242] J. Hou, et al., Segmental bone regeneration using rhBMP-2-loaded collagen/chitosan microspheres composite scaffold in a rabbit model, Biomed. Mater. 7 (3) (2012) 035002.
[243] H. Wu, et al., Reconstruction of large-scale defects with a novel hybrid scaffold made from poly(l-lactic acid)/Nanohydroxyapatite/Alendronate-loaded chitosan microsphere: in vitro and in vivo studies, Sci. Rep. 7 (1) (2017) 359.
[244] C.Z. Wang, et al., The effect of the local delivery of alendronate on human adipose-derived stem cell-based bone regeneration, Biomaterials 31 (33) (2010) 8674–8683.
[245] X. Shen, et al., Alendronate-loaded hydroxyapatite-TiO2 nanotubes for improved bone formation in osteoporotic rabbits, J. Mater. Chem. B 4 (8) (2016) 1423–1436.
[246] D.X. Wang, et al., Enhancing the bioactivity of Poly(lactic-co-glycolic acid) scaffold with a nano-hydroxyapatite coating for the treatment of segmental bone defect in a rabbit model, Int. J. Nanomed. 8 (2013) 1855–1865.
[247] L.A. Solchaga, et al., Treatment of osteochondral defects with autologous bone marrow in a hyaluronan-based delivery vehicle, Tissue Eng. 8 (2) (2002) 333–347.
[248] G. Kogan, et al., Hyaluronic acid: a natural biopolymer with a broad range of biomedical and industrial applications, Biotechnol. Lett. 29 (1) (2007) 17–25.
[249] X.Z. Shu, et al., Disulfide-crosslinked hyaluronan-gelatin hydrogel films: a covalent mimic of the extracellular matrix for in vitro cell growth, Biomaterials 24 (21) (2003) 3825–3834.
[250] M.N. Collins, C. Birkinshaw, Hyaluronic acid based scaffolds for tissue engineering—a review, Carbohydr. Polym. 92 (2) (2013) 1262–1279.
[251] A. Rajan Unnithan, et al., A unique scaffold for bone tissue engineering: an osteogenic combination of graphene oxide–hyaluronic acid–chitosan with simvastatin, J. Ind. Eng. Chem. 46 (2017) 182–191.
[252] H.X. Zhang, et al., Biocompatibility and osteogenesis of calcium phosphate composite scaffolds containing simvastatin-loaded PLGA microspheres for bone tissue engineering, J. Biomed. Mater. Res. - Part A 103 (10) (2015) 3250–3258.
[253] Q. Yan, et al., Controlled release of simvastatin-loaded thermo-sensitive PLGA-PEG-PLGA hydrogel for bone tissue regeneration: in vitro and in vivo characteristics, J. Biomed. Mater. Res. - Part A 103 (11) (2015) 3580–3589.
[254] J.E. Samorezov, E. Alsberg, Spatial regulation of controlled bioactive factor delivery for bone tissue engineering, Adv. Drug Deliv. Rev. 84 (2015) 45–67.
[255] Y. Zhou, et al., The role of simvastatin in the osteogenesis of injectable tissue-engineered bone based on human adipose-derived stromal cells and platelet-rich plasma, Biomaterials 31 (20) (2010) 5325–5335.
[256] X.I.N. Huang, Z. Huang, W. Li, Highly efficient release of simvastatin from simvastatin-loaded calcium sulphate scaffolds enhances segmental bone regeneration in rabbits, Mol. Med. Rep. 9 (6) (2014) 2152–2158.
[257] J.B. Lee, et al., Poly(l-Lactic acid)/gelatin fibrous scaffold loaded with simvastatin/beta-cyclodextrin-modified hydroxyapatite inclusion complex for bone tissue regeneration, Macromol. Biosci. 16 (7) (2016) 1027–1038.
[258] J. Zhang, et al., Combination of simvastatin, calcium silicate/gypsum, and gelatin and bone regeneration in rabbit calvarial defects 6 (2016) 23422.
[259] J. Jing, H. Rammal, M. Dubus, R. Rahouadj, E. Pauthe, F. Velard, J. Braux, S.C. Gangloff, L. Siad, H. Kerdjoudj, Chitosan/hyaluronic acid porous scaffold for bone tissue engineering, Front. Bioeng. Biotechnol. Conference Abstract: 10th World Biomaterials Congress (2016), https://doi.org/10.3389/conf.FBIOE.2016.01.01918.
[260] C.R. Correia, et al., Chitosan scaffolds containing hyaluronic acid for cartilage tissue engineering, Tissue Eng. Part C Methods 17 (7) (2011) 717–730.
[261] H.J. Kim, et al., Hybrid scaffolds composed of hyaluronic acid and collagen for cartilage regeneration, Tissue Eng. Regen. Med. 9 (2) (2012) 57–62.
[262] Y.-L. Chang, et al., Bone healing improvements using hyaluronic acid and hydroxyapatite/beta-tricalcium phosphate in combination: an animal study, BioMed Res. Int. 2016 (2016) 8.
[263] N. Kasoju, U. Bora, Silk fibroin in tissue engineering, Adv. Healthc. Mater. 1 (4) (2012) 393–412.
[264] B.B. Mandal, et al., High-strength silk protein scaffolds for bone repair, Proc. Natl. Acad. Sci. 109 (20) (2012) 7699–7704.

[265] S. Sofia, et al., Functionalized silk-based biomaterials for bone formation, J. Biomed. Mater Res. 54 (1) (2001) 139–148.
[266] S.L. McNamara, et al., Silk as a biocohesive sacrificial binder in the fabrication of hydroxyapatite load bearing scaffolds, Biomaterials 35 (25) (2014) 6941–6953.
[267] H. Kweon, et al., Hydroxyapatite and silk combination-coated dental implants result in superior bone formation in the peri-implant area compared with hydroxyapatite and collagen combination-coated implants, J. Oral Maxillofac. Surg. 72 (10) (2014) 1928–1936.
[268] S.I. Roohani-Esfahani, et al., Effect of self-assembled nanofibrous silk/polycaprolactone layer on the osteoconductivity and mechanical properties of biphasic calcium phosphate scaffolds, Acta Biomater. 8 (1) (2012) 302–312.
[269] J.J. Li, et al., Multiple silk coatings on biphasic calcium phosphate scaffolds: effect on physical and mechanical properties and in vitro osteogenic response of human mesenchymal stem cells, Biomacromolecules 14 (7) (2013) 2179–2188.
[270] C. Cao, et al., Mechanical reinforcement of injectable calcium phosphate cement/silk fibroin (SF) composite by mineralized SF, Ceram. Int. 40 (9) (2014) 13987–13993.
[271] M.S. Kim, G. Kim, Three-dimensional electrospun polycaprolactone (PCL)/alginate hybrid composite scaffolds, Carbohydr. Polym. 114 (2014) 213–221.
[272] E. Khor, Methods for the treatment of collagenous tissues for bioprostheses, Biomaterials 18 (2) (1997) 95–105.
[273] B.A. Harley, et al., Mechanical characterization of collagen–glycosaminoglycan scaffolds, Acta Biomater. 3 (4) (2007) 463–474.
[274] C.M. Tierney, et al., The effects of collagen concentration and crosslink density on the biological, structural and mechanical properties of collagen-GAG scaffolds for bone tissue engineering, J. Mech. Behav. Biomed. Mater. 2 (2) (2009) 202–209.
[275] P.B. Maurus, C.C. Kaeding, Bioabsorbable implant material review, Operat. Tech. Sports Med. 12 (3) (2004) 158–160.
[276] J.C. Middleton, A.J. Tipton, Synthetic biodegradable polymers as orthopedic devices, Biomaterials 21 (23) (2000) 2335–2346.
[277] S. Wu, et al., Biomimetic porous scaffolds for bone tissue engineering, Mater. Sci. Eng. R Rep. 80 (2014) 1–36.
[278] K.J. Lowry, et al., Polycaprolactone/glass bioabsorbable implant in a rabbit humerus fracture model, J. Biomed. Mater. Res. 36 (4) (1997) 536–541.
[279] B.D. Ulery, L.S. Nair, C.T. Laurencin, Biomedical applications of biodegradable polymers, J. Polym. Sci. B Polym. Phys. 49 (12) (2011) 832–864.
[280] J.M. Williams, et al., Bone tissue engineering using polycaprolactone scaffolds fabricated via selective laser sintering, Biomaterials 26 (23) (2005) 4817–4827.
[281] C.H. Chen, et al., Surface modification of polycaprolactone scaffolds fabricated via selective laser sintering for cartilage tissue engineering, Mater Sci. Eng. C Mater Biol. Appl. 40 (2014) 389–397.
[282] Z. Cheng, S.-H. Teoh, Surface modification of ultra thin poly (ε-caprolactone) films using acrylic acid and collagen, Biomaterials 25 (11) (2004) 1991–2001.
[283] D. Simon, A. Holland, R. Shanks, Poly(caprolactone) thin film preparation, morphology, and surface texture, J. Appl. Polym. Sci. 103 (2) (2007) 1287–1294.
[284] Y.B. Kim, G.H. Kim, PCL/Alginate composite scaffolds for hard tissue engineering: fabrication, characterization, and cellular activities, ACS Comb. Sci. 17 (2) (2015) 87–99.
[285] D.L. Cohen, et al., Direct freeform fabrication of seeded hydrogels in arbitrary geometries, Tissue Eng. 12 (5) (2006) 1325–1335.
[286] S. Ahn, et al., Fabrication of cell-laden three-dimensional alginate-scaffolds with an aerosol cross-linking process, J. Mater. Chem. 22 (36) (2012) 18735–18740.
[287] R.M. Cornelius, et al., Immunoblot analysis of proteins associated with self-assembled monolayer surfaces of defined chemistries, J. Biomed. Mater. Res. Part A 98 (1) (2011) 7–18.
[288] Y. Luo, et al., Hierarchical mesoporous bioactive glass/alginate composite scaffolds fabricated by three-dimensional plotting for bone tissue engineering, Biofabrication 5 (1) (2013) 015005.
[289] K.F. Leong, C.M. Cheah, C.K. Chua, Solid freeform fabrication of three-dimensional scaffolds for engineering replacement tissues and organs, Biomaterials 24 (13) (2003) 2363–2378.
[290] D.W. Hutmacher, Scaffold design and fabrication technologies for engineering tissues — state of the art and future perspectives. Journal of Biomaterials Science, Polym. Ed. 12 (1) (2001) 107–124.
[291] N. Patel, et al., A comparative study on the in vivo behavior of hydroxyapatite and silicon substituted hydroxyapatite granules, J. Mater. Sci. Mater. Med. 13 (12) (2002) 1199–1206.
[292] A. Bianco, et al., Si-substituted hydroxyapatite nanopowders: synthesis, thermal stability and sinterability, Mater. Res. Bull. 44 (2) (2009) 345–354.
[293] M. Griffin, A. Bayat, Electrical stimulation in bone healing: critical analysis by evaluating levels of evidence, Eplasty 11 (2011) e34.
[294] C.P. Huang, X.M. Chen, Z.Q. Chen, Osteocyte: the impresario in the electrical stimulation for bone fracture healing, Med. Hypotheses 70 (2) (2008) 287–290.
[295] S. Meng, M. Rouabhia, Z. Zhang, Electrical stimulation in tissue regeneration, in: G.D. Gargiulo, A. McEwan (Eds.), Applied Biomedical Engineering, InTech, Rijeka, 2011. Ch. 03.
[296] M. Vila, et al., Electrical stimuli to increase cell proliferation on carbon nanotubes/mesoporous silica composites for drug delivery, J. Biomed. Mater Res. A 101 (1) (2013) 213–221.
[297] A. Sarac, et al., The ratio of crystallinity and thermodynamical interactions of polycaprolactone with some aliphatic esters and aromatic solvents by inverse gas chromatography, Polym. Bull. 53 (5) (2005) 349–357.
[298] S. Lauren, et al., Precision extruding deposition (PED) fabrication of polycaprolactone (PCL) scaffolds for bone tissue engineering, Biofabrication 1 (1) (2009) 015003.
[299] A.A. White, S.M. Best, I.A. Kinloch, Hydroxyapatite–carbon nanotube composites for biomedical applications: a review, Int. J. Appl. Ceram. Technol. 4 (1) (2007) 1–13.
[300] A.E. Jakus, et al., Hyperelastic "bone": a highly versatile, growth factor-free, osteoregenerative, scalable, and surgically friendly biomaterial, Sci. Transl. Med. 8 (358) (2016) 358ra127.
[301] W.K. Hsu, et al., Nanocomposite therapy as a more efficacious and less inflammatory alternative to bone morphogenetic protein-2 in a rodent arthrodesis model, J. Orthop. Res. 29 (12) (2011) 1812–1819.
[302] A.E. Jakus, et al., Hyperelastic “bone”: a highly versatile, growth factor–free, osteoregenerative, scalable, and surgically friendly biomaterial, Sci. Transl. Med. 8 (358) (2016), 358ra127-358ra127.
[303] Y.-L. Cheng, et al., Enhanced adhesion and differentiation of human mesenchymal stem cell inside apatite-mineralized/poly(dopamine)-coated poly(?-caprolactone) scaffolds by stereolithography, J. Mater. Chem. B 4 (38) (2016) 6307–6315.
[304] M.N. Cooke, et al., Use of stereolithography to manufacture critical-sized 3D biodegradable scaffolds for bone ingrowth, J. Biomed. Mater Res. B Appl. Biomater. 64 (2) (2003) 65–69.
[305] S.M. Roosa, et al., The pore size of polycaprolactone scaffolds has limited influence on bone regeneration in an in vivo model, J. Biomed. Mater. Res. A 92 (1) (2010) 359–368.
[306] H. Lee, et al., Mussel-inspired surface chemistry for multifunctional coatings, Science 318 (5849) (2007) 426–430.
[307] H. Yang, et al., Inhibition of titanium-particle-induced inflammatory osteolysis after local administration of dopamine and suppression of osteoclastogenesis via D2-like receptor signaling pathway, Biomaterials 80 (2016) 1–10.
[308] B.P. Tripathi, et al., Enhanced hydrophilic and antifouling polyacrylonitrile membrane with polydopamine modified silica nanoparticles, RSC Adv. 6 (6) (2016) 4448–4457.
[309] Y. Xie, et al., Highly sensitive and selective detection of miRNA: DNase I-assisted target recycling using DNA probes protected by polydopamine nanospheres, Chem. Commun. 51 (11) (2015) 2156–2158.
[310] M.F. Maitz, Applications of synthetic polymers in clinical medicine, Biosurf. Biotribol. 1 (3) (2015) 161–176.
[311] M.S. Lopes, A.L. Jardini, R.M. Filho, Poly (lactic acid) production for tissue engineering applications, Procedia Eng. 42 (2012) 1402–1413.
[312] T. Yang, et al., Fabrication of hierarchical macroporous biocompatible scaffolds by combining pickering high internal phase emulsion templates with three-dimensional printing, ACS Appl. Mater Interfaces 9 (27) (2017) 22950–22958.
[313] B. Holmes, et al., A synergistic approach to the design, fabrication and evaluation of 3D printed micro and nano featured scaffolds for vascularized bone tissue repair, Nanotechnology 27 (6) (2016) 064001.
[314] Z. Ren, et al., Repairing a bone defect with a three-dimensional cellular construct composed of a multi-layered cell sheet on electrospun mesh, Biofabrication 9 (2) (2017) 025036.
[315] Q. Yao, et al., Three dimensional electrospun PCL/PLA blend nanofibrous scaffolds with significantly improved stem cells osteogenic differentiation and cranial bone formation, Biomaterials 115 (2017) 115–127.
[316] T. Xu, et al., Electrospun polycaprolactone 3D nanofibrous scaffold with interconnected and hierarchically structured pores for bone tissue engineering, Adv. Healthc. Mater. 4 (15) (2015) 2238–2246.
[317] L.S. Nair, C.T. Laurencin, Biodegradable polymers as biomaterials, Prog. Polym. Sci. 32 (8–9) (2007) 762–798.
[318] K.G. Marra, et al., In vitro analysis of biodegradable polymer blend/hydroxyapatite composites for bone tissue engineering, J. Biomed. Mater. Res. 47 (3) (1999) 324–335.
[319] Z. Pan, J. Ding, Poly(lactide-co-glycolide) porous scaffolds for tissue engineering and regenerative medicine, Interface Focus 2 (3) (2012) 366–377.
[320] V.P. Orlovskii, V.S. Komlev, S.M. Barinov, Hydroxyapatite and hydroxyapatite-based ceramics, Inorg. Mater. 38 (10) (2002) 973–984.
[321] M.V. Jose, et al., Aligned bioactive multi-component nanofibrous nanocomposite scaffolds for bone tissue engineering, Macromol. Biosci. 10 (4) (2010) 433–444.
[322] C.-j. Shuai, et al., Preparation of complex porous scaffolds via selective laser sintering of poly(vinyl alcohol)/calcium silicate, J. Bioact. Compat. Polym. 29 (2) (2014) 110–120.
[323] P. Gentile, et al., An overview of poly(lactic-co-glycolic) acid (PLGA)-based biomaterials for bone tissue engineering, Int. J. Mol. Sci. 15 (3) (2014) 3640–3659.
[324] P. Zhang, et al., RGD-conjugated copolymer incorporated into composite of poly(lactide-co-glycotide) and poly(L-lactide)-grafted nanohydroxyapatite for bone tissue engineering, Biomacromolecules 12 (7) (2011) 2667–2680.
[325] R.E. McMahon, et al., Development of nanomaterials for bone repair and regeneration, J. Biomed. Mater Res. B Appl. Biomater. 101 (2) (2013)

Please cite this article in press as: G. Turnbull, et al., 3D bioactive composite scaffolds for bone tissue engineering, Bioactive Materials (2017), https://doi.org/10.1016/j.bioactmat.2017.10.001

387–397.
[326] S.K. Kumar, R. Krishnamoorti, Nanocomposites: structure, phase behavior, and properties, Annu. Rev. Chem. Biomol. Eng. 1 (2010) 37–58.
[327] P.A. Mouthuy, et al., Physico-chemical characterization of functional electrospun scaffolds for bone and cartilage tissue engineering, Proc. Inst. Mech. Eng. H. 224 (12) (2010) 1401–1414.
[328] M.V. Jose, et al., Aligned PLGA/HA nanofibrous nanocomposite scaffolds for bone tissue engineering, Acta Biomater. 5 (1) (2009) 305–315.
[329] Y.P. Yun, et al., Comparison of osteogenic differentiation from adipose-derived stem cells, mesenchymal stem cells, and pulp cells on PLGA/hydroxyapatite nanofiber, Tissue Eng. Regen. Med. 6 (2009) 336–345.
[330] A. Haider, K.C. Gupta, I.K. Kang, Morphological effects of HA on the cell compatibility of electrospun HA/PLGA composite nanofiber scaffolds, Biomed. Res. Int. 2014 (2014).
[331] A.B. Allen, et al., Functional augmentation of naturally-derived materials for tissue regeneration, Ann. Biomed. Eng. 43 (3) (2015) 555–567.
[332] A.K. Bassi, et al., The chemical and physical properties of poly(ε-caprolactone) scaffolds functionalised with poly(vinyl phosphonic acid-co-acrylic acid), J. Tissue Eng. 2011 (2011) 615328.
[333] M.D. Pierschbacher, E. Ruoslahti, Cell attachment activity of fibronectin can be duplicated by small synthetic fragments of the molecule, Nature 309 (5963) (1984) 30–33.
[334] Y.C. Shin, et al., Biomimetic hybrid nanofiber sheets composed of RGD peptide-decorated PLGA as cell-adhesive substrates, J. Funct. Biomater. 6 (2) (2015) 367–378.
[335] E.M. Ahmed, Hydrogel: preparation, characterization, and applications: a review, J. Adv. Res. 6 (2) (2015) 105–121.
[336] B.H. Fellah, et al., Bone repair using a new injectable self-crosslinkable bone substitute, J. Orthop. Res. 24 (4) (2006) 628–635.
[337] J. Kim, et al., Bone regeneration using hyaluronic acid-based hydrogel with bone morphogenic protein-2 and human mesenchymal stem cells, Biomaterials 28 (10) (2007) 1830–1837.
[338] D. Chimene, et al., Advanced bioinks for 3D printing: a materials science perspective, Ann. Biomed. Eng. 44 (6) (2016) 2090–2102.
[339] A.G. Tabriz, et al., Three-dimensional bioprinting of complex cell laden alginate hydrogel structures, Biofabrication 7 (4) (2015) 045012.
[340] M.M. Stanton, J. Samitier, S. Sanchez, Bioprinting of 3D hydrogels, Lab. Chip 15 (15) (2015) 3111–3115.
[341] H.-B. Zhang, et al., Three-dimensional bioprinting is not only about cell-laden structures, Chin. J. Traumatol. 19 (4) (2016) 187–192.
[342] M. Guvendiren, et al., Designing biomaterials for 3D printing, ACS Biomater. Sci. Eng. 2 (10) (2016) 1679–1693.
[343] A.D. Baldwin, K.L. Kiick, Polysaccharide-modified synthetic polymeric biomaterials, Biopolymers 94 (1) (2010) 128–140.
[344] T. Nie, et al., Production of heparin-functionalized hydrogels for the development of responsive and controlled growth factor delivery systems, J. Control. Release 122 (3) (2007) 287–296.
[345] Y. Liang, K.L. Kiick, Heparin-functionalized polymeric biomaterials in tissue engineering and drug delivery applications, Acta biomater. 10 (4) (2014) 1588–1600.
[346] D.A. Ossipov, Bisphosphonate-modified biomaterials for drug delivery and bone tissue engineering, Expert Opin. Drug Deliv. 12 (9) (2015) 1443–1458.
[347] O. Liliang, et al., Effect of bioink properties on printability and cell viability for 3D bioplotting of embryonic stem cells, Biofabrication 8 (3) (2016) 035020.
[348] D. Houzhu, T. Filippos, C.C. Robert, Bioprinting multidimensional constructs: a quantitative approach to understanding printed cell density and redistribution phenomena, Biomed. Phys. Eng. Express 3 (3) (2017) 035016.
[349] D.-J. Cornelissen, A. Faulkner-Jones, W. Shu, Current developments in 3D bioprinting for tissue engineering, Curr. Opin. Biomed. Eng. 2 (1) (2017) 76–82.
[350] Y.R. Lou, et al., The use of nanofibrillar cellulose hydrogel as a flexible three-dimensional model to culture human pluripotent stem cells, Stem Cells Dev. 23 (4) (2014) 380–392.
[351] K. Markstedt, et al., 3D bioprinting human chondrocytes with nanocellulose–alginate bioink for cartilage tissue engineering applications, Biomacromolecules 16 (5) (2015) 1489–1496.
[352] N.T. Khanarian, et al., A hydrogel-mineral composite scaffold for osteochondral interface tissue engineering, Tissue Eng. Part A 18 (5–6) (2012) 533–545.
[353] J.P. Spalazzi, et al., In vivo evaluation of a multiphased scaffold designed for orthopaedic interface tissue engineering and soft tissue-to-bone integration, J. Biomed. Mater Res. A 86 (1) (2008) 1–12.
[354] G. Gao, et al., Inkjet-bioprinted acrylated peptides and PEG hydrogel with human mesenchymal stem cells promote robust bone and cartilage formation with minimal printhead clogging, Biotechnol. J. 10 (10) (2015) 1568–1577.
[355] H.-W. Kang, et al., A 3D bioprinting system to produce human-scale tissue constructs with structural integrity, Nat Biotechnol. 34 (3) (2016) 312–319.
[356] M. Muller, et al., Printing thermoresponsive reverse molds for the creation of patterned two-component hydrogels for 3D cell culture, J. Vis. Exp. (77) (2013) e50632.
[357] M. Di Biase, et al., Inkjet printing and cell seeding thermoreversible photocurable gel structures, Soft Matter 7 (6) (2011) 2639–2646.
[358] N.E. Fedorovich, et al., Evaluation of photocrosslinked lutrol hydrogel for tissue printing applications, Biomacromolecules 10 (7) (2009) 1689–1696.
[359] N.E. Fedorovich, et al., Biofabrication of osteochondral tissue equivalents by printing topologically defined, cell-laden hydrogel scaffolds, Tissue Eng. Part C Methods 18 (1) (2012) 33–44.
[360] E. Lippens, et al., Cell survival and proliferation after encapsulation in a chemically modified Pluronic(R) F127 hydrogel, J. Biomater. Appl. 27 (7) (2013) 828–839.
[361] C.C. Chang, et al., Direct-write bioprinting three-dimensional biohybrid systems for future regenerative therapies, J. Biomed. Mater Res. B Appl. Biomater. 98 (1) (2011) 160–170.
[362] T. Tharmalingam, et al., Pluronic enhances the robustness and reduces the cell attachment of mammalian cells, Mol. Biotechnol. 39 (2) (2008) 167–177.
[363] S.F. Khattak, S.R. Bhatia, S.C. Roberts, Pluronic F127 as a cell encapsulation material: utilization of membrane-stabilizing agents, Tissue Eng. 11 (5–6) (2005) 974–983.
[364] P. Chandaroy, et al., Utilizing temperature-sensitive association of Pluronic F-127 with lipid bilayers to control liposome-cell adhesion, Biochim. Biophys. Acta 1559 (1) (2002) 32–42.
[365] S.Y. Lee, G. Tae, Y.H. Kim, Thermal gellation and photo-polymerization of diacrylated Pluronic F 127, J. Biomater. Sci. Polym. Ed. 18 (10) (2007) 1335–1353.
[366] S. Patra, V. Young, A review of 3D printing techniques and the future in biofabrication of bioprinted tissue, Cell Biochem. Biophys. (2016) 1–6.
[367] V. Mironov, et al., Organ printing: tissue spheroids as building blocks, Biomaterials 30 (12) (2009) 2164–2174.
[368] D.B. Kolesky, et al., Three-dimensional bioprinting of thick vascularized tissues, Proc. Natl. Acad. Sci. 113 (12) (2016) 3179–3184.
[369] M. Michael, et al., Nanostructured Pluronic hydrogels as bioinks for 3D bioprinting, Biofabrication 7 (3) (2015) 035006.
[370] J.P.K. Armstrong, et al., 3D bioprinting using a templated porous bioink, Adv. Healthc. Mater. 5 (14) (2016) 1724–1730.
[371] B. Byambaa, et al., Bioprinted osteogenic and vasculogenic patterns for engineering 3D bone tissue, Adv. Healthc. Mater. 6 (16) (2017) 1700015.
[372] D.W. Thompson, J.T. Butterworth, The nature of laponite and its aqueous dispersions, J. Colloid Interface Sci. 151 (1992) 236–243.
[373] J.R. Xavier, et al., Bioactive nanoengineered hydrogels for bone tissue engineering: a growth-factor-free approach, ACS Nano 9 (3) (2015) 3109–3118.
[374] A. Paul, et al., Nanoengineered biomimetic hydrogels for guiding human stem cell osteogenesis in three dimensional microenvironments, J. Mater Chem. B Mater Biol. Med. 4 (20) (2016) 3544–3554.
[375] J. Wang, et al., Phage nanofibers induce vascularized osteogenesis in 3D printed bone scaffolds, Adv. Mater. 26 (29) (2014) 4961–4966.
[376] C. Marco, et al., 3D bioprinting of BM-MSCs-loaded ECM biomimetic hydrogels for in vitro neocartilage formation, Biofabrication 8 (3) (2016) 035002.
[377] A.C. Daly, et al., 3D bioprinting of developmentally inspired templates for whole bone organ engineering, Adv. Healthc. Mater. 5 (18) (2016) 2353–2362.
[378] H.H. Kim, et al., Surface-modified silk hydrogel containing hydroxyapatite nanoparticle with hyaluronic acid-dopamine conjugate, Int. J. Biol. Macromol. 70 (2014) 516–522.
[379] M.H. Kim, et al., Silk fibroin/hydroxyapatite composite hydrogel induced by gamma-ray irradiation for bone tissue engineering, Biomater. Res. 21 (1) (2017) 12.
[380] X. Ding, et al., Increased stem cells delivered using a silk gel/scaffold complex for enhanced bone regeneration, Sci. Rep. 7 (1) (2017) 2175.
[381] X.-F. Wang, et al., Osteogenic differentiation of three-dimensional bioprinted constructs consisting of human adipose-derived stem cells in vitro and in vivo, PLoS One 11 (6) (2016) e0157214.
[382] M. Maglione, et al., In vivo evaluation of chitosan-glycerol gel scaffolds seeded with stem cells for full-thickness mandibular bone regeneration, J. Oral Sci. 59 (2) (2017) 225–232.
[383] R. Jin, et al., Injectable chitosan-based hydrogels for cartilage tissue engineering, Biomaterials 30 (13) (2009) 2544–2551.
[384] H. Tan, et al., Controlled gelation and degradation rates of injectable hyaluronic acid-based hydrogels through a double crosslinking strategy, J. tissue Eng. Regen. Med. 5 (10) (2011) 790–797.
[385] Y. Wei, et al., A novel injectable scaffold for cartilage tissue engineering using adipose-derived adult stem cells, J. Orthop. Res. 26 (1) (2008) 27–33.
[386] K. Ding, et al., A promising injectable scaffold: the biocompatibility and effect on osteogenic differentiation of mesenchymal stem cells, Biotechnol. Bioprocess Eng. 18 (1) (2013) 155–163.
[387] M. Dessi, et al., Novel biomimetic thermosensitive beta-tricalcium phosphate/chitosan-based hydrogels for bone tissue engineering, J. Biomed. Mater Res. A 101 (10) (2013) 2984–2993.
[388] Y. Jiao, et al., A rheological study of biodegradable injectable PEGMC/HA composite scaffolds, Soft Matter 8 (5) (2012) 1499–1507.
[389] D. Gyawali, et al., Citrate-based biodegradable injectable hydrogel composites for orthopedic applications, Biomater. Sci. 1 (1) (2013) 52–64.
[390] S. Fu, et al., Injectable and thermo-sensitive PEG-PCL-PEG copolymer/collagen/n-HA hydrogel composite for guided bone regeneration, Biomaterials 33 (19) (2012) 4801–4809.
[391] Y. Huang, et al., An injectable nano-hydroxyapatite (n-HA)/glycol chitosan (G-CS)/hyaluronic acid (HyA) composite hydrogel for bone tissue engineering, RSC Adv. 6 (40) (2016) 33529–33536.

Please cite this article in press as: G. Turnbull, et al., 3D bioactive composite scaffolds for bone tissue engineering, Bioactive Materials (2017), https://doi.org/10.1016/j.bioactmat.2017.10.001

[392] J. Yan, et al., Injectable alginate/hydroxyapatite gel scaffold combined with gelatin microspheres for drug delivery and bone tissue engineering, Mater Sci. Eng. C Mater Biol. Appl. 63 (2016) 274–284.
[393] C.K. Kuo, P.X. Ma, Maintaining dimensions and mechanical properties of ionically crosslinked alginate hydrogel scaffolds in vitro, J. Biomed. Mater Res. A 84 (4) (2008) 899–907.
[394] Y. Han, et al., The calcium silicate/alginate composite: preparation and evaluation of its behavior as bioactive injectable hydrogels, Acta Biomater. 9 (11) (2013) 9107–9117.
[395] L. Zhao, M.D. Weir, H.H.K. Xu, An injectable calcium phosphate-alginate hydrogel-umbilical cord mesenchymal stem cell paste for bone tissue engineering, Biomaterials 31 (25) (2010) 6502–6510.
[396] S. Dhivya, et al., Nanohydroxyapatite-reinforced chitosan composite hydrogel for bone tissue repair in vitro and in vivo, J. Nanobiotechnol. 13 (2015) 40.
[397] T.E. Douglas, et al., Injectable self-gelling composites for bone tissue engineering based on gellan gum hydrogel enriched with different bioglasses, Biomed. Mater. 9 (4) (2014) 045014.
[398] Q.Z. Chen, G.A. Thouas, Fabrication and characterization of sol-gel derived 45S5 Bioglass(R)-ceramic scaffolds, Acta Biomater. 7 (10) (2011) 3616–3626.
[399] M.V. Priya, et al., Injectable osteogenic and angiogenic nanocomposite hydrogels for irregular bone defects, Biomed. Mater. 11 (3) (2016) 035017.
[400] A.K. Miri, et al., Ectopic bone formation in rapidly fabricated acellular injectable dense collagen-Bioglass hybrid scaffolds via gel aspiration-ejection, Biomaterials 85 (2016) 128–141.
[401] Y. Li, H. Tian, X. Chen, Hyaluronic acid based injectable hydrogels for localized and sustained gene delivery, J. Control Release 213 (2015) e140-1.
[402] X. Ji, et al., Coaxially electrospun core/shell structured poly(L-lactide) acid/chitosan nanofibers for potential drug carrier in tissue engineering, J. Biomed. Nanotechnol. 9 (10) (2013) 1672–1678.
[403] T.D. Sargeant, et al., An in situ forming collagen-PEG hydrogel for tissue regeneration, Acta Biomater. 8 (1) (2012) 124–132.
[404] A. Fathi, et al., Elastin based cell-laden injectable hydrogels with tunable gelation, mechanical and biodegradation properties, Biomaterials 35 (21) (2014) 5425–5435.
[405] S.J. Bidarra, C.C. Barrias, P.L. Granja, Injectable alginate hydrogels for cell delivery in tissue engineering, Acta Biomater. 10 (4) (2014) 1646–1662.
[406] K. Ren, et al., Injectable glycopolypeptide hydrogels as biomimetic scaffolds for cartilage tissue engineering, Biomaterials 51 (2015) 238–249.
[407] J. Radhakrishnan, et al., Injectable and 3D bioprinted polysaccharide hydrogels: from cartilage to osteochondral tissue engineering, Biomacromolecules 18 (1) (2017) 1–26.
[408] R. Jin, et al., Synthesis and characterization of hyaluronic acid-poly(ethylene glycol) hydrogels via Michael addition: an injectable biomaterial for cartilage repair, Acta Biomater. 6 (6) (2010) 1968–1977.
[409] S. Yan, et al., Injectable in situ self-cross-linking hydrogels based on poly(L-glutamic acid) and alginate for cartilage tissue engineering, Biomacromolecules 15 (12) (2014) 4495–4508.
[410] E.M. Ehlers, et al., Effects of hyaluronic acid on the morphology and proliferation of human chondrocytes in primary cell culture, Ann. Anat. 183 (1) (2001) 13–17.
[411] K. Aibe, J. Ryu, S. Sano, Effects of hyaluronic acid on cartilage metabolism in free chondrocytes, J. Orthop. Sci. 1 (4) (1996) 268–276.
[412] A.M. Patti, et al., Effect of hyaluronic acid on human chondrocyte cell lines from articular cartilage, Tissue Cell 33 (3) (2001) 294–300.
[413] M. Akmal, et al., The effects of hyaluronic acid on articular chondrocytes, J. Bone & Jt. Surg. Br. 87-B (8) (2005) 1143–1149.
[414] Q. Hua, C.B. Knudson, W. Knudson, Internalization of hyaluronan by chondrocytes occurs via receptor-mediated endocytosis, J. Cell Sci. 106 (Pt 1) (1993) 365–375.
[415] O. Ishida, et al., Chondrocytes are regulated by cellular adhesion through CD44 and hyaluronic acid pathway, J. Bone Min. Res. 12 (10) (1997) 1657–1663.
[416] Hyaluronan receptor-directed assembly of chondrocyte pericellular matrix, J. Cell Biol. 120 (3) (1993) 825–834.
[417] H. Park, et al., Injectable chitosan hyaluronic acid hydrogels for cartilage tissue engineering, Acta Biomater. 9 (1) (2013) 4779–4786.
[418] Y. Guo, et al., Hydrogels of collagen/chondroitin sulfate/hyaluronan interpenetrating polymer network for cartilage tissue engineering, J. Mater Sci. Mater. Med. 23 (9) (2012) 2267–2279.
[419] F. Yu, et al., An injectable hyaluronic acid/PEG hydrogel for cartilage tissue engineering formed by integrating enzymatic crosslinking and Diels-Alder "click chemistry", Polym. Chem. 5 (3) (2014) 1082–1090.
[420] F. Chen, et al., Self-crosslinking and injectable hyaluronic acid/RGD-functionalized pectin hydrogel for cartilage tissue engineering, Carbohydr. Polym. 166 (2017) 31–44.
[421] L. Bacakova, K. Novotna, M. Parizek, Polysaccharides as cell carriers for tissue engineering: the use of cellulose in vascular wall reconstruction, Physiol. Res. 63 (1) (2014) S29–S47.
[422] F. Munarin, et al., Pectin-based injectable biomaterials for bone tissue engineering, Biomacromolecules 12 (3) (2011) 568–577.
[423] B. Choi, et al., Cartilaginous extracellular matrix-modified chitosan hydrogels for cartilage tissue engineering, ACS Appl. Mater. Interfaces 6 (22) (2014) 20110–20121.
[424] H. Park, K.Y. Lee, Cartilage regeneration using biodegradable oxidized alginate/hyaluronate hydrogels, J. Biomed. Mater. Res. A 102 (12) (2014) 4519–4525.
[425] H. Park, et al., Alginate hydrogels modified with low molecular weight hyaluronate for cartilage regeneration, Carbohydr. Polym. 162 (2017) 100–107.
[426] J.C. Lee, et al., Synovium-derived mesenchymal stem cells encapsulated in a novel injectable gel can repair osteochondral defects in a rabbit model, Tissue Eng. Part A 18 (19–20) (2012) 2173–2186.
[427] C. Fan, D.-A. Wang, A biodegradable PEG-based micro-cavitary hydrogel as scaffold for cartilage tissue engineering, Eur. Polym. J. 72 (2015) 651–660.
[428] Y. Hwang, N. Sangaj, S. Varghese, Interconnected macroporous poly(ethylene glycol) cryogels as a cell scaffold for cartilage tissue engineering, Tissue Eng. Part A 16 (10) (2010) 3033–3041.
[429] W.K. Lee, et al., Novel poly(ethylene glycol) scaffolds crosslinked by hydrolyzable polyrotaxane for cartilage tissue engineering, J. Biomed. Mater Res. A 67 (4) (2003) 1087–1092.
[430] Zhang, K., et al., ASC spheroids formed in poly(L-glutamic acid)/chitosan scaffold to enhance hyaline-like cartilage regeneration. Front. Bioeng. Biotechnol. Conference Abstract: 10th World Biomaterials Congress. doi: 10.3389/conf.FBIOE.2016.01.00906 .
[431] A. Dubbini, et al., Injectable hyaluronic acid/PEG-p(HPMAm-lac)-based hydrogels dually cross-linked by thermal gelling and Michael addition, Eur. Polym. J. 72 (2015) 423–437.
[432] M.H. Anthony, et al., Rising to the challenge: applying biofabrication approaches for better drug and chemical product development, Biofabrication 9 (3) (2017) 033001.
[433] C.H. Evans, Barriers to the clinical translation of orthopedic tissue engineering, Tissue Eng. Part B Rev. 17 (6) (2011) 437–441.
[434] P.G. Robey, Cell sources for bone regeneration: the good, the bad, and the ugly (but promising), Tissue Eng. Part B Rev. 17 (6) (2011) 423–430.
[435] C. Colnot, Cell sources for bone tissue engineering: insights from basic science, Tissue Eng. Part B Rev. 17 (6) (2011) 449–457.
[436] A. Stolzing, et al., Age-related changes in human bone marrow-derived mesenchymal stem cells: consequences for cell therapies, Mech. Ageing Dev. 129 (3) (2008) 163–173.
[437] G.F. Muschler, et al., Age- and gender-related changes in the cellularity of human bone marrow and the prevalence of osteoblastic progenitors, J. Orthop. Res. 19 (1) (2001) 117–125.
[438] M. Kahle, et al., Embryonic stem cells induce ectopic bone formation in rats, Biomed. Mater. Eng. 20 (6) (2010) 371–380.
[439] D.J. Illich, et al., Concise review: induced pluripotent stem cells and lineage reprogramming: prospects for bone regeneration, Stem Cells 29 (4) (2011) 555–563.
[440] P.W.M. Ferry, et al., Hydrogel-based reinforcement of 3D bioprinted constructs, Biofabrication 8 (3) (2016) 035004.
[441] S. Kedong, et al., Development and fabrication of a two-layer tissue engineered osteochondral composite using hybrid hydrogel-cancellous bone scaffolds in a spinner flask, Biomed. Mater. 11 (6) (2016) 065002.
[442] Z. Ting, et al., Biomimetic design and fabrication of multilayered osteochondral scaffolds by low-temperature deposition manufacturing and thermal-induced phase-separation techniques, Biofabrication 9 (2) (2017) 025021.
[443] F.P. Melchels, et al., Additive manufacturing of tissues and organs, Prog. Polym. Sci. 37 (8) (2012) 1079–1104.
[444] L. Riccardo, et al., Biofabrication of tissue constructs by 3D bioprinting of cell-laden microcarriers, Biofabrication 6 (3) (2014) 035020.
[445] M. Orciani, et al., Biofabrication and bone tissue regeneration: cell source, approaches, and challenges, Front. Bioeng. Biotechnol. 5 (17) (2017).
[446] S. Morgan, et al., The cost of drug development: a systematic review, Health Policy 100 (1) (2011) 4–17.
[447] J.A. DiMasi, R.W. Hansen, H.G. Grabowski, The price of innovation: new estimates of drug development costs, J. Health Econ. 22 (2) (2003) 151–185.
[448] M.A. Rodgers, et al., Reporting of industry funded study outcome data: comparison of confidential and published data on the safety and effectiveness of rhBMP-2 for spinal fusion, BMJ Br. Med. J. (2013) 346.
[449] C.H. Evans, Barriers to the clinical translation of orthopedic tissue engineering, Tissue Eng. Part B Rev. 17 (6) (2011) 437–441.
[450] S.J. Hollister, W.L. Murphy, Scaffold translation: barriers between concept and clinic, Tissue Eng. Part B Rev. 17 (6) (2011) 459–474.
[451] M. Dickson, J.P. Gagnon, Key factors in the rising cost of new drug discovery and development, Nat. Rev. Drug Discov. 3 (5) (2004) 417–429.
[452] N. Vermeulen, et al., 3D bioprint me: a socioethical view of bioprinting human organs and tissues, J. Med. Ethics 43 (9) (2017) 618–624.
[453] P.H. Li, 3D bioprinting technologies: patents, innovation and access, Law Innov. Technol. 6 (2) (2014) 282–304.
[454] X. Wang, Y. Yan, R. Zhang, Recent trends and challenges in complex organ manufacturing, Tissue Eng. Part B Rev. 16 (2) (2010) 189–197.
[455] V. Mironov, V. Kasyanov, R.R. Markwald, Organ printing: from bioprinter to organ biofabrication line, Curr. Opin. Biotechnol. 22 (5) (2011) 667–673.
[456] P.M. Tsimbouri, et al., Stimulation of 3D osteogenesis by mesenchymal stem cells using a nanovibrational bioreactor, Nat. Biomed. Eng. 1 (9) (2017) 758–770.
[457] P.R. Baraniak, T.C. McDevitt, Scaffold-free culture of mesenchymal stem cell spheroids in suspension preserves multilineage potential, Cell Tissue Res. 347 (2012).

Please cite this article in press as: G. Turnbull, et al., 3D bioactive composite scaffolds for bone tissue engineering, Bioactive Materials (2017), https://doi.org/10.1016/j.bioactmat.2017.10.001

[458] T.J. Bartosh, et al., Aggregation of human mesenchymal stromal cells (MSCs) into 3D spheroids enhances their antiinflammatory properties, Proc. Natl. Acad. Sci. U. S. A. 107 (2010).
[459] L.-W. Xia, et al., Nano-structured smart hydrogels with rapid response and high elasticity 4 (2013) 2226.
[460] J. An, et al., Design and 3D printing of scaffolds and tissues, Engineering 1 (2) (2015) 261–268.
[461] C. Huang, J. Geng, S. Jiang, MicroRNAs in regulation of osteogenic differentiation of mesenchymal stem cells, Cell Tissue Res. 368 (2) (2017) 229–238.
[462] Y. Tian, et al., MicroRNA-30a promotes chondrogenic differentiation of mesenchymal stem cells through inhibiting Delta-like 4 expression, Life Sci. 148 (2016) 220–228.
[463] S.J. Lee, et al., Surface modification of 3D-printed porous scaffolds via mussel-inspired polydopamine and effective immobilization of rhBMP-2 to promote osteogenic differentiation for bone tissue engineering, Acta Biomater. 40 (Supplement C) (2016) 182–191.
[464] K.M. Woo, et al., Nano-fibrous scaffolding promotes osteoblast differentiation and biomineralization, Biomaterials 28 (2) (2007) 335–343.
[465] H. Sun, et al., Osteogenic differentiation of human amniotic fluid–derived stem cells induced by bone morphogenetic Protein-7 and enhanced by nanofibrous scaffolds, Biomaterials 31 (6) (2010) 1133.
[466] L.A. Smith, et al., The enhancement of human embryonic stem cell osteogenic differentiation with nano-fibrous scaffolding, Biomaterials 31 (21) (2010) 5526–5535.
[467] H. Cao, et al., The topographical effect of electrospun nanofibrous scaffolds on the in vivo and in vitro foreign body reaction, J. Biomed. Mater Res. A 93 (3) (2010) 1151–1159.
[468] A.R. Amini, C.T. Laurencin, S.P. Nukavarapu, Bone tissue engineering: recent advances and challenges, Crit. Rev. Biomed. Eng. 40 (5) (2012) 363–408.
[469] J.M. Karp, G.S. Leng Teo, Mesenchymal stem cell homing: the devil is in the details, Cell Stem Cell 4 (3) (2009) 206–216.

Please cite this article in press as: G. Turnbull, et al., 3D bioactive composite scaffolds for bone tissue engineering, Bioactive Materials (2017), https://doi.org/10.1016/j.bioactmat.2017.10.001